

**Genetic manipulation of chlorophyll
metabolism in *Arabidopsis thaliana* to
prevent singlet oxygen-induced stress
and programmed cell death.**

Thesis submitted to

JAWAHARLAL NEHRU UNIVERSITY

For the award of the degree of

DOCTOR OF PHILOSOPHY

Garima Chauhan

2019



SCHOOL OF LIFE SCIENCES
JAWAHARLAL NEHRU UNIVERSITY
NEW DELHI-110067



School of Life Sciences
Jawaharlal Nehru University

New Delhi-110 067, INDIA

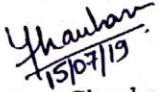
Dr. Baishnab C. Tripathy, FNA, FNASC, FNAAS
Professor
J.C. Bose National Fellow

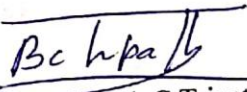
Phone : 91-11-26704524
Fax : 91-11-26742558
E-mail : bctripathy@mail.jnu.ac.in
baishnabtripathy@yahoo.com

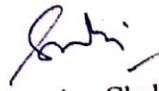
CERTIFICATE

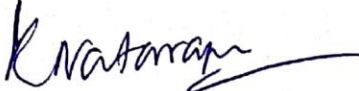
This is to certify that the research work embodied in this thesis entitled "**Genetic manipulation of chlorophyll metabolism in *Arabidopsis thaliana* to prevent singlet oxygen-induced oxidative stress and programmed cell death**" submitted for the award of Degree of **Doctor of Philosophy**, has been carried out by **Ms. Garima Chauhan** under the supervision of **Prof. Baishnab C Tripathy** and **Prof. Supriya Chakraborty** in the School of Life Sciences, Jawaharlal Nehru University, New Delhi, India.

This work is original and has not been submitted so far, in part or in full for any degree or diploma of any other university.


Garima Chauhan
(Candidate)


Prof. Baishnab C Tripathy
(Supervisor)


Prof. Supriya Chakraborty
(Jt. Supervisor)


Prof. K. Natarajan
(Dean, SLS, JNU)

ABBREVIATIONS

$^{\circ}\text{C}$	Degree Celsius
$^1\text{O}_2$	Singlet oxygen
ALA	5-Aminolevulinic acid
APX	Ascorbate Peroxidase
CAT	Catalase
Chl	Chlorophyll
Chlide	Chlorophyllide
CLH	Chlorophyllase
d	Dark
DIC	Differential interference contrast
EDTA	Ethylenediaminetetraacetic acid
EEE	Excess excitation energy
ETR	Electron transport rate
FCC	Fluorescent chlorophyll catabolite
Fig	Figure
h	hour
HL	High light
IRGA	Infrared gas analyzer
L	Liter
l	Light
LHC	Light harvesting complex
$\text{m}^{-2} \text{s}^{-1}$	meter square per second
MCS	Metal chelating substance
mM	millimolar
min	Minute
ms	milli second
ml	milliliter
MS	Murashige and Skoog
NCC	Nonfluorescent chlorophyll catabolite

NPQ	Non-photochemical quenching
nm	Nanometer
ns	Nanosecond
PAM	Pulse amplitude modulation
PAO	Pheide a oxygenase
Pchl _a	Protochlorophyll _a
Pheide a	Pheophorbide a
POR	Protochlorophyllide oxidoreductase
PSI	Photosystem I
PSII	Photosystem II
RCC	Red chlorophyll catabolite
RCCR	Red chlorophyll catabolite reductase
ROS	Reactive oxygen species
rpm	Revolutions per minute
RT	Room temperature
SD	Standard deviation
SE	Standard error
Sec	Seconds
SOSG	Singlet oxygen sensor green
TBA	Thio barbituric acid
TCA	Trichloroacetic acid
TBARS	Thiobarbituric acid reactive substance
TE	Tris EDTA
Tris	Tris (hydroxymethyl) aminomethane
Vol	Volume
μg	Microgram
μl	Microliter
μmol	micromol

TABLE OF CONTENTS

Introduction	7
Objectives	9
Review of literature	10
Singlet oxygen production in plants.	10
Reaction center and antenna complex	11
Cyt b6f complex	12
Chlorophyll biosynthetic intermediates	12
Chlorophyll catabolic intermediates	16
Singlet oxygen-induced oxidative stress	18
Singlet oxygen-induced lipid peroxidation.	19
Degradation of protein in response to singlet oxygen stress	20
DNA fragmentation	21
Role of singlet oxygen in programmed cell death	21
Manipulating chlorophyll metabolic pathway to reduce singlet oxygen-induced damage	23
Protochlorophyllide oxidoreductase (POR)	24
Pheophorbide a Oxygenase (PAO)	26
Red chlorophyll catabolite reductase (RCCR)	27
Materials and Methods	28
Surface sterilization of <i>Arabidopsis</i> seeds	28
General sterilization procedures	28
Nutrient media	28
Spectrophotometry	30
Chlorophyll and carotenoid estimation	30
Pulse amplitude modulation (PAM) measurements	31
ALA treatment	33
Light treatment	33
Imaging PAM	33

Protein extraction	34
Catalase (CAT) activity (EC 1.11.1.6)	34
Ascorbate Peroxidase (APX) activity (EC 1.11.1.11)	34
Protoplast Isolation	34
Singlet oxygen imaging by SOSG	35
Terminal deoxynucleotidyl transferase nick end labeling (TUNEL) Assay	35
Estimation of lipid peroxidation	36
Handy PEA	37
High light treatment	37
Carbon dioxide assimilation analysis by Infrared gas analyzer (IRGA)	38

Results

39

Comparison of photosynthetic parameters of WT, PORCx, and <i>porC-2</i> mutant	39
Plant phenotype	39
Pigment content in WT, PORCx, and <i>porC-2</i> plants	39
Analysis of chlorophyll a fluorescence parameter by Pulse amplitude modulation	39
Measurement of photosynthetic CO ₂ assimilated by plants	41
Antioxidative enzyme activities	42
Impact of singlet oxygen-induced oxidative stress causes severe photooxidative stress in <i>porC-2</i> mutant	43
Morphological changes	43
Chlorophyll a fluorescence imaging	43
Singlet oxygen generation in response to Pchl _a accumulation	43
Singlet oxygen-induced damage to photosynthetic apparatus	44
Cell death due to singlet oxygen induced oxidative stress	45
Photooxidative stress in high light	45
Generation of singlet oxygen from the leaves in high light	46
Pulse amplitude modulation (PAM) measurement after high light stress	46
Chlorophyll a fast fluorescence kinetics	47
Analysis of lipid peroxidation	50

Evans blue staining	50
Analysis of ¹ O ₂ in protoplast	50
Induction of cell death in response to high light stress	51
TUNEL assay	51
Genetic manipulation of chlorophyll catabolic enzymes to prevent oxidative stress	51
Total chlorophyll	52
Carotenoid content	52
Imaging PAM analysis	52
Chlorophyll a fluorescence parameters	52
Antioxidative enzyme activities	54
Impact of high light stress	54
High light induced photo bleaching of leaves	55
Singlet oxygen accumulation in response to high light stress.	55
Chlorophyll a fluorescence parameters	55
Chlorophyll a fluorescence JIP-Test	56
MDA assay	59
Evans blue staining	59
Discussion	60
Summary	74
References	77
Appendix	90

Introduction

Singlet oxygen ($^1\text{O}_2$) is one of the reactive oxygen species that is produced mostly in light via type II photosensitization reactions of tetrapyrroles in the oxygenic world. Reduced amount of $^1\text{O}_2$ is readily quenched by carotenoids, tocopherols, histidine and possibly detoxified by ascorbate. Elevation in the level of $^1\text{O}_2$ occurs when plants are subjected to extreme environmental fluctuations like high light, extreme temperature, salinity, and drought stress. The overaccumulation of $^1\text{O}_2$ induces oxidative stress in plants. Highly reactive $^1\text{O}_2$ oxidizes various biologically relevant biomolecules such as lipids, proteins, and nucleic acids and ultimately impairs their function. The intensive damage to cellular machinery ultimately leads to programmed cell death.

In higher plants, the major site of $^1\text{O}_2$ production is in the chloroplast. When plants receive surplus light, the excess energy that is absorbed, excites chlorophyll and its metabolic intermediates to their triplet excited state. The increased life span of triplet excited state allows interaction with molecular oxygen to give rise to singlet oxygen. Presence of parallel spin electrons in the outer orbital of oxygen reduces the reactivity of oxygen. However, the absorption of excess energy removes the spin restriction. Hence non-reactive oxygen gets converted into most reactive, singlet oxygen via type II photosensitization reaction. Elevated singlet oxygen induces oxidative stress in plants and activates a downstream signaling pathway that leads to programmed cell death. Analysis of conditional mutants such as *flu*, *tigrina*, *chlorina 1* has paved the way to understand the signaling cascade initiated by singlet oxygen in a controlled manner. Elevation of $^1\text{O}_2$ level induces activation of stress-responsive genes that are specific to $^1\text{O}_2$ and not induced by other ROS such as superoxide and hydrogen peroxide.

Various enzymes tightly regulate chlorophyll biosynthesis and degradation pathway. Some of the intermediates involved in both biosynthesis and degradation pathways are photodynamic. When plants are exposed to sun light, these intermediates absorb the excess energy and return to their ground state by transferring their energy to nearly available molecular oxygen. During chlorophyll biosynthesis, the photodynamic intermediate protochlorophyllide accumulates in the dark. Its conversion is catalyzed by a light dependent Protochlorophyllide oxidoreductase

enzyme which requires NADPH as a co-factor. The surplus availability of PORC enzyme during high light stress will ensure maximum conversion of dark accumulated pchl_a into chl_a. The minimum level of potent singlet oxygen generator in high light condition will minimize the Pchl_a derived singlet oxygen-induced oxidative stress in plants.

Chlorophyll degradation generally takes place during senescence. The presence of photodynamic intermediates in the pathway need to be rapidly converted into non-photodynamic form. Therefore, chlorophyll degradation pathway is tightly regulated to prevent the catabolic intermediate induced formation of singlet oxygen. Degradation of chlorophyll molecule majorly involves the removal of phytol tail and magnesium ion. It is followed by the oxygenic opening of the macrocyclic chlorine ring which is mediated by NADPH dependent Pheophorbide a oxygenase (PAO). It catalyzes the conversion of photodynamic green-colored closed tetrapyrrole pheophorbide a into red colored open chain tetrapyrrole called red chlorophyll catabolite (RCC). In this case, both the intermediates formed are photosensitizers. The conversion of red chlorophyll catabolite into non-fluorescent chlorophyll catabolite (nFCCs) is mediated by Red chlorophyll catabolite reductase (RCCR). Together, PAO and RCCR, forms a ternary complex with the pheophorbide a and they convert it into colorless non-photodynamic intermediate nFCCs, that are exported to the vacuole for further degradation. In the present study, the role of PAO, as well as RCCR, is studied by using the double overexpressor AtPAO and AtRCCR in *Arabidopsis*. Under high light stress, it is assumed that the overexpression of PAO and RCCR will enable the plant to tolerate the stress by decreasing the accumulation of photodynamic intermediates, pheophorbide a and red chlorophyll catabolite.

In this study, we present a different aspect to reduce ¹O₂ mediated cytotoxic damage. It involves reducing the accumulation of photosensitive chlorophyll metabolic intermediates by overexpressing enzymes of the same pathway that convert them into a non-photosensitive compound. Hence, by reducing the accumulation of potential singlet oxygen generators, a plant system can be established where a reduction in singlet oxygen production will not only protect plants from toxic effects of singlet oxygen but also will enable plants to tolerate photooxidative stress.

To implement the above strategy, the transgenic plants previously generated in our laboratory were treated with light to increase or minimize the generation of singlet oxygen via type II photosensitization reactions of chlorophyll anabolic or catabolic products.

Objectives

1. To characterize chlorophyll biosynthetic mutant of Protochlorophyllide Oxidoreductase C (*porC-2*) and its overexpressor (*AtPORCx*) in *Arabidopsis thaliana*.
2. To study the impact of light stress on photosynthetic efficiency, singlet oxygen production, and cell death mechanism in the above chlorophyll biosynthetic mutant and its overexpressor.
3. To characterize Chlorophyll catabolic mutant of Pheophorbide a Oxygenase (*pao*) and double overexpressor of Pheophorbide a Oxygenase C (PAO) + Red Chlorophyll Catabolite Reductase (RCCR) (*AtPAOx/AtRCCRx*) in *Arabidopsis thaliana*.
4. To study the impact of high light stress on photosynthetic efficiency, singlet oxygen production, and cell death mechanism in the above chlorophyll catabolic mutants and their overexpressors.

Review of literature

Photosynthesis is an indispensable process for survival on Earth. It utilizes solar energy to convert inert inorganic components into utilizable biochemical energy, which is necessary for nearly all forms of life to thrive. Oxygen is produced as a byproduct, whereas carbohydrates are produced to carry out metabolic processes in photosynthesizing organisms. The rise in oxygen level in the primitive reduced atmosphere of earth paved the way for the evolution of advanced /complex forms of life. However, living in an oxygen-rich world also increases the risk of oxidative stress. Molecular oxygen in its ground (Triplet) state is kinetically slow. The parallel spin of two unpaired electrons in the outermost orbit restrain oxygen molecule from interacting with other molecules. However, the spin restriction can be removed by applying energy, which is enough to change the spin of one of the electrons. The antiparallel spin of electrons in the outermost orbital of excited oxygen creates highly reactive singlet oxygen. In plants, chloroplasts serve as the major source of singlet oxygen in response to photooxidative stress (Rebeiz et al. 1988; Triantaphylides et al. 2008a). It readily oxidizes biologically significant molecules and renders them non-functional and cause cytotoxic damage. Exposure to extreme environmental fluctuation results in a rapid accumulation of singlet oxygen. When the damage is beyond repair, it induces the expression of a distinct set of genes that lead the cell towards programmed cell death (Gutiérrez et al. 2011).

Singlet oxygen production in plants.

In a plant cell, the impact of oxidative stress induced by singlet oxygen is greatly affected by the site of its production. Singlet oxygen cannot diffuse to long-distance (Gorman and Rodgers 1992), and its life span is restricted to 200 ns (Sies and Menck 1992). The location of singlet oxygen generation becomes the primary target of $^1\text{O}_2$ -mediated oxidation events. ROS like hydrogen peroxide, superoxide are formed by transfer of electrons, whereas singlet oxygen is produced by the transfer of energy. Therefore, the production of singlet oxygen primarily takes place in sites where energy transfer events are prominent. During

photosynthesis, where solar energy is absorbed by the chlorophylls, and its derivative can induce the formation of singlet oxygen.

Reaction center and antenna complex

Chlorophyll pigment absorbs light and converts solar energy into electrical energy by charge separation. It is a tetrapyrrole pigment with a central magnesium ion and a phytol tail. The presence of conjugated double bonds in the chlorophyll molecule allows it to absorb light energy. Therefore, it is present in the light-harvesting complex as well as in the reaction center. Upon receiving photons, the chlorophyll molecule is excited from a lower energy ground state to higher energy singlet state. The excited chlorophyll molecules at the antenna complex transfer their energy to the adjacent chlorophyll molecule by resonance and return to its ground state. The subsequent transfer of energy within the antenna ultimately reaches chlorophyll *a* in the P680 reaction center. Pheophytin (Pheo) is the intermediary acceptor in photosystem II. It receives electrons from excited $p680^*$ at Photosystem II to form ion-radical pair $P680^+Pheo^-$. Since $Pheo^-$ is unstable, it readily gives its electron to the first stable plastoquinone electron acceptor Q_A . After gaining an electron, the reduced Q_A^- transfer it to the second plastoquinone electron acceptor Q_B molecule located at D1 protein within the photosystem II. Another light reaction results in the formation of Q_B^{2-} which utilize 2 protons and a bicarbonate ion (Stemler 1973; Shevela et al. 2012) to give rise to Q_BH_2 (Plastoquinol). This mobile electron carrier leaves D1 protein to transfer electrons to the cytochrome b_6f complex which not only take part in subsequent transfer of electrons to PSI but also result into formation of a proton gradient across thylakoid lumen and stroma. Establishment of a proton motive force and activation of ATP Synthase in the thylakoid membrane synthesize ATP by utilizing ADP and inorganic phosphate.

When plants receive light energy, which is more than their requirement for photochemistry, the over-reduction of the electron transport chain takes place. The unavailability of oxidized Q_B favors charge recombination reactions (Vass 2011) between $p680$ and pheophytin, giving rise to triplet $^3p680^*$ (Aro et al. 1993). This energy transfer between an excited triplet $^3p680^*$ to molecular oxygen results into

production of singlet oxygen (Shook, F. C., & Abakerli 1984). In the light-harvesting complex where the chlorophyll molecules are in abundance, the proximity with zeaxanthin or other carotenoids quenches the energy excitation energy in the form of heat (Baroli et al. 2000). The distance between the excited state of chlorophyll and carotenoid is directly related to efficient heat dissipation. However, in the reaction center, the distance between the excited chlorophyll molecule and carotenoids is too large to allow the quenching, which eventually leads to the formation of singlet oxygen in the reaction center. The distant Carotenoid present in the reaction center reacts with the singlet oxygen produced from the $^3\text{p680}^*$. And thus, prevent singlet oxygen-mediated damage to D1 protein.

Cyt b6f complex

Experiments done on sub thylakoid preparations suggested that electron transport activity of isolated PS II core complex was majorly affected when irradiated with bright light. The increase rate of PS II photoinactivation was prominent due to the inclusion of cytochrome b6/f, whereas, addition PSI to the sample had no effect on the photoinactivation. Consequently, detection of singlet oxygen by chemical trapping method indicate the role of and cytochrome b6/f as a photosensitizer (Suh et al. 2000). However, to protect itself from the oxidative effects of singlet oxygen, it requires a neighboring beta- carotene to quench the singlet oxygen produced in light (StroebeI et al. 2003). Contribution of cytochrome b6/f in singlet oxygen generation is minor in comparison to PSII-mediated singlet oxygen production.

Chlorophyll biosynthetic intermediates

Chlorophyll biosynthesis is a tightly regulated process that takes place in the stroma as well as in the thylakoid membrane. All the enzymes that participate in the biosynthesis pathway are encoded by nuclear genes. Their synthesis takes place in the cytoplasm, and after post-translational modification, they are transported to their respective site of action. The whole process of chlorophyll biosynthesis can be subdivided into the following parts (i) formation of 5-aminolevulinic acid (ALA) (ii) synthesis of protoporphyrin IX from ALA (iii) formation of chlorophyll. Early steps of the chlorophyll biosynthesis pathway take place in the stroma, but the later steps are carried out in the thylakoid membrane

due to the hydrophobic nature of the enzymes catalyzing the process (Mohapatra and Tripathy 2007). Among the various chlorophyll biosynthetic intermediates, membrane-bound Protoporphyrin IX, Mg-protoporphyrin IX, and Protochlorophyllide are photodynamic. When illuminated, similar to chlorophyll molecule, these intermediates absorb energy and gets excited to their respective higher energy state and revert to the ground state by transferring energy to the molecular oxygen which leads to singlet oxygen production via type II photosensitization reaction (Foote 1991) and induces oxidative stress in plants (Chakraborty and Tripathy 1992).

Aminolevulinic acid (ALA)

5- Aminolevulinic acid (ALA) is a natural nonproteinogenic metabolite which is the common precursor to all the tetrapyrroles such as chlorophyll, sirohaem, haem, and phytychromobilins. Since most of the chlorophyll biosynthetic intermediates are photodynamic, therefore their production is strictly regulated to reduce the formation of light-induced singlet oxygen. Therefore, the synthesis of ALA serves as the rate-determining/limiting step for the tetrapyrrole biosynthesis.

Exogenous application of ALA on cucumber seedlings inhibited the PSII-dependent oxygen evolution by 60% within 30 minutes of exposure to sunlight. Consequently, in a different experiment, ALA treated plants were dark-adapted after illumination for 15 min, to analyze the reversibility of the photodynamic stress. Chlorophyll fluorescence induction kinetics of dark-adapted samples showed 50% decline in variable fluorescence, which declined further irrespective of the time. After, 12 h of dark incubation, plants exhibited visible damage in the form of necrotic lesions. It was concluded that the photodynamic damage induced by ALA could not be reversed by putting plants in the dark. The elicitation of singlet oxygen, within 15 min of light exposure is sufficient to induce permanent damage to plants (Tripathy and Chakraborty 1991; Chakraborty and Tripathy 1992).

Photodynamic properties of ALA are also utilized in the animal system to selectively target cancerous and malignant tissues. In animals, ALA is synthesized in mitochondria from succinyl Co-A and Glycine. Further conversion into haem requires additional enzymes in a coordinated way to reduce the accumulation of

photodynamic intermediate Protoporphyrin IX. For therapeutic use, ALA is administered topically or systemically where it is metabolized into Protoporphyrin IX. Distinct characteristics of tumorous cells facilitate overaccumulation of PPIX. Site-specific irradiation activates photochemical production of singlet oxygen in the localized area of interest and induces photooxidative stress, ultimately leading to cell death (Muchowicz et al. 2011; Valdes et al. 2014).

Protoporphyrin IX

Protoporphyrin IX (PPIX) is a common precursor for both chlorophyll and heme biosynthesis. It is a heterocyclic tetrapyrrole which is capable of chelating metal transition metal to form metalloporphyrin. It is formed by oxidation of unstable Protoporphyrinogen IX by Protoporphyrinogen oxidase (PPOX). It requires flavin as a cofactor, and oxygen is used as a terminal electron acceptor (Poulson and Polglase 1974). It serves as the precursor of heme and mg protoporphyrin IX. External application of PPOX inhibitors such as AF-Na (Acifluorfen-Na) not only halts the chlorophyll and heme biosynthesis pathway but also result in an accumulation of photodynamic Protoporphyrin IX that absorb sunlight to give rise to singlet oxygen via type II photosensitization reaction. Induction of singlet oxygen burst impairs photosynthetic electron transport rate by damaging PSI and PSII activities (Tripathy et al. 2007).

In humans, the absence of functional PPOX gene leads to variegate porphyria, which is an autosomal dominant disease. Accumulation of PPIX causes extremely photosensitive skin, gallstones, and damage to the liver (Sachar et al. 2016). Exposure of sunlight leads to severe blistering due to excess production of singlet oxygen from the accumulated Protoporphyrin IX. However, the characteristic feature of PPIX to induce singlet oxygen production can be utilized for therapeutic purpose. Photodynamic therapy is a clinically approved procedure which is minimally invasive and selectively cytotoxic towards malignant cells. Recent studies have shown that encapsulation PPIX in Achieved Silica Nanoparticle (SiNPs) greatly increases its efficiency to destroy osteosarcoma (Makhadmeh and Abdul Aziz 2018).

Mg Protoporphyrin IX

Addition of Mg^{2+} to PPIX divert the tetrapyrrole biosynthesis pathways towards chlorophyll formation. The reaction is catalyzed by a multi-subunit Mg-

chelataze enzyme to form Mg-protoporphyrin (Mg-PPIX). The Mg-chelataze enzyme has three subunits (CHLI, CHLD, and CHLH) that take part in sequential ATP-dependent activation step followed by ATP-dependent chelation step. Another subunit has been identified as CHLM that encode methyltransferase enzyme that catalyzes the formation of Mg-protoporphyrin monomethyl ester (MPE). Seedlings grown in Norflurazon supplemented media showed ten times the accumulation of Mg-PPIX following ALA feeding compared to non-treated plants (Strand et al. 2003). Downregulation of nuclear photosynthetic genes in response to elevated Mg²⁺-PPIX level indicates its role in retrograde signaling (Pontier et al. 2007). However, subsequent reports were unable to confirm Mg²⁺-PPIX mediated regulation of gene expression, as supplementing ALA externally induced photosynthesis-related nuclear genes. Rather a prominent role of singlet oxygen as a signal was observed (Moulin et al. 2008).

Protochlorophyllide

The photosensitive intermediate Protochlorophyllide (Pchlde) is formed from Mg-PPIX monomethyl ester by the help of enzyme Mg-PPIX monomethyl ester cyclase. In angiosperms, the accumulation of Pchlde in dark halts the chlorophyll biosynthesis pathway by blocking ALA synthesis. The suspension of chlorophyll biosynthesis by feedback inhibition is a characteristic feature in higher plants. This efficient strategy is employed to reduce the damage that may occur due to the accumulation of unbound tetrapyrrole intermediates. Previous studies have shown the involvement of heme as an effector in regulating the negative feedback mechanism. Inactivation of heme degradation enzyme, heme oxygenase leads accumulation of heme, that downregulate not only ALA synthesis but also reduces the build-up of Pchlde (Muramoto et al. 1999). Conversely, by chelating unbound Fe²⁺/³⁺ by adding an iron chelator reduces heme level and result in upregulation of Pchlde (Duggan and Gassman 2008). Since the content of heme and chlorophyll cannot be the same, hence, Heme cannot be solely responsible for regulating the feedback machinery. Identification of *flu* mutant has paved a way to understand singlet oxygen-induced regulation of gene expression in *Arabidopsis* (Meskauskiene et al. 2001). The *fluorescent in blue light (flu)* mutant was identified from wildtype by irradiating the etiolated seedlings with blue fluorescent light. Emission of bright red fluorescence in the *flu* mutant was

observed due to the accumulation of pchl_{ide} in the dark. Upon illumination, activation of enzyme Protochlorophyllide oxidoreductase (POR) converts Pchl_{ide} into Chlorophyllide. In etiolated angiosperm seedlings, Pchl_{ide} is found in association with NADPH: POR in the prolamellar bodies (PLB). The decrease in Pchl_{ide} level release the block on ALA formation and thus the chlorophyll biosynthesis resume in light. When *flu* mutant seedlings were grown under continuous light, no difference in phenotype was observed. However, when etiolated *flu* mutant seedlings were shifted to light, it resulted in rapid photobleaching and ultimately followed by cellular death. External application of ALA on plants disrupts the feedback inhibition machinery. Excess ALA overproduces photodynamic tetrapyrroles that ultimately reaches a bottleneck at the light-dependent step. Due to limited availability of POR enzyme results into an accumulation of Pchl_{ide} and thus it induces a rapid burst of singlet oxygen in the chloroplast compartment.

External application of ALA induces overproduction of singlet oxygen in plants (Tripathy and Chakraborty 1991). Since it is the precursor of all the tetrapyrroles, its synthesis is tightly regulated by a negative feedback mechanism. But when it is externally applied to plants, it disrupts the feedback inhibition and results into overproduction of photosensitive intermediates and thus cause singlet oxygen-mediated oxidative stress. A genetic approach was made to screen out the additional regulators of tetrapyrrole synthesis to understand more about the regulation of ALA synthesis.

Chlorophyll catabolic intermediates

Chlorophyll degradation takes place during senescence, fruit ripening or due to exposure to extreme environmental fluctuations. During favorable conditions, chlorophyll is catabolized in a steady-state, but when plants are under stress, a large amount of chlorophyll is degraded in a short period. Similar to chlorophyll biosynthesis pathway, few chlorophyll catabolic intermediates are also photosensitizers. Hence, the chlorophyll degradation pathway is also tightly regulated by 6 enzymatic and 1 nonenzymatic reaction. It involves the sequential removal of phytol tail followed by the opening of the macrocyclic ring of chlorophyll, which is regarded as an important event in downstream processing of

the photosensitive chlorophyll breakdown products (Hörtensteiner and Kräutler 2011).

Pheophorbide a

The Chlorophyll degradation is initiated by chlorophyllase enzyme which removes the phytol tail from the chlorophyll to form green colored chlorophyllide. Mg-dechelating substance (MDS) removes the central magnesium ion from the chlorophyllide to form colorless pheophorbide a. Conversion of Pheophorbide, a to red chlorophyll catabolite, is catalyzed by an Iron-Rieske dependent monooxygenase, Pheophorbide *a* oxygenase that opens the oxygenic ring C4 and C5 position (Hirashima et al. 2009).

Earlier, it was proposed that in the absence of PaO activity will lead to inhibition of chlorophyll degradation pathway, and the plant will exhibit stay green phenotype. The *Arabidopsis* genome was analyzed to search for PAO-encoding gene having sequences homologs with the known iron-containing Rieske- type monooxygenase sequences. Three open reading frames were identified as- Tic-55, ACD1, and ACD1 like. Analysis of antisense *ACD1* transgenic revealed the role of ACD1 in PAO activity. Plants lacking PAO activity showed no phenotypic difference from the wild type plant. However, accumulated large amount of pheophorbide a when illuminated to normal light after five days of dark incubation followed by the death of plant due to photooxidative damage (Tanaka et al. 2003; Hirashima et al. 2009). Since pheophorbide a is a photosensitizer, its accumulation in *AsACD1* resulted into production of singlet oxygen which induces the photobleaching. Pheophorbide mediated singlet oxygen production is clinically utilized in photodynamic therapy as a photosensitizer to induce localized production of singlet oxygen for the treatment of cancer (Busch et al. 2009).

Red chlorophyll catabolite

Conversion of pheophorbide a into primary fluorescent chlorophyll catabolite was thought to be a major step in the degreening process involving primarily PAO enzyme. But the enzymatic reaction involved in the oxygenolytic opening of the macrocyclic ring has been characterized only partially. Studies done on *Chlorella protothecoides* speculated the role of a red-colored bilin pigment excreted by the alga when grown in a nitrogen-deficient, glucose-rich medium. Later experiments

involving isotope-labeled oxygen, ^{18}O showed the participation of a red-colored bilin derived intermediate (Curty et al. 1995). This compound was produced as a result of monooxygenase –catalyzed oxygenation, which suggested the involvement of C4/C5 double bond. Hydrolysis of epoxide followed by intramolecular ring arrangement resulted in the opening of the macrocyclic ring. For the opening of the ring by the mechanism above, it would require the addition of two atoms each of oxygen and hydrogen into the pheide a molecule. Hence, it was assumed that the conversion of pheide a to FCCs (Fluorescent chlorophyll catabolite) requires two enzymatic steps (Rodoni et al. 1997). Later, a red-colored intermediate was identified as red chlorophyll catabolite (RCC) that acts as an immediate precursor of FCCs (Wüthrich et al. 2000). Further confirmation was done by chemical degradation of pheophorbide a (Krautler et al. 1997). RCC in the unbound form is a photosensitizer and induce the formation of singlet oxygen upon absorbing light. Also, it readily binds to PAO enzyme, thus preventing it from acting on the pheide a molecule. Therefore, a cytosolic reductase enzyme, Red chlorophyll catabolite reductase (RCCR) directly reduces the bound RCC and sets free the primary fluorescent chlorophyll catabolite (pFCC). Formation of blue fluorescent chlorophyll catabolite from pheide a require cooperation between PAO and RCC reductase to reduce the photodynamic RCC intermediate into FCC. This transformation also requires reduced ferredoxin and stroma proteins.

Similar to chlorophyll biosynthetic intermediates, degradation products of chlorophyll are also photodynamic. Therefore, their biosynthesis and breakdown processes are highly compartmentalized and tightly regulated. Accumulation of chlorophyll degradation derivatives can induce cell death as the plant's exhibit induction of defenses in pathogen resistance. Treating plants with *Pseudomonas syringae* effector, Coronatine, induced lesion mimic phenotype in light-exposed plants. However, complete suppression in cell death was observed in plants kept in the dark.

Singlet oxygen-induced oxidative stress

Plants utilize solar energy to fix atmospheric carbon dioxide by the process of photosynthesis. The absorption of solar energy is carried out by chlorophyll and its accessory pigments such as Carotenoids and phycobilins. Together they

efficiently absorb light energy to drive photochemical reactions. However, when plants are exposed to saturating light intensities, the excess excitation energy is also absorbed by the pigments, and they get excited to their triplet state. Interaction with molecular oxygen results into formation of singlet oxygen. Since singlet oxygen has a short life span and low diffusion rate, the major damage due to singlet oxygen is caused at the site of its maximum production.

Singlet oxygen-induced lipid peroxidation.

During chlorophyll biosynthesis, the intermediates from Protoporphyrin IX onwards are hydrophobic. Therefore they are found embedded in the thylakoid membrane (Mohapatra and Tripathy 2002, 2007). Their ability to absorb energy allows them to convert molecular oxygen into singlet oxygen. When these intermediates are accumulated in response to external application of ALA, rapid burst of singlet oxygen primarily oxidizes the polyunsaturated fatty acids to lipid hydroperoxide that further breaks down into several products of lipid peroxidation. However, the addition of singlet oxygen quenchers such as histidine and sodium azide protected isolated chloroplasts from ALA-induced oxidative stress as analyzed by measuring the Thiobarbituric acid reactive substances (TBARS) (Chakraborty and Tripathy 1991). Lipid peroxidation is mediated by two nonenzymatic reactions that ultimately produce a specific pattern of PUFA oxidation product (Stratton and Liebler 1997). Type I reactions involve free radicals with high redox potential like hydroxyl radicals, organic oxyl, and peroxy radicals. Initiation of type I reaction is mediated by free radicals that have high redox potential. However, free radicals such as superoxide ion and hydrogen peroxide are not sufficient to readily oxidize the PUFA. Instead, they require a transition metal ion, Fe^{2+} to mediate the formation of hydroxyl radical by a non-enzymatic Fenton reaction. Type II reactions are mediated by singlet oxygen. Production of singlet oxygen by the membrane-bound chlorophyll intermediates primarily targets α -Linolenic acid, which is present in the majority in the chloroplast membrane (Murakami et al. 2002). In plant system, lipid peroxidation is considered one of the markers to study oxidative stress (Mueller et al. 2006) and the resulting peroxidation products have been involved in regulating various developmental processes (Mueller et al. 2006).

To discriminate between free radical and singlet, oxygen-induced lipid peroxidation in plants, quantification of oxidized hydroxyl fatty acids were analyzed with HPLC-tandem mass spectrometry (MS/MS) after treating plants with hydrogen peroxide and methylene blue to trigger free radical (FR) and singlet oxygen production respectively. Differential oxidation of hydroperoxy PUFAs, linoleic (18:2) acid and linolenic acid (18:3) was determined by HPLC- negative electrospray ionization-MS/MS. Hydroxy fatty acid isomer specific to singlet oxygen was exclusively enhanced in response to methylene blue in the photosynthetic tissues. Further, exposure of singlet oxygen-sensitive double mutants *vte1 npq* with photooxidative conditions significantly increased the accumulation of singlet oxygen specific 10-HOTE and 15-HOTE hydroxyl fatty acid isomer and intensified cell death progression (Triantaphylides et al. 2008b). In a different experiment, leakage of plastidic protein into the cytosol was observed in response to singlet oxygen stress. In flu seedlings, the loss of chloroplast integrity as a result of singlet mediated lipid peroxidation resulted in the release of chloroplast protein. Smaller subunit of Rubisco (SSU) was tagged with a green fluorescent protein to study its localization in response to singlet oxygen-generating conditions. When WT plants were kept in high light ($270\mu\text{mol photons m}^{-2}\text{s}^{-1}$), for a different period of time, loss in plastid integrity was visualized by a fluorescent microscope. The evident release of plastidic SSU-GFP in the cytoplasm 96 h of high light stress indicate singlet oxygen-mediated disintegration of plastidic membrane increase protein leakage into the cytoplasm (Kim et al. 2012).

Degradation of protein in response to singlet oxygen stress

Exposure of saturating light intensities over reduce the electron transport chain and favors the formation of excited chlorophyll molecules. Unable to transfer their energy into photochemical reactions, these excited chlorophyll molecules interact with molecular oxygen to form singlet oxygen. Presence of carotenoids in the antenna system prevents the formation of singlet oxygen by absorbing energy and dissipating it as heat. But in the reaction center, presence of 2 β -carotene molecules are not enough to prevent singlet oxygen formation. Since the Vanderwal distance between the reaction center chlorophyll molecule and the b

carotene molecule is large, it prohibits the transfer of energy from an excited reaction center molecule to the beta carotene (Loll et al. 2005).

When plants are exposed to high light, the overproduction of singlet oxygen in the reaction center oxidizes D1 protein and initiate its degradation. Since D1 protein allows the reduction of P680⁺ through its Tyr-Z residue present at 161 position abstracts an electron from the water evolution complex. In the absence of functional D1 protein, photoinhibition of PSII results into decrease in the electron transfer efficiency of plants. Furthermore, studies have shown that the excess of active oxygen in the vicinity of PSII hampers the D1 repair machinery, thereby causing permanent damage to the electron transport chain. Studies done on *Arabidopsis* cell suspension culture explained that the addition of singlet oxygen generators such as methyl viologen, rose Bengal, and indigo carmine oxidizes D1 protein of the PSII reaction center. Even the low concentration of the photosensitizers was capable of inducing protein degradation in all the illuminated samples (Gutiérrez et al. 2014).

DNA fragmentation

Overaccumulation of singlet oxygen is known to cause programmed cell death in plants (op den Camp 2003). In animal cells, a series of biochemical and molecular changes precede apoptosis. The major events include cell shrinkage, loss of membrane integrity, leakage of cytochrome c, membrane blebbing, chromatin condensation, and fragmentation of chromosomal DNA. Activation of indigenous endonucleases cleaves DNA at specific sites to form different sizes of degraded DNA. Resolving those fragments on Agarose gel exhibit a ladder-like pattern corresponding to the DNA fragments. Detection of these fragments by in situ labeling methods can serve as a marker of apoptosis. Terminal deoxynucleotidyl transferase BrdUTP nick end labeling assay (TUNEL) utilize Terminal deoxynucleotidyl transferase enzyme to incorporate Br-labelled dUTP in a template-independent manner. Incubation of the labeled DNA with a fluorophore-conjugated antibody specific to Br-dUTP provide an accurate measure to check free 3'OH ends generated in response to singlet oxygen-induced oxidative stress (Ambastha et al. 2017).

Role of singlet oxygen in programmed cell death

Singlet oxygen production in plants and animals in response to stress conditions is well documented. In plants, exposure to saturating light intensity enhances singlet oxygen production in chloroplasts as a result of absorption of excess excitation energy, which cannot be utilized in photochemistry (Niyogi 2002). However, the induction of the cell death pathway in response to pathogen infection is regarded as a controlled hypersensitive reaction to restrict the invasion of the pathogen and is described as an important element of their defense machinery against the pathogen (León and Montesano 2013).

Irradiating *flu* seedlings after dark incubation induces phenotypic alterations as observed by necrotic lesions followed by cell death. However, in wild type plants, the intensity of light, the duration of stress, and ultimately, the level of singlet oxygen determines the fate of the cell. Experiments were conducted on *flu* mutant to identify second-site mutations that could negate the cytotoxic effect induced by singlet oxygen. It was revealed that a plastid protein EXECUTOR 1 (EX1), regulate the singlet oxygen-induced retrograde signaling (Wagner et al. 2004). Double mutants of *executor1/flu* accumulated Pchlide similar to *flu* mutant when kept in the dark. However, upon reillumination, the double mutant does not exhibit any necrotic patches, unlike *flu* mutant, which showed visible symptoms of photobleaching. In a different experiment, plants were treated with DCMU under high light conditions generate singlet oxygen. Leaves from the plants were floated onto different concentrations of DCMU. Analysis of cell death was done by checking the electrolytic leakage from the treated vs. control leaves with respect of time. Mutation in the Executor 1 protein abrogated singlet oxygen-induced cell damage and cell death. It was concluded that the presence of EXECUTOR 1 is required for the induction of singlet oxygen-induced response (Wagner et al. 2004). Another nuclear-encoded protein is identified as EXECUTOR 2, which, along with EX1, play a role in regulating downstream signaling initiated by singlet oxygen (Lee et al. 2007). Genes expressed in response to singlet oxygen has been identified by transcriptome profiling (Ramel et al. 2013). Among the upregulated gene, OXI 1 kinase was identified as one of the genes getting upregulated in response to singlet oxygen-induced cell death. OXI 1 kinase is a serine-threonine kinase which was known to regulate ROS influenced developmental processes. Strong induction of OXI 1 kinase mRNA

transcript was observed in the conditional *chlorina 1* mutant in response to high light exposure. A null mutant of *oxil* exhibited a drastic decrease in the extent singlet oxygen-induced photooxidative damage and thus, a significant reduction in plant cell death. Similar to the Executor proteins studied previously, OXI1 also play a role in regulating the retrograde signaling associated with singlet oxygen (Shumbe et al. 2016a). However, the gene expression profile studied in *oxil*, and *chl1* mutants seem to work independently of executor proteins. Another study on the *Arabidopsis* cell suspension culture showed that induction of singlet oxygen genes in response to a photosensitizer rose Bengal is independent of executor proteins. These experiments suggest that $^1\text{O}_2$ mediated downstream signaling to modulate gene expression is regulated by more than one intermediate signaling regulators that work independently of each other. It is speculated that the different site of singlet oxygen generation may play a role in defining the $^1\text{O}_2$ regulatory network within a cell. Moreover, the involvement of intermediate signaling molecules such as beta cyclocitral and dihydroactinidiolide cannot be overlooked (D'Alessandro and Havaux 2019).

Manipulating chlorophyll metabolic pathway to reduce singlet oxygen-induced damage

Chlorophyll biosynthesis and degradation pathways are strictly regulated to prevent the accumulation of photodynamic intermediates. The presence of conjugated bonds within their structure allows them to absorb light energy. However, in the absence of a reaction center molecule in their vicinity, the excess absorbed energy cannot be used to drive photochemical reactions. Instead, interaction with nearly available molecular oxygen gives rise to active singlet oxygen. Overproduction of singlet oxygen in response to stress is correlated with the accumulation of photodynamic chlorophyll intermediates and its derivatives. Strategies can be employed to reduce their accumulation by targeting an enzyme that catabolizes them into their nonphotodynamic forms without altering the pathway.

In the chlorophyll biosynthesis pathway, PORC enzyme plays a prominent role in converting dark accumulated Pchl_{id} into chl_{id}.

Protochlorophyllide oxidoreductase (POR)

In higher plants, chlorophyll biosynthesis reaches a checkpoint during the synthesis of protochlorophyllide (Pchl_{id}). The accumulation of Pchl_{id} in dark initiate a feedback signal to the precursor ALA to reduce the biosynthesis process. At the checkpoint, a second regulation was done by light-dependent Protochlorophyllide oxidoreductase. In the chlorophyll biosynthesis pathway, this step is the only light-dependent step that requires photoactivation of POR enzyme and, NADPH as a cofactor to donate electron during the reduction of Pchl_{id}. Together, POR:Pchl_{id}: NADPH form a ternary complex and accumulate in the prolamellar bodies (PLBs), formed from the convoluted membrane to form a crystalline structure in the etioplasts of the dark-grown seedlings (Dehesh and Ryberg 1985). It specifically adds two hydrogen atoms at C17 and C18 position on the D-ring of protochlorophyllide. NADPH: Pchl_{id} reductase (E.C.1.3.1.33) is a nuclear-encoded protein localized in the chloroplast envelop membrane. Multiple forms of POR are synthesized in the cytosol as large precursors (pPORs) that are later transported to chloroplast after post-translational modification. Association of mediator protein assists in the translocation of the mature protein to the chloroplast. Suppression in the activity of protein which interacts during POR import resulted in blockage of POR transport across the chloroplast and resulted in accumulation of Pchl_{id} and thus result into formation of Pchl_{id} derived 102 (Reinbothe et al. 2015).

POR proteins are members of the RED (Reductase, Epimerase, Dehydrogenase) superfamily that is involved in NADP(H) or NAD(H) dependent reactions (Wilks and Timko). Analysis of the CD spectra of POR showed the relative amount of the secondary structures in the POR protein. It was estimated that POR enzyme carries 13% alpha-helix, 19 % beta-sheet, an approximate of 20 % turn and 28 % random coil. It is speculated that it is anchored to the hydrophobic membrane using a beta-sheet or alpha helix carrying a tryptophan residue. However, the presence of a hydrophobic loop can also involve in membrane anchorage. Furthermore, experiments were conducted to study the catalytic activity of the enzyme. Clustered charge to alanine scanning mutagenesis study revealed that out of the 37 mutants enzymes only 5 retained their enzymatic activity, 14 were catalytically inactivated, and the rest of them showed altered

enzymatic activity (Dahlin et al. 2002). Mutation in the beta-sheets of the protein structure negatively affects the enzymatic activity. On the contrary, no difference in the enzymatic activity was observed when the mutation was in the alpha helix. To study the involvement of amino acid in protein folding and membrane anchorage, replacement of the charged amino acid at N and C terminal region of the protein showed alterations in the protein assembly. Conversely, a mutation in the central core of protein greatly reduces its attachment with the thylakoid membrane (Dahlin et al. 2002).

In the model plant *Arabidopsis*, multiple isoforms of POR exist. Namely, POR A, POR B, and POR C. In the etiolated seedlings, POR A take part in the greening of the leaves. However, its mRNA decreased drastically afterward. *Arabidopsis* WT plants, when grown under controlled far-red light, exhibited similar growth as with the plants grown under white light. However, the far-red light seedlings were yellow in color due to limited POR A indicate direct involvement of POR A in the greening process (Sperling et al. 1997). POR B mRNA transcripts were present in etiolated and green seedlings (Armstrong et al. 1995a). Although both POR B and PORC mRNA are influenced with diurnal fluctuations, but only POR B mRNA exhibited circadian regulations (Su et al. 2001).

POR enzymes are highly evolutionary conserved as they show more than 74% amino acid sequence similarity. Variation among the POR sequences can be attributed by N-terminal transit peptide. Sequence alignment studies between PORC and previously identified POR A and POR B showed 82.8 % and 83.2 % aminoacid similarity. However, analysis of the N-terminal of the POR C protein shows divergence from the POR A and POR B sequences. Furthermore, phylogenetic analysis of the POR protein to understand its evolutionary relationship indicated that PORC diverges early, whereas POR A and POR B are recent (Oosawa et al. 2000).

In rice, analysis of the OsPORA function was studied in *faded green leaf* mutant that exhibits severe necrotic lesions and variegation due to a mutation in the PORA gene. Accumulation of Pchl_{ide} also induces phototoxicity in the mutant. By complementing the function of OsPORA by OsPORB rescued the lesion mimic phenotype in the *fgl* mutant (Kwon et al. 2017). Similarly,

overexpression of ZmPORB in maize plant increased the Tocopherol content in the leaves and kernels (Zhan et al. 2019). Overexpression of POR enzymes can provide an efficient solution to prevent the accumulation of Pchl_a derived singlet oxygen production and prevent oxidative stress conditions in the high amplitude of light.

Pheophorbide a Oxygenase (PAO)

Chlorophyll degradation is one of the events that take place during senescence. In plants, chlorophyll is degraded in specialized plastids, gerontoplast. The chlorophyll degradation process is also regulated by a number of enzymes as similar to chlorophyll biosynthesis; the chlorophyll catabolic intermediates are also photosensitive. Major events during chlorophyll degradation involve removal of phytol tail and central Mg²⁺ ion, breaking of the chlorine ring and transport of the non-fluorescent catabolite to the vacuole for further degradation. The first step in the Chl degradation involves the conversion of Chl b into Chl a by Chl b reductase and 7-hydroxymethyl Chl reductase (Hörtensteiner et al. 2002). Hence it is the Chl a that participate in the Chl catabolic pathway. The removal of phytol tail from the porphyrin ring is mediated by Chlorophyllase, to form chlorophyllide a. Magnesium ion is removed by Mg-dechelating substance to form a pheophorbide a. This green-colored pigment is photodynamic as described above. Its conversion is regulated by a Fe-dependent monooxygenase that requires NADPH and ferredoxin to produce red chlorophyll catabolite (Curty et al. 1995). Pheophorbide a oxygenase is a nuclear-encoded membrane-localized Rieske-type-iron-sulphur-cluster containing enzyme. To study the biochemical features of the enzyme, several attempts were made to purify the PAO protein by using the classical approach were futile. Functional genomics approach was utilized to identify putative candidate genes that exhibit PAO like activity. In *Arabidopsis*, Accelerated cell death 1 has been identified (At3g44880), that showed PAO like activity when cloned in *E.coli* (Pruzinska et al. 2003). Earlier it was assumed that by reducing the activity of the chlorophyll degrading enzyme, the chlorophyll degradation process can be abrogated and thus the plant will stay green forever. On the contrary, the accumulation of pheophorbide a in the antisense ACD lines induced severe photobleaching and oxidative stress in plants (Tanaka et al. 2003).

Similarly, in maize, its homologous gene was identified as lethal leaf spot 1. The *lls1* mutant exhibited an autonomous induction of necrotic lesions that induced programmed cell death in the leaves (Gray et al. 1997).

PAO catalyze the oxygenic ring-opening of the pheophorbide a between C4 and C5 (Hörtensteiner et al. 2002). Pheophorbide b present nearby inhibit the enzyme activity in a competitive manner (Hörtensteiner et al. 1995). Presence of 2 transmembrane domain in its C-terminal allow it to anchor to the inner membrane of the chloroplast membrane.

Red chlorophyll catabolite reductase

The RCC formed by the action of pheophorbide a Oxygenase on the green-colored pheophorbide a, inhibit the action of PAO enzyme by strongly binding to it. Therefore, the existence of another enzyme was speculated (Mach et al. 2001). A cytosolic RCC reductase bind to the PAO: RCC complex and release the non-fluorescent chlorophyll catabolite for further degradation (Rodoni et al. 1997). Crystal structure analysis speculated the significant role of glutamic acid 154 and aspartic acid 291 in regulating the substrate binding and catalytic site on ACD2. In *Arabidopsis*, Accelerated cell death 2 is identical to RCCR. In-plant cell, the ACD2 is localized in the chloroplasts of the mature leaves. In the early stage of development, ACD2 is present in both chloroplasts and mitochondria. The *acd2* mutant exhibited runaway cell death phenotype due to limited RCCR enzyme. To further elucidate that the necrotic lesions are formed because of accumulation of RCC, exogenous application of Chl biosynthetic photodynamic intermediate PPIX induced apoptotic like events in a light-dependent manner (Yao and Greenberg 2006). Similarly, overproduction of ACD2 reduced the pathogen-induced disease symptoms and cell death upon infection with virulent *P.syringae* (Mach et al. 2001).

Materials and Methods

Surface sterilization of *Arabidopsis* seeds

50-60 *Arabidopsis* seeds were soaked in double-distilled water and kept in 4°C for stratification. After 48 h, seeds were sterilized with 2 ml of sterilization solution (2% Sodium hypochlorite with 1µl/ml of 20% Triton X-100) in culture hood. Seeds were gently mixed by inverting the centrifuge tube for 10-15 min. Before plating the seeds on MS plates, the sterilization solution is removed by 5 times washing with distilled water. Seeds were germinated in half-strength MS media pH 5.7.

General sterilization procedures

Culture media, glassware, and tissue culture tools were sterilized by autoclaving at 121 °C and 15lb/inch² for 15 min.

Nutrient media

Half strength MS media (1.1 g) is added to half a liter of double-distilled water. The pH is maintained by adding 1M-KOH to make MS plates. The media is solidified by adding 0.8% agar-agar.

Table-1 Composition of the GM medium (Gamborg et al. 1968)

Constituents	Concentration
0.5X MS salt with macro-and micronutrients, Vitamins (Sigma)	2.2 g/L
1% Sucrose	10 g/L
0.8 % Agar-agar	8 g/L

Table-2 List of various specific chemical used

Material	Source
----------	--------

FDA (Fluorescein diacetate)	Calbiochem
DAPI (4',6-diamidino-2-phenylindole)	Invitrogen, Eugene, Oregon, USA
Evan's blue	HIMEDIA
Cellulase R-10	Yakult, Minatoku, Tokyo, Japan
Macerozyme R-10	Yakult, Minatoku, Tokyo, Japan
SOSG	Molecular Probes, Thermo Fisher Scientific
General chemicals	Amersham, Biorad, Qualigen, Sigma, SRL

Table-3 Plant materials and their sources.

Plant	Specification	Source
<i>Arabidopsis</i> (wild type)	<i>Arabidopsis thaliana</i> (Col-0)	Delhi University (South campus)
<i>Arabidopsis</i> (<i>porc2</i> mutant)	<i>Arabidopsis thaliana</i> (Col-0) POR C Mutant having T-DNA insertion in the fourth exon of PORC, (Masuda et al., 2003)	Received with thanks from Prof. T. Masuda. Graduate School of Bioscience and Biotechnology, Tokyo Institute of Technology, 4259 Nagatsuta, Midori-Ku, Yokohama, 226-8501 Japan.

<i>Arabidopsis</i> (PORC overexpressor)	<i>Arabidopsis thaliana</i> (Col-0) over expressing PORC, Line T-13. (Pattanayak and Tripathy)	Transgenic developed at Prof. B.C.Tripathy's lab, SLS, JNU, New Delhi, 110067, India
<i>Arabidopsis</i> (<i>AtPaOx/RCCRx</i> overexpressor)	<i>Arabidopsis thaliana</i> (Col-0) over expressing At PAO/At RCCR, Line-D26	Transgenic developed at Prof. B.C.Tripathy's lab, SLS, JNU, New Delhi, 110067, India
<i>Arabidopsis</i> (<i>AtPaOx</i> overexpressor)	<i>Arabidopsis thaliana</i> (Col-0) over expressing At PAO Line-PS51	Transgenic developed at Prof. B.C.Tripathy's lab, SLS, JNU, New Delhi, 110067, India
<i>Arabidopsis</i> (<i>pao mutant</i>)	<i>Arabidopsis thaliana</i> (Col-0)	Received with thanks from Prof. Stefan Hortensteiner

Spectrophotometry:

Spectrophotometric studies were done on UV-160A (Shimadzu Corporation, Kyoto, Japan), Lambda-35 (Perkin Elmer) and Cary 300 Bio UV-visible (Varian) double-beam spectrophotometers.

Chlorophyll and carotenoid estimation:

Leaf tissue was homogenized in 90% chilled ammoniacal acetone (10 ml) in a pre-chilled mortar and pestle under safe green light. For preparing 90% ammoniacal acetone, 1 N ammonia solution (7.48 ml in 100 ml distilled water) was prepared and then was diluted ten times. This 0.1N ammonia solution was taken, and acetone was added to obtain 90% ammoniacal solution. Four replicates were taken for each batch. Homogenate was centrifuged at 10,000 rpm for 10 min at 4⁰C. The supernatant was taken for estimating Chl and carotenoids. Absorbance was recorded at 663 nm, 645 nm, and 470 nm. Reference cuvette contained 90% ammoniacal acetone. Chl was calculated as described by (Porra et al. 1989) and carotenoids were calculated as described by (Wellburn and Lichtenthaler 1984)

$$\text{Chl (a+b)} = (9.05 \times \lambda_{663} + 22.2 \times \lambda_{645}) V/W$$

$$\text{Carotenoids} = (1000 \times \lambda_{470} - \{3.27 \times \text{Chl a} - 1.04 \times \text{Chl b}\}/5) V/227 \times W$$

Pulse amplitude modulation (PAM) measurements

F_v/F_M , electron transport rate (ETR), quantum yield of photosystem II (yield), non-photochemical quenching (NPQ), and coefficient of photochemical quenching (qP), yield of non-regulated energy dissipation Y(NO) of high light treated and untreated plants were measured at room temperature by a Dual PAM-100 Chlorophyll fluorimeter (Walz, Germany). Plants were incubated in the dark for 20 min to relax all the reaction centers. Red actinic illumination (wavelength, 655nm) provided by five LEDs (H3000); (Stanley, Irvine, CA, USA) focused onto the leaf surface (79 mm²). Two other H-3000 LEDs that emit 650-nm pulses were used as measuring light. Leaf clip holder 2030-B, equipped with a micro quantum sensor, monitored photosynthetically active radiation. Chl fluorescence was detected by a photodiode (BYP 12; Siemens, Munich, Germany) that was shielded by a long-pass-far-red filter (RG9; Schott, Southbridge MA, USA) and a heat filter. The different photosynthetic parameters were calculated according to the equations mentioned below:

$$F_v/F_M = (F_M - F_0)/F_M$$

(F_v is the difference between maximum and minimum fluorescence)

$$\text{Yield} = (F_m' - F_t) / F_m'$$

(F_m' is the maximum fluorescence yield, when the sample is pre-illuminated, and F_t is the fluorescence yield at any given time).

$$q_P = (F_m' - F_t) / (F_m' - F_o)$$

(F_o is the minimum fluorescence of the dark-adapted leaves when all the reaction centers are open)

$$q_L = (F_m' - F_t) / (F_m' - F_o) \times F_o' / F$$

(F_m is the maximum fluorescence when all the reaction centers are closed)

$$\text{ETR} = \text{Yield} \times \text{PAR} \times 0.5 \times 0.84$$

(Yield is overall photochemical quantum yield; PAR is flux density of incident photochemically active radiation measured in $\mu\text{moles photons m}^{-2} \text{ s}^{-1}$; 0.5 factor is transport of one electron requires for absorption of two quanta, as two photosystems are involved; 0.84 is 84% of the incident quanta are absorbed by the leaf).

$$Y(\text{NPQ})$$

Quantum yield of regulated energy dissipation in PS II.

$$Y(\text{NPQ}) =$$

$$1 - Y(\text{II}) - 1 / (\text{NPQ} + 1 + q_L (F_m / F_o - 1))$$

$$Y(\text{NO})$$

Quantum yield of nonregulated energy dissipation in PS II.

$$Y(\text{NO}) = 1 / (\text{NPQ} + 1 + q_L (F_m / F_o - 1))$$

ALA treatment

1 mM aqueous ALA solution was used to spray on three-week-old pot grown *Arabidopsis* plants. Later, plants were covered with aluminum foil and kept in the dark for 12 hours to accumulate Pchl_a. Control plants were sprayed with distilled water.

Light treatment

After 12 h of dark incubation, ALA-treated and untreated plants were exposed to low light ($75 \mu\text{mol photons m}^{-2} \text{s}^{-1}$) for different time intervals.

Imaging PAM

After completion of light treatment, plants were again incubated in the dark for 20 min to open all the reaction centers. Images were captured from IMAGING PAM MAXI chlorophyll fluorometer (Walz, Germany) and the fluorescence parameters were calculated from ImagingWin software (Walz, Germany).

Chlorophyll fluorescence parameters such as the maximum quantum yield of PS II (F_v/F_m) was determined by the equation $F_v/F_m = (F_m - F_o) / F_m$ where F_o is the dark fluorescence yield, F_m is the maximum fluorescence yield and $(F_m - F_o)$ is the variable fluorescence (F_v). Maximum efficiency of the water diffusion-reaction is analyzed from the ratio of variable to minimum fluorescence yield (F_v / F_o). Other parameters such as Electron transport rate of photosystem II was calculated from the equation $\text{ETR (II)} = \phi \text{ PS II} \times \text{PAR} \times 0.5 \times 0.84$ where $\phi \text{ PS II}$ is effective PSII quantum yield (calculated by $(F'_m - F_t) / F'_m = \Delta F / F'_m$ where F'_m is referred as the maximum fluorescence yield when the samples are illuminated, and F_t is the fluorescence yield at any given time (t). PAR abbreviates for photosynthetically active radiation, 0.5 is the factor of the ratio of PS II and PS I (1:1), 0.84 is the value that correlates with the percentage of incident photons are absorbed by the leaf to drive photosynthesis. The nonphotochemical quenching of the maximum fluorescence was calculated by $(F_m - F'_m) / F'_m$. Quantum yield of nonregulated energy dissipation $Y(\text{NO})$ is calculated by the equation $1 / (\text{NPQ} + 1 + qL (F_m / F_o - 1))$, where qL represents the fraction of reaction centers that are open according to the lake model (Baker 2008).

Protein extraction

Leaves (100mg) were harvested and immediately frozen in liquid nitrogen and pulverized. Total protein was extracted in extraction buffer (0.1% Triton X-100, 0.1% SLS, 0.01 M EDTA, 0.01 M β -ME, 0.05 M Na_2HPO_4 , pH 7.0). The homogenates were centrifuged at 12,000 rpm for 30 min at 4°C. Protein concentrations of the supernatants were determined using the Bradford method (Bradford, 1976).

Catalase (CAT) activity (EC 1.11.1.6)

Three-week-old WT, PORCx and *porC-2* plants were grown under control light. 50 mg tissue was harvested, and their total protein was isolated in 50 mM phosphate buffer (pH 7), and its concentration was determined by Bradford assay (Bradford 1976). Catalase activity was measured by a UV double beam spectrophotometer at 250 nm by monitoring the consumption of H_2O_2 (Extinction coefficient= $39.4 \text{ mM}^{-1}\text{cm}^{-1}$) by the enzyme present in the protein extract with respect to time.

Ascorbate Peroxidase (APX) activity (EC 1.11.1.11)

The H_2O_2 dependent oxidation of ascorbate was determined at 290 nm using the extinction coefficient of ascorbate ($E=2.8 \text{ mM}^{-1}\text{cm}^{-1}$). The reaction mixture contained 10 mM ascorbic acid, 10 mM H_2O_2 and 40 microgram protein.

Protoplast Isolation

Protoplasts were isolated using Tape *Arabidopsis* method (Wu et al. 2009). Leaves (width: 2 cm, length: 5 cm in optimal light condition; width: 0.5 cm; length: 2.5 cm in low light conditions) were collected from 3 to 5-week-old plants grown under optimal light conditions. Selected leaves were used in a 'Tape-*Arabidopsis* Sandwich' experiment. The upper epidermal surface was stabilized by affixing a strip of Time tape while the lower epidermal surface was affixed to a strip of magic tape. The Magic tape was then carefully pulled away from the Time tape, peeling away the lower epidermal surface cell layer. The peeled leaves (7 to 10 optimal-light-growth leaves, about 1-2 g, up to 5 g), still adhering to the Time tape, were transferred to a Petri dish containing 10 mL of enzyme solution [1% cellulase

'Onozuka' R10 (Yakult, Tokyo, Japan), 0.25% macerozyme 'Onozuka' R10 (Yakult), 0.4 M mannitol, 10 mM CaCl₂, 20 mM KCl, 0.1% BSA and 20 mM MES, pH 5.7]. The leaves were gently shaken (40 rpm on a platform shaker) in light for 20 to 60 min until the protoplasts were released into the solution. The protoplasts were centrifuged at 100 × g for 3 min in an Eppendorf A-4-44 rotor, washed twice with 25 mL of pre-chilled modified W5 solution (154 mM NaCl, 125 mM CaCl₂, 5 mM KCl, 5 mM glucose, and 2 mM MES, pH 5.7) and incubated on ice for 30 min. During the incubation period, protoplasts were counted using a hemocytometer under a light microscope. The protoplasts were then centrifuged and resuspended in modified MMg solution (0.4 M mannitol, 15 mM MgCl₂, and 4 mM MES, pH 5.7) to a final concentration of 2 to 5 × 10⁵ cells/mL.

Singlet oxygen imaging by SOSG

For ¹O₂ detection, protoplasts were incubated with the SOSG (100 μM) in the dark for one hour, then washed with the protoplast suspension buffer and exposed to light for 30 min and visualized in Nikon-Ti-E microscope at 60x magnification. For staining whole leaf Plantlets, prior to the transfer and at the end of the treatment, were immersed and infiltrated in the dark under vacuum with a solution of 100 μM Singlet Oxygen Sensor Green[®] reagent (SOSG) (S36002, Invitrogen) in 50 mM phosphate potassium buffer (pH 7.5). Infiltrated plantlets were then placed again on control and treatment media for 30 minutes in the light before being photographed under the microscope.

Terminal deoxynucleotidyl transferase nick end labeling (TUNEL)

Assay

DNA nicks formed as a result of the initiation of PCD was visualized by TUNEL assay. Incorporation of deoxyuridine (BrdUTP) to the free 3'-OH in the DNA strand was detected by fluorophore-labeled antibody (Alexa-488) specific for BrdUTP. Addition of BrdUTP to the exposed 3'- hydroxyl end is catalyzed by Terminal deoxynucleotidyl transferase in a template-independent manner. Labeling of DNA nicks can be visualized by using excitation-emission spectra similar to fluorescein. Before DNA labeling, the protoplasts from the treated and untreated samples were washed with suspension buffer and immediately fixed with 2% paraformaldehyde and 2.5 % glutaraldehyde in 50mM sodium phosphate buffer (pH 7.2) for 1 h at 4°C. Fixed protoplasts were washed gently with 50 mM phosphate

buffer pH 7.2 and finally suspending in 1 ml phosphate buffer. To increase the permeability, protoplasts were sequentially dehydrated in an increasing gradient of alcohol (from 20% to 100%) for half an hour. Dehydrated protoplasts were finally incubated in 100% absolute alcohol at -20°C for 2 days. The treatment of protoplast with alcohol also removed the chlorophyll pigments making the protoplast colorless. The decolorized protoplasts were again rehydrated with 50mM phosphate buffer pH 7.0, and TUNEL assay was performed using APO-BrdU™ TUNEL Assay Kit (Invitrogen) according to the manufacturer's protocol. After TUNEL labeling, the protoplasts were counterstained with DAPI and observed under a fluorescent microscope to localize nucleus. Green fluorescence of Alexa-488 under blue filter marks the site at which TdT-mediated incorporation of fluorescein-labeled BrdUTP occurs during the fragmentation of the DNA.

Estimation of lipid peroxide

The level of lipid peroxidation products was estimated using 200 mg fresh tissue according to the method of (Hodges et al. 1999) and were expressed as thiobarbituric acid reactive substances (TBARS). Plant samples were extracted in 0.25% 2-thiobarbituric acid (TBA) in 10% TCA using a mortar and pestle. Contents were heated at 95°C for 30 minutes and the quickly cooled in an ice bath and centrifuged at 12,000 rpm for 10 min. The absorbance of the supernatant was read at 532 nm, and correction for unspecific turbidity was done by subtracting the absorbance of the same at 600 nm. The blank was 0.25% TBA in 10% TCA. The concentration of lipid peroxides, together with oxidatively modified proteins, were quantified and expressed as total TBARS in terms of nmol g⁻¹ fresh weight using an extinction coefficient of 155 nM⁻¹ cm⁻¹. TBARS are an index of lipid peroxidation. To increase the accuracy of determining TBA-MDA levels by correcting for compounds other than MDA, which absorb at 532 nm, subtraction of the absorbance at 532 nm of a solution containing plant extract incubated without TBA from an identical solution containing TBA was done. *Arabidopsis* WT and transgenic plants samples were homogenized in (i) -TBA solution comprised of 20 % (w/v) trichloroacetic acid (-TBA) or (ii) TBA solution containing the above plus 0.25% TBA (+TBA). Samples were then mixed vigorously, heated at 95°C in a water bath for 25 min, cooled, and centrifuged at 12,000 rpm for 10 min. Absorbances were read (Shimadzu, Japan) at

440 nm, 532 nm, and 600 nm. Malondialdehyde equivalents were calculated in the following manner:

$$1) [(\lambda_{532+TBA}) - (\lambda_{600+TBA}) - (\lambda_{532-TBA}) - (\lambda_{600-TBA})] = A;$$

$$2) [(\lambda_{440+TBA} - \lambda_{600+TBA}) 0.0571] = B;$$

$$3) \text{MDA equivalents (nmol.ml}^{-1}\text{)} = (A-B/157000) \times 10^6.$$

Handy PEA

Chlorophyll a fluorescence induction was measured using Handy PEA (Plant Efficiency Analyzer), Hansatech Instruments, UK. *Arabidopsis* seedlings were pre-darkened for 20 min at room temperature. Chlorophyll a fluorescence induction transients were measured, up to 2 s, by excitation with 650 nm light of high intensity ($3500 \mu\text{mol photons m}^{-2} \text{s}^{-1}$), as provided by an array of 3 LEDs. These data were then analyzed by the so-called OJIP-test (Stirbet et al. 2018), here, O (origin) is the (measured) initial minimum fluorescence, which is followed by a rise to a J level (2 ms), an inflection I (30 ms), and then finally the peak P (260 ms). Parameters labeled as PI (performance index), RC/ABS (estimated ratio of reaction center to PSII antenna absorption), F_V/F_O (variable to minimal fluorescence), and an area over the fluorescence induction curve were obtained by using ‘‘PEA plus software’’ (Strasser et al. 2005).

In addition, we measured 2 other parameters: (i) variable to minimum fluorescence (F_V/F_O), which is considered to be proportional to the activity of the water-splitting complex on the donor side of the PSII; and (ii) Area, the area above the chlorophyll fluorescence curve between F_O and F_M , which estimates the size of the plastoquinone pool. To examine the OJIP data from different samples, fluorescence transients were normalized at the F_O (the O level).

In addition, we also calculated $V_{OP} = (F_t - F_O) / (F_P - F_O)$

and $V_{IP} = (F_t - F_I) / (F_P - F_I)$.

High light treatment

High light exposure was given in the Votsch plant growth chamber. The intensity of light was measured by Fluorometer (LiCOR). Plants were kept at top rack where the intensity was measured to be $800 \mu\text{mol photons m}^{-2} \text{s}^{-1}$. For reducing

damage due to heat, the temperature was reduced to 18⁰C such that temperature on the rack was maintained to 21⁰c

Carbon dioxide assimilation analysis by Infrared gas analyzer (IRGA)

Photosynthetic carbon dioxide assimilation of 6-week-old plants grown under short-day condition (8h L/16h D) in soil, were measured using an Infrared gas analyzer (Portable Gas Exchange Fluorescence System GFS3000, Walz) using a standard head, for known leaf areas. The CO₂ concentration in the sample chamber was maintained at 400 ppm, block temperature at 22°C, and relative humidity at 50 %. For measurements of stomatal conductance (gs), transpiration rate (E), and water use efficiency (WUE), we used a light intensity of 400 μmol photons m⁻² s⁻¹(von Caemmerer and Farquhar 1981).

Results

Comparison of photosynthetic parameters of WT, PORCx, and *porC-2* mutant

Plant phenotype

WT, overexpressor of Protochlorophyllide oxidoreductase C (PORCx), and its knock-down mutant (*porC-2*) were grown at 21⁰C under 10h L and 14h D photoperiod in cool-white-fluorescent light (100 $\mu\text{mol photons m}^{-2} \text{s}^{-1}$) for up to five weeks. Images captured indicate that they are almost similar in appearance (Fig. 1).

Pigment content in WT, PORCx, and *porC-2* plants

Total chlorophyll (Chl), and carotenoid content were measured in three-week-old WT, PORCx and *porC-2* plants grown at 21⁰C under 10h L and 14h D photoperiod in cool-white-fluorescent light (100 $\mu\text{mol photons m}^{-2} \text{s}^{-1}$). Overproduction of PORC increased chlorophyll and carotenoid content in PORCx in comparison to WT plants. PORCx plants had 17 % more Chl than *porC-2* and WT. Likewise, carotenoid content was higher in PORCx plants, i.e., 30% higher than WT (Fig. 2a, 2b).

Analysis of chlorophyll a fluorescence parameter by Pulse amplitude modulation

Analysis of chlorophyll a fluorescence in response to modulated pulses of light provides an important tool to study the photosynthetic efficiency of a plant in a quick and non-invasive manner. The chlorophyll molecules absorb light energy, and its subsequent de-excitation takes place through one of the three inter-competitive processes, i.e., energy being utilized in photochemical reaction, thermal dissipation, or Chl a fluorescence. Analysis of Chl a fluorescence kinetics has paved the way for better understanding of the complex events involving the electron transport.

Minimum fluorescence (F_0)

Before measurement, all plants were incubated in the dark for 20 minutes so that all reaction centers remain uniformly open. The Chl a fluorescence was monitored by Dual PAM 100 spectrofluorometer (Walz, Germany). Exposure of

plants to measuring light (ML) gives the minimum fluorescence yield (F_0). Under control conditions, there was no significant difference in the minimum fluorescence level of WT and PORCx and *porC-2* plants (Fig. 3a).

Maximum fluorescence (F_m)

Exposure to a short pulse of saturating light determines F_m , which indicate maximum reduction of the primary electron acceptor Q_A . No significant difference was observed in the maximum fluorescence of WT, PORCx, and *porC-2* plants in control conditions (Fig. 3b).

F_v/F_m

Variable fluorescence can be determined by calculating the difference between maximum to minimum chlorophyll fluorescence. Plants growing under control conditions have a higher and almost similar value of F_v/F_m ratio. The F_v/F_m ratio was approx ~ 0.80 in WT, PORCx, and *porC-2* plants, which indicated that the quantum efficiency of dark-adapted plants was almost similar (Fig. 4a).

F_v/F_0

The ratio of variable to minimum fluorescence gives an insight regarding the activity of oxygen evolution complex on the donor side of PSII. In control conditions, the F_v/F_0 ratio of WT, PORCx, and *porC-2* plants were almost similar (Fig. 4b).

Quantum yield of photosystem II (ϕ PSII)

It represents the fraction of photons that are utilized to drive photosynthetic machinery. The ϕ PSII decreased in response to light intensity. The PSII quantum yield of PORCx plants was 12% higher than the WT in most light intensities. The *porC-2* mutant had a very small decrease of ϕ PSII quantum yield (Fig. 5a).

Electron transport rate of PSII (ETR II)

The PSII-dependent electron transport rate increased with an increase in light intensity. The calculated electron transport rate (ETR II) was plotted against photosynthetic active radiation ($\mu\text{mol photons m}^{-2} \text{s}^{-1}$) to form a light response curve. In the absence of any stress, the ETR of PORCx was 11% higher than WT. The *porC-2* plants had almost similar ETR values with respect to WT (Fig. 5b).

Non-photochemical quenching (NPQ)

NPQ corresponds to the activation of a heat dissipation machinery to protect PSII from excess excitation energy. The NPQ increased in response to higher light

intensities. The *porC-2* mutant had 27% higher NPQ than the WT. The NPQ of PORCx plants was slightly lower than the WT in higher light intensities (Fig. 6a).

Quantum yield of non-regulated energy dissipation Y(NO)

Y (NO) is a measure of non-regulated energy dissipation in PSII. It involves light-induced processes that in addition to basal energy loss contribute to non-radiative decay by photo-inhibition. The Y(NO) values of WT, PORCx, and *porC-2* plants were almost similar in the control condition. (Fig 6 b)

Coefficient of photochemical quenching (qP)

The qP denotes the fraction of reaction centers in the open state, i.e. having oxidized Q_A . It is based on the puddle model that does not take into account the connectivity of PSII reaction centers. In PORCx, a 14.8% increase in the qP value indicates that its photochemical efficiency of PSII is more in higher light intensities. In the *porC-2* mutant, qP values were similar to that of WT (Fig 7a).

Coefficient of photochemical quenching (qL)

This parameter indicates the fraction of reaction centers that are open in PSII according to the lake model that assumes that all or most of the PSII complexes are interconnected. A higher value of qL in PORCx, i.e., 30% more than WT, suggesting that a larger fraction of open reaction centers that can efficiently utilize absorbed energy into photochemical energy. The *porC-2* mutant had almost similar qL as compared to WT (Fig. 7b).

Measurement of photosynthetic CO₂ assimilated by plants

Five-week-old *Arabidopsis* plants were used to analyze their carbon dioxide assimilation efficiency as described in the materials and methods. Before measurements, leaves were pre-illuminated at 400 $\mu\text{mol photons m}^{-2} \text{s}^{-1}$ for 25 min. The rest of the parameters were monitored in the same light intensity, and 400 $\mu\text{mol (mol)}^{-1}$ of CO₂ and the leaf temperature was maintained of 25⁰C using LiCOR (6400) Infrared gas analyzer.

CO₂ assimilation rate (An)

The An of PORCx plant was 16% higher than WT. However, the carbon assimilation rates of WT and *porC-2* plants were almost similar (Fig. 8a).

Stomatal conductance (g_s)

It measures the rate of CO₂ intake or release of water vapors through stomatal pores present in the leaves. Maximum stomatal conductance was observed in PORCx plants. The stomatal conductance of PORCx plants was 20% higher than the WT. In contrast, the *porC-2* mutants had 18% lower g_s than the WT. (Fig. 8b)

Transpiration rate

It is a measure of the transfer of water from the plant to the atmosphere by evaporation predominantly through stomata. In consonance with stomatal conductance, the transpiration rate in *porC-2* plants was lowest. However, under identical conditions, the PORCx had 10% increase in the transpiration rate with respect to WT plants (Fig. 9a).

Water use efficiency (WUE)

It is calculated by taking the ratio of photosynthetic rate to the transpiration rate. The WUE denotes the amount of water used to fix CO₂. Maximum WUE was observed in *porC-2* plants due to reduced transpiration rate. They had 70% higher WUE than the WT. However, the WUE of PORCx plant was almost similar to the WT (Fig. 9b).

Antioxidative enzyme activities

Presence of any kind of stress illicit formation of reactive oxygen species in plants. As a result, the presence of inbuilt antioxidant enzyme-mediated defense machinery readily increases for detoxification of the free radicals produced in response to stress.

Catalase activity

It mostly detoxifies hydrogen peroxide produced during photorespiration or by β -oxidation of fatty acid. In control conditions, the activity of catalase was 15 % less in PORCx plants than WT plants. The *porC-2* plants had 19% higher catalase activity (Fig. 10a).

Ascorbate Peroxidase activity

It utilizes ascorbic acid for the reduction of hydrogen peroxide into water and oxygen. In PORCx plants, the APX activity was reduced by 14% in comparison to WT. However, in *porC-2* mutants, the APX activity was higher by 7% (Fig. 10b).

Impact of singlet oxygen-induced oxidative stress causes severe photooxidative stress in *porC-2* mutant

Morphological changes

Three-week-old WT, PORCx and *porC-2* plants were sprayed with 1 mM ALA or distilled water (control) and incubated in the dark for 12 h to accumulate the Chl biosynthetic intermediate Pchl_{ide}. After dark-incubation, plants were exposed to low light (75 $\mu\text{mol photons m}^{-2} \text{s}^{-1}$) for up to 2 h. As shown in Figure. 11, the *porC-2* mutants had the most visible photooxidative damages. Under identical conditions, the visible damage to PORC plants was minimal.

Chlorophyll a fluorescence imaging

The severity of ALA-induced stress on plant photosynthetic efficiency was determined by using Imaging PAM MAXI (Walz, Germany). The Fv/Fm false-color images of plants overexpressing PORC enzyme demonstrated that it was least affected in PORCx plants whereas *porC-2* plants had the highest decrease of Fv/Fm in the image after 2 h light exposure (Fig. 12)

Ft false-color image

False-color images of Chl a fluorescence at a time t (Ft), from WT, PORCx and its knock-down mutant *porC-2* plants treated without or with 1 mM ALA, were obtained from Imaging PAM (Fig. 13). In ALA-treated *porC-2* mutants, the fluorescence was seen from only a few partially green patches of bleached leaves. Under identical conditions, the overexpressor plants had a lot of fluorescence emanating from greener leaves whose images were recorded by the fluorometer.

Singlet oxygen generation in response to Pchl_{ide} accumulation

To monitor the $^1\text{O}_2$ generated via type II photosensitization reaction of the photosensitizer Pchl_{ide}, leaves were harvested and treated with singlet oxygen sensor green (SOSG) to monitor the $^1\text{O}_2$ -induced green fluorescence in a fluorescence microscope (Fig. 14a). Results demonstrate that the maximum amount of $^1\text{O}_2$ was produced from the photosensitizer Pchl_{ide} by ALA-treated *porC-2* plants exposed to

light for 2 h. The minimal SOSG fluorescence was produced from ALA-treated and light-exposed PORCx plants (Fig. 14b).

Singlet oxygen-induced damage to photosynthetic apparatus

Fv/Fm ratio

To ascertain the ALA-induced oxidative stress, the Fv/Fm ratio was quantified in both control and ALA-treated samples after 1 h and 2 h of light exposure (Fig.15a). The Fv/Fm ratio of dark incubated ALA-treated WT and *porC-2* plants was reduced by 8% and 14% after 1 h of light treatment. Under identical conditions, the Fv/Fm ratio of PORCx plants was unaffected. After 2 h of light treatment, the Fv/Fm ratio declined by 14% in WT, 20% in *porC-2* and to a smaller extent (5%) in PORC overexpressors.

Fv/Fo ratio

To ascertain the intensity of damage caused by $^1\text{O}_2$ to the oxygen evolution complex, the Fv/Fo ratio in ALA-treated dark-incubated plants was monitored upon light exposure (Fig.15b). The Fv/Fo ratio denotes the activity of water splitting complex of PSII. Due to the limited availability of PORC enzyme in *porC-2* and WT plants, the accumulation of Pchl_a caused a burst in $^1\text{O}_2$ production that significantly damaged the oxygen-evolving complex. The maximum decrease in Fv/Fo ratio was observed in *porC-2* plants followed by WT, whereas PORCx plants had smaller impairment of photosynthetic oxygen evolution machinery. The Fv/Fo ratio declined by 23% and 18% after 2 h of light exposure in *porC-2* and WT plants, respectively. However, under identical conditions, the Fv/Fo ratio of PORCx plants remained unaffected.

Quantum yield of photosystem II (ϕ PS II)

The impact of $^1\text{O}_2$ -induced oxidative stress on the overall photochemical quantum yield of PSII (ϕ PSII) was determined at 530 $\mu\text{mol photons m}^{-2} \text{s}^{-1}$ light intensity using the equation described in materials and methods. In ALA-treated dark incubated *porC-2* plants, the effective quantum yield of PS II decreased by 50.3% within an hour of light exposure that later declined to 72.6 % after 2 h of light treatment (Fig.16a). In the WT plants, the effective quantum yield decreases from 35% and 63% due to 1h and 2h of light treatment, respectively. Under identical condition, the ϕ PSII pfPORCx plants were affected to a smaller extent (15%-20%).

Electron transport rate (ETR II)

The PSII-dependent ETR measured at $530 \mu\text{mol photons m}^{-2} \text{s}^{-1}$ was determined in control and ALA-treated plants. ALA-sprayed and dark-incubated *porC-2* and WT plants, exposed to light $75 \mu\text{mol photons m}^{-2} \text{s}^{-1}$ for 2 h had 50% and 35% reduction in ETR respectively (Fig. 16b). However, the ETR of PORCx plants declined by 17% after 2 h of light exposure.

Non-photochemical quenching (NPQ)

It is a measure of non-photochemical fluorescence quenching, reflecting photoprotection by heat dissipation machinery in response to stress. Increased NPQ in PORC overexpressor indicates the activation of proton gradient-dependent heat dissipation machinery (Fig.17a). However, *porC-2* and WT, the decrease in NPQ indicate the absence of activation of the protective mechanism.

Quantum yield of non-regulated energy dissipation Y(NO)

In the control conditions, the Y(NO), that denotes quantum yield of energy dissipation in PS II, were similar in all the three types of plants (Fig.17b). After ALA treatment, the increase in Y(NO) in *porC-2* and WT indicates that both the processes of photochemical energy conversion and protective regulatory mechanisms are unable to cope up even with the low light ($75 \mu\text{mol photons m}^{-2} \text{s}^{-1}$). Under identical conditions in PORCx plants, the decrease in the Y(NO) indicates that due to excess of PORC enzyme, the Y(NO) remained unaffected after 2 h of light exposure.

Cell death due to singlet oxygen-induced oxidative stress

After completion of low light exposure, the ALA treated and untreated plants were stained with Evans blue dye. Maximum inclusion of Evans blue dye was observed in the *porC-2* mutant after 2 h of low light exposure. In contrast, the PORCx plants had marginal inclusion of the dye demonstrating that overexpression of PORC enzyme reduced singlet oxygen-induced cell death, (Fig.18)

Photooxidative stress in high light

Because of the presence of higher concentration of the photo-sensitizer Pchl_a in ALA-treated and dark-incubated plants, the $^1\text{O}_2$ production was triggered even by very low light intensity ($75 \mu\text{mol photons m}^{-2} \text{s}^{-1}$). To study further, the $^1\text{O}_2$ generation in plants was triggered by exposing plants to high light ($800 \mu\text{mol photons m}^{-2} \text{s}^{-1}$) without prior ALA treatment. The excess light energy absorbed by

Chl molecules cannot be utilized in photochemical reactions; instead, the excitation energy is transferred to O₂ to generate ¹O₂.

Five-week-old WT, PORC_x, and *porC-2* plants grown in 100 μmol photons m⁻² s⁻¹ were exposed to high light (800 μmol photons m⁻² s⁻¹) to induce the formation of triplet excited state of Chl molecules that transfer their energy to oxygen to generate singlet oxygen. High light intensity was provided from metal halide lamps within the plant growth chamber maintained at 21 °C (Votsch, Germany). Immediately after stress treatment, pictures were taken to visualize high-light-induced photobleaching in plants. From figure 19 it is apparent that a number of leaves from *porC-2* mutant were bleached. WT plants also had visible photodamage to their leaves. However, PORC_x overexpressor had little visible damage to the rosette structure.

Generation of singlet oxygen from the leaves in high light

To monitor ¹O₂ level in the absence of stress, three-week-old WT, PORC_x, and *porC-2* plants were grown under cool-white fluorescent light (100 μmol photons m⁻² s⁻¹) in *Arabidopsis*-growth-room were exposed to the same light intensity in the plant growth chamber. Leaves were excised using a sharp razor and infiltrated with SOSG solution. Fluorescence microscopy revealed that *porC-2* mutant emitted 40% higher SOSG fluorescence than WT. In control conditions, PORC_x plants generated lower ¹O₂ than the WT. Maximum SOSG fluorescence in control conditions can be attributed by the presence of a higher amount of Pchl_a in *porC-2* mutants (Fig. 20-21).

Upon high light treatment (800 μmol photons m⁻² s⁻¹) of WT, PORC_x and *porC-2* plants in plant growth chamber maintained at 21 °C, the SOSG fluorescence substantially increased in all. However, the leaves of PORC_x plants emitted the lowest amount of SOSG fluorescence. However, maximum SOSG fluorescence was recorded from *porC-2* mutants in high light. It was 76% higher than the WT. The PORC_x leaves emitted 59% lower singlet-oxygen-induced SOSG fluorescence (Fig. 20-21).

Pulse amplitude modulation (PAM) measurement after high light stress

To quantitate the high-light-induced damage to the photosynthetic apparatus, five-week-old WT, PORCx and *porC-2* plants were exposed to high light (800 $\mu\text{mol photons m}^{-2} \text{s}^{-1}$) for 16 h. Control plants were kept under their growth light intensity (100 $\mu\text{mol photons m}^{-2} \text{s}^{-1}$). After 16 h light treatment, plants were incubated in the dark for 20 min to uniformly open all the reaction centers. Their photosynthetic functions were measured using Chl a fluorescence as a non-invasive tool.

Quantum yield of photosystem II (ϕ PS II)

In PORCx plants, 5 % decline in the PSII yield was observed after 16 h HL treatment. In *porC-2*, the ϕ PSII yield was reduced by 29%. (Fig. 22a).

Electron transport rate (ETR II)

After 16 h of high light stress, maximum reduction of 38 % in ETR II was observed in *porC-2* mutant with respect to its control plant. However, only 7 % decline in ETR II was observed in PORCx plants in response to high light (Fig. 22b).

Non-photochemical quenching (NPQ)

In PORCx plants, NPQ increases by 53% in response to high light stress. Activation of NPQ mediates heat dissipation machinery involving the establishment of a proton gradient across the thylakoid membrane. Severe reduction of NPQ in WT and *porC-2* plants exposed to HL suggests damage in their NPQ machinery in stress condition (Fig. 23a).

Quantum yield of non-regulated energy dissipation Y(NO)

Higher values of Y(NO) indicate that at that point of time, the photochemical energy conversion and heat dissipation machinery are unable to tolerate the stress. In response to high light, the Y(NO) increased by 50% in WT and 69% in the *porC-2* mutant. However, there was no increase of Y(NO) in PORC overexpressors (Fig. 23b).

Chlorophyll a fast fluorescence kinetics

Chlorophyll fluorescence parameters serve as a versatile tool to study the function of the photosynthetic apparatus. When plants are incubated in the dark for 20 min, all the reaction centers remain open. Illumination with a short pulse of saturating light uniformly reduce most Q_A centers that result in maximum fluorescence signal (F_m). Irradiation with actinic light (light intensity sufficient to

initiate photochemical reaction) for a short period results into a characteristic induction in Chl fluorescence as explained by *Kautsky effect*. Upon plotting the fluorescence induction kinetics on the logarithmic time scale, distinct inflections can be seen which are collectively referred to as OJIP curve. The O stands for the origin of Chl a fast fluorescence induction kinetics; it denotes the initiation of reduction of primary plastoquinone acceptor Q_A . On the other side, the J and I represent the intermediate process involving the reduction of plastoquinol pool and reduction of ferredoxin at PS I and P denote the peak. Analysis of Chl a fluorescence kinetics can give insight into interconnecting processes during photosynthesis.

OJIP curve

Comparison of the OJIP curves obtained in control and 16 h high light stress revealed that the Fm rise was highest in PORCx plants. It indicates efficient electron transfer from PSII to PSI via all the intermediary steps. However, a delay in the Fm rise was obtained in the *porC-2* mutant indicating an interruption in the electron transport due to the presence of reduced electron acceptors. (Fig. 24).

Double normalization at O and P

The OJIP curve is normalized at both O (20 μ s) and P (270ms). A significant J-rise was obtained in the *porC-2* mutant in response to HL stress. (Fig. 25).

Double normalization at I and P

The OJIP curves were normalized at I (30ms) and P (270ms). Early IP rise may indicate the effective transfer of electrons from PSII to PSI and its subsequent conversion into reducing equivalents such as NADPH. Under control conditions, all the plants showed an early rise from I to P. However, under HL stress, the PORCx plants showed early IP rise followed by WT and delayed rise was observed in *porC-2* mutant plants. A quick IP rise may indicate the productivity of the plant in terms of higher photosynthetic rate and growth as observed in rice plants (Hamdani et al. 2015) (Fig. 26).

Normalization at I

By normalizing the transient curve datapoints only at 30 ms which corresponds to the, I phase, early rise in the PORC overexpressor after high light stress indicate that the absorbed energy is effectively utilized in the photochemical reaction without reducing its efficiency (Fig. 27).

Minimum fluorescence (Fo)

In response to high light stress, the Fo increased in all the plants. However, the increase of Fo in *porC-2* plants was 25 % higher in high light. Likewise, WT plants had 11.1 % higher Fo values than its control. Under identical conditions, PORCx plants had 4 % increase in Fo (Fig. 28a).

Maximum fluorescence (Fm)

Under control conditions, the value of maximum fluorescence was almost similar in WT, PORCx, and *porC-2* plants. Subsequent exposure to high light stress for 16 h reduced the Fm values in WT and *porC-2* mutant. (Fig. 28b).

Fv/Fm

In control conditions, the maximum PSII quantum yield was almost similar in all the plants. Exposure to high light stress prominently reduces the Fv/Fm in the *porC-2* mutant by 15.6%. Likewise, WT plants had 5.9 % lower Fv/Fm. Conversely, the PORCx plants showed less than 5% decline in Fv/Fm after 16 h of high light exposure (Fig. 29a).

Fv/Fo

Exposure to high light intensity greatly reduces the D1 protein turnover. As a result, exposure to high light intensity reduced the water-splitting activity in all the plants types. A maximum decline of 33.8% was observed in the *porC-2* mutant, followed by 29 % decline in the high light treated WT plants. Under similar conditions, PORCx had less than 17% decline the Fv/Fo ratio (Fig. 29b).

Radar plot

In order to summarize most of the relevant chlorophyll fluorescence parameters (Fig. 30), a radar plot was prepared to easily compare with respect to WT control, which is used as a reference.

Parameters used

Fo, that denotes the minimum chlorophyll a fluorescence increased in *porC-2* plants

Fm, the Maximum fluorescence upon exposure to short pulse of saturating light, was similar in among all the control and treatment plants

Fv/Fo, the maximum efficiency of water water-splitting activity in the PSII is declined in *porC-2* after high light treatment.

Area, the area above the OJIP curve which is a measure of redox status of the plastoquinol pool, was higher in PORCx plants

10RC/CS_M, represents the efficiency index, expressed as the density of reaction center per chlorophyll molecule. It was minimum in highlight treated *porC-2* plants

DIo/ CS_M -Represents the energy that is not utilized by the reaction center. Instead the absorbed energy is dissipated as heat. Maximum loss of energy was observed in *porC-2* high light treated plants.

ETo/ CS_M—It indicates the rate of electron transport by one reaction center. PORCx plants had maximum rate.

Tro/ CS_M—Energy flux trapped by one active reaction center. Maximum utilization of energy into photosynthetic reactions was observed in PORCx plants.

Analysis of lipid peroxidation

Generation of singlet oxygen in the plastidic membrane primarily targets membrane-bound polyunsaturated fatty acids (PUFAs). Estimation of the extent of lipid peroxidation serves as a marker for photooxidative stress. It can be measured by quantifying the oxidized product malonaldehyde, through MDA assay. Under control conditions, the MDA content in all the plant types was similar. However, after 16 h of HL stress, the MDA content increased by 216% in WT, whereas in *porC-2* it increased by 768%. On the contrary, PORCx had only 266% increase in the MDA content. (Fig. 31),

Evans blue staining

Elevation in singlet oxygen damages the cell membrane by rapidly oxidizing the structural membrane-bound lipids. Loss of membrane integrity can be observed by staining tissues with Evans blue dye that selectively penetrate nonviable cells. Maximum dye-inclusion was observed in *porC-2* mutant, whereas PORCx plants had minimum inclusion of dye with respect to WT and *porC-2*. (Fig. 32),

Analysis of ¹O₂ in protoplast

To check the induction of ¹O₂ at a cellular level in response to HL stress, four-week-old plants were kept under high light intensity for 16 h. Later, their protoplasts were isolated by using cellulose and macerozyme. Protoplasts were immediately

stained with SOSG dye and imaged under a fluorescent microscope. Nearly 57% increase in the SOSG signal was observed from the *porC-2* protoplast. Under identical conditions, PORCx protoplasts had 34% less SOSG fluorescence than WT. (Fig. 33),

Induction of cell death in response to high light stress

Excessive accumulation of $^1\text{O}_2$ rapidly oxidizes nearly available molecules and render them non-functional, thus causing cytotoxic damage to the cell. When the rate of damage exceeds the rate of repair, the cell undergoes programmed cell death. The characteristic features of programmed cell death involve fragmentation of DNA, condensation of chromatin, and blebbing of cell membrane. By incorporating fluorophore-labeled deoxynucleotide, the formation of DNA nicks during stress can be analyzed.

TUNEL assay

Terminal deoxynucleotidyl transferase nick end labeling (TUNEL) of the protoplast indicate the presence of DNA break by utilizing Alexa-fluor-labeled antibody specific to the modified deoxynucleotide. After completion of HL stress, protoplasts were harvested from the stressed leaves. Further processing of protoplasts was done as described in the materials and methods. Analysis of the labeled protoplasts under FITC channel showed TUNEL positive nuclei in the *porC-2* and WT protoplasts. However, very few TUNEL positive nuclei were observed from PORCx protoplasts. (Fig. 34),

Genetic manipulation of chlorophyll catabolic enzymes to prevent oxidative stress

During senescence and stress conditions the Chl molecules are extensively degraded, leading to the buildup of tetrapyrrolic Chl catabolites. These act as photosensitizers and generate $^1\text{O}_2$ in the presence of light and causes photooxidative damage to plants. Previously in our laboratory, the Chl catabolic enzyme pheophorbide a oxygenase was overexpressed in *Arabidopsis thaliana* to minimize the accumulation of pheophorbide a in stress conditions. The other enzyme in the Chl catabolic pathway, i.e., red chlorophyll catabolite reductase (RCCR) was also

previously overexpressed in our laboratory along with pheophorbide a oxygenase (PAO) in *A. thaliana* to minimize the accumulation of both the photosensitizers, i.e., Pheo a and RCC to prevent singlet-oxygen-induced oxidative stress.

In the present study, the impact of overexpression of *AtPAO* alone and overexpression of both the Chl catabolic genes *AtPAO/AtRCCR* on high-light-induced photooxidative stress is studied.

The Double overexpressor *Arabidopsis thaliana* (*AtPAO/AtRCCR*) line D26, the single overexpressor *AtPAOx*, line PS51, its mutant *pao*, and WT were grown at 21⁰C under 10h L and 14h D photoperiod in cool-white-fluorescent light (100 $\mu\text{mol photons m}^{-2} \text{ s}^{-1}$) for up to five-weeks. Their images were captured to observe any difference in appearance due to genetic manipulation (Fig. 35). There was no significant difference in growth in D26, PS51, and *pao* mutant plants.

Total chlorophyll

Total Chl content in WT, D26, PS51, and *pao* mutant were almost similar demonstrating that upregulation or down regulation of Chl catabolic enzymes did not have any impact on their Chl biosynthesis potential in controlled growth conditions (Fig. 36a).

Carotenoid content

In the D26, PS51, and *pao* mutant, the carotenoid content was almost similar to WT plants under control conditions (Fig. 36b).

Imaging PAM analysis

Fv/Fm false-color image

Four-week-old WT, D26, PS51 and *pao* mutant plants were grown under cool-white-fluorescent light (100 $\mu\text{mol photons m}^{-2} \text{ s}^{-1}$) light. Before capturing an image, plants were dark-adapted for 20 min to uniformly open the reaction centers. The Fv/Fm images revealed that all the plants had similar color at the maximum, which signifies that the plants used for the study were healthy and devoid of any other stress (Fig. 37).

Chlorophyll a fluorescence parameters

Minimum fluorescence (Fo)

The fluorescence measurements were taken using a Dual PAM 100 (Walz, Germany) spectrofluorometer. In control conditions when plants are dark-adapted, all the primary electron acceptors become oxidized, and thus the reaction center is said to be in open state. The Fo values of D26, PS51, *pao* were similar to the WT (Fig. 38a).

Maximum fluorescence (Fm)

Exposure with a short saturating pulse to dark-adapted plants yielded the maximum fluorescence Fm. The Fm values were almost the same in WT, D26, PS51, and *pao* mutant (Fig. 38b).

Fv/Fm

The ratio of the variable to maximal fluorescence determines the overall photosynthetic efficiency of the plant. As this parameter is very sensitive to stress, its analysis under the control condition indicated that all the plants had similar ~ 0.8 Fv/Fm values (Fig. 39a).

Fv/Fo

The ratio of variable to minimum fluorescence determine the activity of oxygen evolution complex at the donor side of PSII. In control conditions, D26, PS51, and WT and *pao* plants had almost similar Fv/Fo ratio (Fig. 39b).

Quantum yield of photosystem II (ϕ PSII)

Under control conditions, the D26 plants had 25.6 % higher ϕ PSII than WT. Similarly, PS51 had a small increase (6%) of ϕ PSII than WT. The *pao* mutant and WT had almost similar yield (Fig. 40a).

PSII-dependent electron transport rate

Analysis of the PSII-dependent electron transport rate in control conditions indicated that D26 plants had 25% higher ETR than the WT. Likewise, in PS51 7% increase was observed. The ETR was almost similar to the WT and *pao* plants (Fig. 40b).

Non-photochemical quenching (NPQ)

The activation of heat dissipation machinery was observed in *pao* mutant even in control non-stressed conditions. The NPQ was 32% higher than the WT in control conditions (Fig. 41a) suggesting that *pao* mutant keeps its heat dissipation machinery active in control conditions.

Quantum yield of non-regulated energy dissipation Y(NO)

This parameter is an indirect measure to study the relative functioning of photochemical and heat dissipation reactions. Under control conditions, the photochemical reactions increased with an increase in light intensity. Since the maximum energy received by the plants is utilized in photochemistry, minimum values of Y(NO) indicated the absence of any stressful condition. The D26, PS51, and *pao* mutant had almost similar values (Fig. 41b).

Coefficient of photochemical quenching (qL)

This parameter indicates the fraction of PSII reaction centers that are open according to the lake model that assumes that all or most of the PSII complexes are interconnected. The higher amount of open reaction center will ensure the channeling of the absorbed light energy to drive photosynthetic reactions. Higher qL value in D26 plants with respect to WT indicates efficient utilization of absorbed energy (Fig. 42a).

Coefficient of photochemical quenching (qP)

The qP denotes the fraction of reaction centers in the open state, i.e. having oxidized Q_A . It is based on the puddle model that does not take into account the connectivity of PSII reaction centers. Higher qL values with respect to WT in D26 plants indicate efficient utilization of absorbed energy (Fig. 42b).

Antioxidative enzyme activities

Under control conditions, the cellular status of antioxidant enzyme determines the presence of free radical at the basal level. Three-week-old plants were grown under controlled light and temperature. Protein isolated was estimated by Bradford assay. Equal quantity of protein was used in all the reactions.

Catalase (CAT) activity

In comparison to WT samples, *pao* mutant had 33% higher CAT activity. Its activities were almost similar in WT, D26, and PS51 samples under control conditions (Fig. 43a).

Ascorbate Peroxidase (APX) activity

The *pao* samples had 25% higher APX activity than WT. On the contrary, D26 and PS51 samples showed 9% and 14% decline in the CAT activity under control conditions (Fig. 43b).

Impact of high light stress

Exposure to high irradiance induces the formation of reactive oxygen species. Excess production of ROS greatly hampers the photosynthetic efficiency and growth of the plant. The Chl degradation becomes high in stress conditions leading to the production of Pheo a and RCC. These act as photosensitizers and generate $^1\text{O}_2$ that causes photooxidative damage.

High light-induced photo bleaching of leaves

Five-week-old WT, D26, PS51, and *pao* mutant plants were exposed to either their growth light intensity, i.e., control ($100 \mu\text{mol photons m}^{-2}\text{s}^{-1}$) or high light ($800 \mu\text{mol photons m}^{-2}\text{s}^{-1}$) for 16 h. Photooxidative stress-induced damage to the leaves was observed in the *pao* mutant and WT plants. However, minimum bleaching was observed in D26 and PS51 lines (Fig. 44).

Singlet oxygen accumulation in response to high light stress.

Involvement of singlet oxygen in high light stress was studied by exposing three-week-old plants to high light for 2 hours. The accumulation of singlet oxygen was studied by SOSG staining of leaves (Fig. 45a). In WT control plants that are exposed to low light for 2 hours, minimum SOSG fluorescence was recorded. However, upon exposing WT plants to high light for 2 h, rapid build-up of SOSG fluorescence could be observed. In WT in response to 2 h high light treatment, the SOSG fluorescence increased by 11-fold. As compared to WT treated samples, HL-treated *pao* mutants had 18-fold increase in SOSG fluorescence. Under identical conditions, D26 plants had only 4-fold increase in $^1\text{O}_2$ -induced SOSG fluorescence (Fig. 46).

Chlorophyll a fluorescence parameters

After completion of high light stress, plants were incubated in the dark. Chlorophyll fluorescence parameters such as electron transport rates, the quantum yield of PSII photochemistry, non-photochemical quenching, and various other parameters were calculated by using Dual-PAM software.

Quantum yield of photosystem II (ϕ PSII)

Exposure of 16 h high light decreases in the photosynthetic efficiency, i.e., the quantum yield of PS II. In WT plants, high irradiance decreased the ϕ PSII by 38% whereas in *pao* mutant the decline was more than 51%. The same of double and single overexpressor was reduced by 18% and 23% respectively (Fig. 47a).

Electron transport rate (ETR II)

Transfer of electrons through the PSII can be calculated from the chlorophyll fluorescence. When plants were exposed to high light stress, the WT plants had 38% reduction in the ETR. The D26 and PS51 transgenic lines had 19% and 23% decrease in the ETR. Under identical conditions, *pao* plants had 51% decrease of PSII activity (Fig. 47b).

Nonphotochemical quenching (NPQ)

When the intensity and duration of light intensity is more than the requirement, the excess energy absorbed need to be dissipated immediately to prevent buildup of free radicals and to reduce potential damage to the photosynthetic machinery. After light stress, activation of NPQ resulted in photoprotection in the D26 plants. D26 high light treated plants had 6% increase in NPQ. In PS51, 25% decrease in of NPQ was observed in response to high light. Conversely, in *pao* mutant, due to lack of functional enzyme Pheophorbide a oxygenase, the accumulation of pheophorbide in response to high light stress increases the level of $^1\text{O}_2$ severely affected the pH gradient dependent photoprotective machinery that resulted in 75% decline of NPQ (Fig. 48a).

Quantum yield of non-regulated energy dissipation Y(NO)

The Y(NO) increased in the WT by 28% in response to high light treatment. Under identical conditions, the *pao* mutants had 110% increase in Y(NO). Conversely, both the D26 transgenic line did not have any significant increase in Y(NO) (Fig. 48b).

Chlorophyll a fluorescence JIP-Test

Analysis of Chl a fluorescence in plants exposed to high light stress can provide an insight to study the series of events that leads to the formation of reducing equivalents.

OJIP- Curve

Analysis of chlorophyll a fluorescent transient showed that due to high light stress, as compared to WT, the P rise severely declined in high-light treated *pao* mutants. The overexpressors, especially D26 had higher P values than the WT. (Fig. 49).

Double normalization at O to P

The double normalization plot both at O (20 μ s) level and P (270 μ s) revealed an early rise from O to I in *pao* mutants in stress condition. Under identical conditions, O to I rise was slower in overexpressors (Fig. 50).

Double normalization at I to P

Analysis of I to P rise in the double normalized Chl fluorescent transient curve indicates the effective transfer of electrons to ferredoxin via PSI. The I to P rise was slower in high-light-treated *pao* mutants. Early I to P rise in the light stressed D26 line can be correlated with higher photosynthesis and productivity (Fig. 51).

Single normalization at I

In high light treated plants, the chlorophyll fluorescence transient curve is normalized at I phase (30ms). D26 line showed an early I rise, followed by PS51 after 16 h HL treatment. It indicates the reduced impact of high light stress on the photochemical reactions in the transgenic plants. On the contrary, in *pao* mutant, delayed I rise signifies the oxidative stress-induced inhibition of the electron transport (Fig. 52).

Minimum fluorescence (Fo)

In response to high light stress, the F_o increased in all the plants. However, the increase of F_o in *pao* plants was 82 % higher in high light. Likewise, WT plants had 44 % higher F_o values than its control. Under identical conditions, D26 plants had 22 % increase in F_o (Fig. 53a).

Maximum fluorescence (Fm)

Under control conditions, the value of maximum fluorescence was almost similar in WT, D26, PS51, and *pao* plants. Subsequent exposure to high light stress for 16 h reduced the F_m values in WT and *pao* mutant. After high light stress, in *pao* plants, the F_m declined by 25%, whereas, WT had 22% decrease in the F_m value. In contrast to D26 and PS51 plants had less than 20% decline in F_m (Fig. 53b).

Fv/Fm

Analysis of the ratio of variable to maximum fluorescence provides information regarding the efficiency with which plant can utilize absorbed energy to drive photochemistry. This parameter is highly sensitive to stress conditions. Hence, it is widely utilized as a marker to study photooxidative stress. In control conditions, the

maximum PSII quantum yield was almost similar in all the plants. Exposure to high light stress prominently reduces the Fv/Fm in the *pao* mutant by 27%. Likewise, WT plants had 17 % lower Fv/Fm. Conversely, the D26 and PS51 plants showed less than 10% decline in Fv/Fm after 16 h of high light exposure (Fig. 54a).

Fv/Fo

The ratio of variable to minimum fluorescence represents the activity of water splitting complex that donates electrons to the oxidized P680 reaction center during the electron transport. The function of water splitting complex is dependent on the working status of the D1 protein. Damage to the D1 protein indirectly halts the electron transport activity and result into the formation of oxidative radicals. Exposure to high light intensity greatly reduces the D1 protein turnover. As a result, exposure to high light intensity reduced the water-splitting activity in all the plants types. A maximum decline of 70% was observed in the *pao* mutant, followed by 54 % decline in the high light treated WT plants. Under similar conditions, D26 and PS51 plants had less than 40% decline the Fv/Fo ratio. (Fig. 54b).

Radar plot

In order to summarize most of the relevant chlorophyll fluorescence parameters, a radar plot was prepared to easily compare with respect to WT control, which is used as a reference. (Fig. 55).

Parameters used

Fo, the minimum chlorophyll fluorescence increased in *pao* mutant in response to high light stress

Area-The area above the OJIP curve, which is a measure of the redox status of the plastoquinol pool was higher in D26 and PS51 lines respectively.

10RC/CS_M, It represents the efficiency index, expressed as the density of reaction center per chlorophyll molecule, was higher in the transgenic D26 and PS51 line

DIo/ CS_M, the energy that is not utilized by the reaction center; instead, the absorbed energy is dissipated as heat, was higher in the high light treated *pao* mutant.

ETo/ CS_M, the rate of electron transport by one reaction center, was higher in D26 and PS51 lines after 16 h high light stress.

Tro/ CS_M, energy flux trapped by one active reaction center was lower in the *pao* mutant.

Psi/(1-psi)- It represents the ratio of electrons leaving the system to the electrons accumulated in the system. It was least affected in D26 and PS51 after high light stress.

Phi/(1-phi) – It denotes the ratio of efficiency of primary photochemical reactions. Maximum efficiency was observed in the high light treated D26, and PS51 lines in comparison to high light treated WT and *pao* plants.

MDA assay

Spectrophotometric analysis of thiobarbituric acid reactive substances is an indirect method to interpret malonaldehyde produced due to ¹O₂-mediated lipid peroxidation. Production of ¹O₂ in the membrane primarily target the membrane lipids and oxidizes them. In WT, in response to high light stress the MDA content increased by 280%. In the *pao* mutant, high light increased the MDA content by 360%. In the *AtPAO/AtRCCRx* D26 plants, the MDA content increased by 120% that was substantially lower than WT (Fig. 56).

Evans blue staining

Elevation in singlet oxygen damages the cell membrane by rapidly oxidizing the structural membrane-bound lipids. Loss of membrane integrity due to cell death could be observed by staining tissues with Evans blue dye that selectively penetrate non-viable cells. Maximum dye-inclusion was observed in *pao* mutant, whereas D26 and PS51 plants had reduced inclusion of dye with respect to WT (Fig. 57) demonstrating the protection of plants from ¹O₂-induced cell death in high light.

Discussion

Evolution of oxygenic photosynthesis paved the way for the emergence of higher and complex life forms on earth. The primitive reduced atmosphere was gradually converted into oxygen-rich due to the development of unicellular photosynthesizing blue-green algae. With the evolution of oxygenic photosynthetic organisms that oxidized H_2O to O_2 to generate the reductant NADPH for the reduction of carbon dioxide into energy-rich molecules resulted in the formation of the present oxygenic world. The increased oxygen concentration in the atmosphere posed a threat to the cell. Oxygen was utilized by cells to generate reactive oxygen species (Dat et al. 2000). Accumulation of oxidized molecular intermediates signals the cell to induce programmed cell death (Gutiérrez et al. 2011). This greatly reduces the vitality and therefore decreases the photosynthetic efficiency of the plant (Nishiyama et al. 2001). Reduction in the supply of energy-rich molecules reduces the growth and therefore, the yield of the plant. Therefore, strategies must be devised such that plants can tolerate oxidative stress without limiting their productivity.

With an increase in light intensity, i.e., from the early morning to noon, light absorption by Chl molecules increases almost linearly. However, the rate of photosynthesis reaches a maximum much before the linear increase in light absorption ceases. Therefore, plants end up in absorbing excess light that could be utilized in photosynthesis. The excess light, that remains un-utilized in photosynthesis, is often dissipated as heat via specific carotenoids that are in close proximity to Chl in light-harvesting chlorophyll-complexes (Björkman and Demmig 1987; Niyogi 2002; Asada 2006; Rossel et al. 2007; Ruban et al. 2012). However, plants often fail to dissipate all the unutilized solar energy absorbed by the pigment bed. The excess light energy, not utilized in photosynthesis, causes an accumulation of excited states of Chl ($^1\text{Chl}^*$) that are subsequently converted to triplet-excited states of Chls ($^3\text{Chl}^*$), which can transfer their energy to molecular oxygen (O_2). The resulting reactive form of O_2 , i.e., singlet oxygen ($^1\text{O}_2$) (Foster, 1991) causes photooxidative damage such as photooxidation of membrane lipids (Farmer and Mueller 2013) and ultimately cell death.

Upon excess illumination, not only Chl, but its biosynthetic tetrapyrrolic intermediates produce $^1\text{O}_2$ in plants and cause oxidative damage (Rebeiz et al. 1988; Chakraborty and Tripathy 1992; op den Camp 2003; Mohapatra and Tripathy 2007; Pattanayak and Tripathy 2011). Therefore, to prevent the $^1\text{O}_2$ -mediated oxidative damage that is due to the accumulation of Chl biosynthetic intermediates, it is essential to minimize their steady-state concentrations in plants during the daytime. The other forms of active oxygen species, such as superoxide (O_2^-) and hydrogen peroxide (H_2O_2) could be detoxified by enzymes like superoxide dismutase, ascorbate peroxidase and dehydroascorbate reductase (Asada 1984), glutathione reductase (Foyer and Shigeoka 2011) and glutathione peroxidase (Fischer et al. 2012). However, there is no enzymatic means available for plants to detoxify $^1\text{O}_2$. Recently, a few attempts have been made to reduce $^1\text{O}_2$ -mediated damage in *Arabidopsis* via *executer1* (*ex1*) and *executer 2* (*ex2*) mutations (Wagner et al. 2004; Lee et al. 2007) or over-expressing glutathione peroxidase and glutathione s-transferase in *Chlamydomonas*. These approaches strive to limit the injury to plants after $^1\text{O}_2$ is produced. However, it is essential to limit the light-mediated $^1\text{O}_2$ generation from the tetrapyrrolic intermediates in order to protect the plants from oxidative damage. Since carotenoids prevent the generation of $^1\text{O}_2$ by quenching the triplet excited states of Chl, many attempts have been made previously to increase their pool size. Increase in the carotenoid pool size may not be always enough to control oxidative stress, as the $^1\text{O}_2$ produced from Chl biosynthetic intermediates is not effectively quenched by them. Chl biosynthetic intermediates are not part of pigment-protein complexes in light-grown plants, and consequently, they cannot transfer their energy to the reaction center for its utilization in photosynthesis. Instead, the light energy absorbed by these intermediates is utilized to produce $^1\text{O}_2$ via type II photosensitization reaction. Therefore, to prevent $^1\text{O}_2$ -induced oxidative damage during the daytime, it is essential to minimize the steady-state concentration of Chl biosynthetic intermediates in plants.

In plants, 5-aminolevulinic acid (ALA) is synthesized from glutamic acid and is metabolized to Protochlorophyllide (Pchl) in the dark. Pchl, one of the major Chl biosynthetic intermediates, accumulates in the dark and provokes cell death in light by producing $^1\text{O}_2$ endogenously. The Pchl that accumulates overnight is photoconverted to Chlorophyllide (Chl) at daybreak by a light-dependent enzyme Protochlorophyllide Oxidoreductase (POR). In etiolated angiosperms, POR is

localized primarily in the prolamellar bodies; however, in light-grown seedlings, POR is found in the thylakoid and envelope membranes of chloroplasts (Barthelemy et al., 2000). In different plant species, gene organization and expression of POR have been shown to be quite different. Two POR genes have been identified from tobacco (Masuda et al. 2003), and three (PORA, PORB, and PORC) from *Arabidopsis* (Armstrong et al. 1995b; Sperling et al. 1997; Oosawa et al. 2000; Pattanayak and Tripathy 2002). In *Arabidopsis*, the expression of POR A rapidly declines after illumination of etiolated seedlings, POR B expression is partially reduced (Armstrong et al., 1995), whereas the POR C expression is induced by light and the transcript abundance increases in response to increasing light-intensity (Masuda et al., 2003; Pattanayak and Tripathy, 2002; Su et al., 2001).

One of the goals of the present investigation was to minimize the generation of $^1\text{O}_2$ by reducing the steady-state concentration of the photosensitizer Pchl_{id} in the plant cell. This was achieved *via* a genetic approach, i.e., overexpression of POR C that could efficiently photo-transform Pchl_{id} to Chl_{id} in light-grown plants. POR C was chosen over its other light-downregulated isoforms, i.e., POR A and POR B (Sperling et al., 1997) as it is light-inducible and its expression increases in response to higher light intensity and, therefore, it is a better candidate to photo-transform Pchl_{id} to Chl_{id} in high-light-grown-plants. Conversely, the *porC-2* mutant is more sensitive to high light and $^1\text{O}_2$ -induced photo-oxidative stress. It generates higher amounts of photosensitizer Pchl_{id}. To probe further, both PORC overexpressed, and *porC-2* mutants were taken for further study.

Solar energy is indispensable for survival on earth as the maximum biomass produced is contributed by photosynthesis. Plants utilize solar energy to drive photochemical reactions by trapping the light through an array of chlorophyll molecules arranged closely in association with proteins in the light-harvesting complex. The absorbed energy from individual chlorophyll is transferred among other chlorophyll molecules through resonance energy transfer until it reaches the reaction center chlorophyll. The primary event in photosynthesis involves the conversion of light energy into photochemical energy. It is mediated by the charge separation events that take place between the reaction center Chl (P680) and the intermediary electron acceptor pheophytin (Pheo) (Mamedov et al. 2015). Upon receiving light, the P680 molecule goes from ground state to excited level. Subsequent charge transfer de-

excites the Chl leads to the formation of a charged radical pair. The electron gained by the pheophytin is transferred to the first stable electron acceptor, Plastoquinone Q_A located on the D2 protein ($P680^+ \text{Pheo}^- Q_A \rightarrow P680^+ \text{Pheo} Q_A^-$) is the 1st stable acceptor of electrons in PSII (Hankamer et al. 1997). Meanwhile, the oxygen evolution complex split water molecule to provide electrons to reduce $P680^+$. The water-splitting activity requires D1 protein, as electron from its 161-Tyrz position is abstracted to reduce the PSII reaction center. From Q_A^- electron is transferred to Q_B on the D1 protein ($Q_A^- Q_B \rightarrow Q_A Q_B^-$). The subsequent transfer of another electron from the Q_A^- leads to the formation of Q_B^{2-} . After receiving 2 protons, plastoquinol (PQH_2) is formed which dissociate itself from the D1 protein to transfer electrons further to Rieske iron-sulfur cluster and cytochrome b6f complex. The electrons are channeled towards copper-containing mobile carrier plastocyanin. The released protons are pumped out of the lumen to form a proton gradient across the thylakoid membrane to activate ATP synthase. The electrons from plastocyanin reduce the $P700^+$ at PSI. The efficient electron transfer from PSII to PSI results in the formation of energy-rich reducing equivalents such as NADPH. The formation of proton gradient across the membrane activates the ATP Synthase complex to generate ATP from ADP and inorganic phosphate. Any interruption in the scheme of electron transport thus greatly affects the photosynthesis reactions.

Illuminations with high light intensity saturate the electron flow in the linear electron transport pathway and promote the generation of excited chlorophyll derived singlet oxygen that severely damages the oxygenic photosynthetic apparatus. On the acceptor side of PSII, the overreduction of the electron transport chain allows charge recombination reactions between ($P680^+ \text{Pheo}^-$) to give rise to $P680^+P680^-$ that interact with molecular oxygen to produce singlet oxygen. Apart from the chlorophyll molecules, their metabolic intermediates produce singlet oxygen upon light exposure. Presence of a conjugated bond system in the intermediates allows them to absorb light. However, they cannot channelize their absorbed energy to drive photochemistry. Instead, they return to the ground state by transferring their energy to molecular oxygen. Under control conditions, singlet oxygen so produced is kept in check by singlet oxygen quenchers such as carotenoids, and tocopherols. Exposure to saturating light intensity perturbs the balance, resulting in its accumulation. Generation of singlet oxygen from membrane-bound pigment complexes primarily

target the D1 protein. However, the chloroplast can recover the damaged D1 protein by enhancing its selective degradation by series of enzymatic steps and allowing de-novo synthesis of nascent D1 protein to replace the non-functional protein (Edelman and Mattoo 2008). Light-induced damage to D1 protein occurs concurrently with the light absorption. Therefore, the coherent repair machinery supplies functional D1 protein to maintain electron transport. When the damage exceeds the capacity of the D1 repair machinery, the accumulated singlet oxygen along with inactivated PSII invokes photoinhibition. Addition of singlet oxygen quencher such as histidine, rutin, diazobicyclooctane partially prevented the singlet oxygen-induced photoinhibition (Chakraborty and Tripathy, 1992; Baroli & Melis, 1998). Drastic reduction in the quantum yield and electron transport rate of PSII mark the induction of photooxidative stress in plants.

The extent of damage to the photosynthetic apparatus can be interpreted from modulated chlorophyll fluorescence in a quick way (Pintó-Marijuan and Munné-Bosch 2014). After absorbing light, an excited chlorophyll molecule can return to the ground state either by transferring its energy to the reaction center molecule to initiate photochemical reactions, or it can dissipate energy in the form of heat, or it can re-emit the energy as fluorescence. These three processes work competitively; therefore, by analyzing the chlorophyll fluorescence yield, the efficiency of photosynthetic machinery and activation of heat-dissipating mechanisms can be understood. Dark adaptation of leaf sample for up to 20 min relaxes the reaction centers, and it represents the successful transfer of electrons from Q_A to Q_B^- . Exposure to a weak modulating light beam (ML) measures the minimum fluorescence (F_0). Subsequent exposure to a saturating pulse results into maximum fluorescence (F_m) by closing the reaction centers. Difference between the maximum to minimum fluorescence determine the variable fluorescence ($F_m - F_0 = F_v$). The ratio of variable to maximum fluorescence denotes the maximum quantum yield of the PSII (F_v/F_m) in dark-adapted plants, which is used as a prominent marker to determine the health status of the plant. In plants, under control and non-stressed condition, the F_v/F_m value remains ~ 0.84 . Any kind of stress that affects the PSII photochemistry results in a decline in the parameter.

Actinic light (light capable of initiating photochemical events) is switched on while the samples are flashed with pulses of saturating light. The maximum

fluorescence thus obtained in the illuminated state is termed as F_m' . Initially, it is higher, but with time, it declines (quenching), which indicates the existence of competitive photochemical and non-photochemical processes. Value of F_m' will always be lower than F_m . Since in the dark-adapted state, the dissipation of energy in the form of heat is close to the minimum, whereas, in the illuminated state, the non-photochemical quenching of Chl a fluorescence is prevalent. Analysis of the ratio of variable fluorescence after light exposure (difference of maximum and minimum fluorescence in the light-adapted state) to the maximum fluorescence in the light-adapted state provide information regarding the effective proportion of absorbed light energy in driving photochemical reactions ($(F_m' - F_o')/F_m' =$ Quantum yield of PSII) (Björkman and Demmig 1987). The difference between the maximum fluorescence in the dark-adapted state and the light-adapted state can be used to estimate the loss of energy in the form of heat called non-photochemical quenching. The ratio of difference between the maximum fluorescence in dark and light-adapted state to the maximum fluorescence in the light-adapted state determines the non-photochemical quenching ($(F_m - F_m')/F_m' =$ NPQ). Exposure to high irradiance activates the proton gradient-dependent non-photochemical quenching pathway to release the excess absorbed energy as heat. Analysis of qP indicates the openness in the reaction centers. The yield of non-regulated energy dissipation $Y(NO)$ is an indicator of photodamage. An increase in the $Y(NO)$ under high light indicate damage in the PSII apparatus and the impairment of D1 protein turnover.

In the present study, we had observed that in the *porC-2* mutant (Masuda et al. 2003) accumulate Pchl_a derived singlet oxygen in light. The quantum yield and PSII-dependent electron transport chain remain unaffected under control conditions. On the contrary, the exogenous application of chlorophyll precursor ALA on the *porC-2* plants drastically reduced the quantum yield and electron transport rates (Tripathy and Chakraborty 1991; Chakraborty and Tripathy 1992). Dark incubation after ALA treatment allowed plants to accumulate photodynamic Pchl_a. Exposure to light-activated the protochlorophyllide oxidoreductase C enzyme in the PORC_x overexpressor, which rapidly converted the excess Pchl_a into Chl_a (Pattanayak and Tripathy 2002, 2011). However, in the *porC-2* mutant, the insertion of T-DNA in the 4th exon resulted in a scarcity of photoactive PORC enzyme. Its unavailability caused accumulated of un-catalyzed Pchl_a in the *porC-2* plant leaves. Subsequent

exposure to low light ($75 \mu\text{mol photons m}^{-2} \text{ s}^{-1}$) was sufficient to induce singlet oxygen production via type-II photosensitization reaction of Pchl_a (Foote, 1991, Tripathy and Chakraborty, 1991, Chakraborty and Tripathy, 1992). This is evident from 1O₂-induced SOSG fluorescence. Maximum Evans blue dye inclusion further validates that the singlet oxygen produced from ALA-derived Pchl_a induced cell death in *porC-2* plants (Shumbe et al. 2016b). Minimum dye inclusion in PORC overexpressor suggests that excess of PORC in plants rapidly converted the dark accumulated Pchl_a into chl_a and thus provided tolerance.

Optimum absorption of light is crucial for plants to carry out photosynthesis for their growth and development. Efficient utilization of light energy requires chlorophyll molecules. In plants, the synthesis of chlorophyll is regulated by a number of enzymes since some of the chlorophyll metabolic intermediates are photosensitive, i.e., they generate singlet oxygen upon exposure to light (Hukmani and Tripathy 1992). Under high light conditions, Chl intermediates along with chl molecules present in the antenna and reaction center get excited and result into a burst of singlet oxygen (Triantaphylides et al. 2008b; Tripathy and Pattanayak 2010; Pattanayak and Tripathy 2011). In response to high light stress, the accumulation of singlet oxygen was monitored by staining high light treated leaves with Singlet oxygen sensor green (SOSG) (Shao et al. 2013). After 2 h of high light stress ($800 \mu\text{mol photons m}^{-2} \text{ s}^{-1}$), maximum SOSG fluorescence was observed from the *porC-2* leaves, whereas, reduced SOSG fluorescence was observed from the PORC overexpressor leaves. It demonstrated that after high light stress, the photodynamic intermediate derived singlet oxygen-induced photooxidative stress was maximum in *porC-2* as observed by the increase in SOSG fluorescence. However, PORCx plants effectively tolerated the photooxidative stress by reducing the buildup of Pchl_a derived singlet oxygen.

Analysis of chlorophyll a fluorescence indicated a maximum decrease in the quantum yield and PSII-dependent electron transport rates of *porC-2* plants. Elevation of non-photochemical quenching in the PORCx plants after 16 h of high light stress clearly demonstrated the activation of zeaxanthin mediated photoprotective machinery in response to high light stress. Over-reduction of electron transport chain causes acidification of thylakoid lumen. Lowering of pH activate redox-regulated violaxanthin de-epoxidase. It mediates the conversion of violaxanthin into zeaxanthin (Dall'Osto et al. 2012). Along with activated Psbs protein, they induce changes in the

confirmation of the PSII antenna complex to modulate and dissipate the excess energy absorbed as heat (Ruban et al. 2012). Conversely, higher Y(NO) in *porC-2* and WT after HL treatment indicated severe damage to the PSII apparatus due to impairment of the D1 repair machinery (Lu et al. 2019).

To further elucidate the physiological events in response to high light stress, chlorophyll a fast fluorescence kinetics was employed. Similar to the pulse amplitude modulation, the chlorophyll a fast fluorescence measurement involves dark adaptation of the samples to bring all the reaction centers into a relaxed state. In other words, all the electron acceptors are oxidized in the open state of reaction center. Exposure to light reduces the electron acceptors in the photosynthetic pathway. A reaction center is termed as closed until the reduces Q_A doesn't pass the electron further to the secondary electron acceptor, Q_B .

Exposure of a short pulse of saturating light rapidly increases the chlorophyll fluorescence, which later declines with time. By plotting the chlorophyll fluorescence points with respect to the logarithmic time scale for up to 2 sec, distinct polyphasic induction curves are obtained which are collectively known as OJIP curve. The distinct rise in the chlorophyll a fluorescence transient curves gives an insight about the turn of events after absorption of light. The fluorescent transient originated from F_0 level to the maximum level via 2 intermediary steps termed as J and I. The O value represents the initial fluorescence and is associated with the energy losses in the PSII pigment antenna. The fluorescence rise from OJ denotes the reduction of the acceptor side of PSII due to the reduction of Q_A , it is observed between 50 μ s to 2 ms. JI indicate the reduction of Plastoquinone pool, and it is observed in between 2ms to 30ms. IP indicates the reduction of the electron carriers near PSI. Fm state represents the complete reduction of the Plastoquinone pool.

Analysis of the OJIP curve in the high light treated plant samples demonstrated that the PORCx plants had an early JI and IP rise, which indicate the efficient transfer of electron through the electron transport chain. Whereas in the *porC-2* and WT plants, a delayed rise indicates that the singlet oxygen-induced photooxidative stress is interrupting the electron transport chain. Further analysis of the chlorophyll a fluorescent transient, the double normalization at IP phase indicated an early rise in the PORCx plants in response to stress. Various studies correlate the

IP rise with the increase in growth and productivity of the plants however the mechanism with which IP rise is regulating the yield of the plant is yet to be explored (Hamdani et al. 2015; Kandoi et al. 2016). Analysis of the OJIP parameters suggested that in the *porC-2* mutant, the increase in the minimum fluorescence represents the blockage of charge transfer between primary and secondary electron acceptors (Pospíšil et al. 1998). Furthermore, analysis of the ratio of variable to minimal fluorescence (F_v/F_o), which denote the activity of oxygen evolution complex was decreased in the *porC-2* mutant. Whereas, the marginal decrease was observed in the PORCx plants. The presence of functional D1 protein to regulate the oxygen evolution complex is indispensable for efficient electron transport. $P680^+$ and excited chl triplet state molecules irreversibly damage the D1 protein. Excess singlet oxygen in the *porC-2* mutant impairs the water-splitting activity of the oxygen evolution complex as observed by increased F_v/F_o values (Burke 2008). Comparative analysis of the other OJIP parameters by spider plot indicates that in *porC-2* plants, the electron transport (ET_O/CS_M) decreased that was due to lower energy absorption by antenna pigments (ABS/CS_M), energy trapping by reaction centers (TR_O/CS_M) and higher energy loss as heat (DI_O/CS_M). On the contrary, PORCx plants had less damaging effect on the electron transport (ET_O/CS_M), had higher energy trapping by reaction centers (TR_O/CS_M) and lower energy loss as heat (DI_O/CS_M). Studies have shown prominent role of singlet oxygen in inducing lipid peroxidation (Triantaphylides et al. 2008a). Analysis of MDA content is widely used to determine oxidative stress-induced oxidation of polyunsaturated fatty acids (Lu et al. 2017). Higher MDA content in the *porC-2* indicates the generation of singlet oxygen from the membrane-bound intermediate Pchl_{ide} target membrane lipids for peroxidation. The detection of singlet oxygen mediated oxidation products serve as downstream signals and regulate singlet oxygen specific gene expression (D'Alessandro and Havaux 2019). Damage to the membrane integrity allowed inclusion of Evans blue dye in the high light treated *porC-2* plants. Stain uptake by the plants indicates the extent of cell death in response to high light stress. Furthermore, analysis of DNA fragments after high light stress is another parameter to study induction of programmed cell death. Protoplasts isolated from the high light treated plants showed DNA nicks in the *porC-2* protoplasts which demonstrate the role of singlet oxygen in inducing programmed cell death.

Loss of Chl occurs during senescence of vegetative plant organs as well as during fruit ripening. Chl has a half lifetime of around 48 h in high light-grown photosynthetic organism. Furthermore, Chl degradation occurs due to external factors such as injuries sustained by low or high temperature or pathogen attack or high light or other abiotic stresses. Rapid degradation of free Chl or its colored derivatives is necessary to avoid cell damage by their photodynamic action.

Chlorophyll is vital to all of the photosynthetic organisms. Their unique structure allows them to harvest sunlight and convert it into energy-rich molecules. However, this ability of light absorption can be fatal when exposed to high light. As some of the biosynthetic and catabolic intermediates of Chl are photodynamic, therefore their synthesis and degradation pathways are tightly controlled by redox-regulated and light-dependent enzymes. Chlorophyll degradation majorly takes place during senescence or ripening of fruit. The enzymes present in the mature gerontoplast rapidly convert the green-colored chlorophyll into colorless non-chlorophyll catabolites (nCCs) which later is transported to vacuoles for further degradation. However, massive amount of Chls are degraded in response to biotic or abiotic stress. Therefore, quick degradation of Chl intermediates are necessary to prevent the accumulation of intermediates derived singlet oxygen.

The chlorophyll degradation is initiated by chlorophyllase (CLH) enzyme that dephylate chlorophyll a to chlorophyllide. The removal of the phytol tail is followed by removal of magnesium ion by Mg-dechelating substances (MDS) to produce green-colored photodynamic pheophorbide a. The accumulation of pheophorbide a can induce photooxidative stress in the light-exposed plant. Photodynamic properties of Pheophorbide are utilized in photodynamic therapy to treat cancerous tissues (Busch et al. 2009).

The conversion of pheophorbide a into red chlorophyll catabolite is a key event in the chlorophyll degradation pathway as it involves the oxygenic opening of the macrocyclic ring, that provide the structural basis of further degradation steps. Its conversion is mediated by nuclear-encoded Rieske-type iron-sulfur oxygenase pheophorbide a oxygenase (PAO) (Pruzinska et al. 2003; Pruzinska 2005). PAO activity increases during senescence; therefore, play an integral role in chlorophyll degradation. In *Arabidopsis*, it is present in a single copy and is identical to

Arabidopsis accelerated cell death 1 (Hörtensteiner et al. 1995; Pruzinska et al. 2003). Presence of 49 aa transit peptide targets the enzyme to the chloroplast where it binds to the inner plastidic membrane. The red chlorophyll catabolite thus formed remain bound to the PAO enzyme and inhibit its function (Krautler 2008). Identification of another cytosolic reductase Red chlorophyll catabolite reductase is known to play a role in PAO mediated degradation of pheophorbide a. It interacts with the Pheophorbide: PAO enzyme complex to release pFCCs for further downstream degradation. PAO independent conversion of pheophorbide a into pFCCs by RCCR was insufficient (Rodoni et al. 1997). The bacterial two-hybrid system demonstrated that for the conversion of pheophorbide a into pFCCs through the macrocyclic opening require closed association of both PAO and RCCR (Pruzinska et al. 2007).

Exposure to biotic as well as abiotic stress induces leaf necrosis, which is accompanied by chlorophyll degradation. Although PAO expression majorly takes place during senescence, physical injury on the maize leaves increases its expression. Further analysis of gene expression by microarray indicated that infection with virulent pathogen *P. syringae* increases the expression of chlorophyll catabolic genes.

In the recent past, several studies have been carried out using mutants of both PAO and RCCR enzymes to study the characteristic features of both enzymes and their role in Chl degradation. Moreover, the mutant study also characterized other roles played by these enzymes during biotic challenges (plant-pathogen interaction) and PCD (Programmed cell death) (Greenberg *et al.*, 1993; 1994). Mutants defective in PAO and RCCR accumulate excessive amounts of the Chl catabolic intermediates pheophorbide a and RCCs, respectively (Pružinská *et al.*, 2003; 2005; 2007, Tanaka *et al.*, 2003). Cell death execution required light indicating that the accumulating tetrapyrroles act as photosensitizers causing the production of reactive oxygen species (ROS) and ultimately cell death (Pružinská *et al.*, 2007, Mach *et al.*, 2001, Hörtensteiner et al., 2004). However, excess accumulation of pheophorbide in the dark could cause light-independent cell death as it is toxic to plants (Hirashima et al. 2009)(Tanaka *et al.*, 2009).

Both PAO and RCCR together are involved in the degradation of Pheide a to non-toxic pFCC during senescence. They both form a complex and work in close vicinity of each other as part of the multienzyme complex during Chl degradation.

They could possibly regulate each other's catalytic activity. To understand the significance of increased expression of PAO during high light-stress, both PAO and RCCR were overexpressed together to form double transgenic plants.

Most plants are sensitive to high light. To assess the protective role of *PAO* and *RCCR*, the WT and *AtPAO/RCCR*x plants were exposed to high light ($800 \mu\text{mol m}^{-2} \text{s}^{-1}$), and their response was monitored. Under identical growth conditions, phenotypically the *AtPAO/RCCR*x plants were greener and were able to withstand stress as compared to WT and *pao* mutants.

Under control conditions, all the plants exhibited a similar phenotype, which indicated that the genetic manipulation had not affected the morphology of the plants. Analysis of chlorophyll fluorescence parameters suggested that in the absence of stress D26 line had higher electron transport rate. WT, D26, and *pao* mutant had an almost similar rate. The absence of stress in plants was further checked by studying the quantum yield of non-regulated energy dissipation $Y(\text{NO})$, which was almost similar in WT, D26, PS51, and *pao*.

By irradiating the plants with high light, a sharp decline in the quantum yield of PSII and PSII-dependent electron transport rate was observed in the *pao* mutant. On the contrary, the electron transport rates of both single and double overexpressor were only marginally affected in response to high light stress. The decrease in the ETR in the mutant can be attributed by overaccumulation of photodynamic pheophorbide a in the *pao* mutant. Limited availability of PAO, therefore leads to the formation of singlet oxygen from the pheophorbide via type II photosensitization reactions (Foote 1991) in response to high light stress. The accumulation of singlet oxygen in response to high light was observed by staining the high light-exposed plants with singlet oxygen sensor green (SOSG) (Ambastha et al. 2017). Analysis of the SOSG fluorescence indicates that minimum level of singlet oxygen is produced from the D26 plants due to the rapid opening of macrocycle ring of chlorine ring, which facilitated the further downstream degradation events. Consequently, maximum SOSG fluorescence was observed from the PAO mutant in high light condition.

Chlorophyll a fast fluorescence transient curve demonstrated early P rise in the D26 plants after 16 h of HL exposure. Further investigation on the polyphasic chlorophyll a fluorescence curve showed efficient transport of electrons from the PSII

to PSI which ensures the optimum working of electron transport even in high light conditions. The effective transport of electron through various electron acceptors can be attributed from the rises obtained after double normalization between I to P phase. Analysis of other fast fluorescence parameters suggest that the rate of electron transport per reaction center and the area which depicts the level of plastoquinone in D26 plants was only marginally affected by the high light stress

The impact of elevated singlet oxygen on the PSII apparatus can be seen by monitoring the NPQ and YNO values (Lu et al. 2017). Under stress conditions, the acidification of thylakoid lumen activates the xanthophylls cycle, which absorbs the excess energy and releases them in the form of heat (Niyogi 2002). But for the establishment of the proton gradient, the integrity of the membrane is crucial. Excess production of singlet oxygen at the membrane primarily target the polyunsaturated fatty acids that constitute the membrane (Birtic et al. 2011). Furthermore, the cell death and membrane leakage due to loss of functional lipids in the membrane allowed the uptake of Evans blue stain (Shumbe et al. 2016a).

It has been previously observed in *pao mutant* plants that due to disruption of PAO, its substrate pheophorbide a accumulate. Pheophorbide a is highly photodynamic in nature and after absorbing light goes to an excited state and on returning to ground state transfers energy to oxygen, in turn, generating singlet oxygen species (1O_2). Due to high light stress chlorophyll degradation occurs, pheophorbide a could accumulate leading to the generation of 1O_2 via type 2 photosensitization reaction. As compared to WT, the overexpressors accumulated reduced amount of photosensitizer pheophorbide a in high light- stressed plants. This led to reduced generation of 1O_2 in transgenic plants in stress conditions. As both PAO and RCCR enzymes form a complex during degradation (Hörtensteiner *et al.* 2010) so it was not possible to measure RCC accumulation during light stress. RCC is not usually detected in *Arabidopsis* WT plants, as is immediately degraded by RCCR, however in RCCR mutants RCC could be detected (Pruzunskia et al., 2007)

Peroxidation of membrane lipids is one of the phytotoxic consequences of oxidative stress (Kenyon and Duke, 1985; Duke and Kenyon, 1986; Gupta and Tripathy, 2000). Lipid peroxidation is a complex process where 1O_2 reacts directly

with the electron-dense polyunsaturated membrane lipids to form semi-stable hydroperoxides (Pryor, 1976). Singlet oxygen, the dominant active oxygen species produced from the tetrapyrrolic photosensitizers, i.e., biosynthetic and catabolic intermediates, is responsible for causing cellular damage. This was elucidated from the observation that the $^1\text{O}_2$ quencher histidine protected the photosynthetic membranes from the photosensitizer-induced damage. The superoxide scavenger SOD or OH^- scavenger formate failed to protect the same (Chakraborty and Tripathy, 1992a, b; Gupta and Tripathy, 1999). MDA production is considered as an index of lipid peroxidation. High-light stress-induced oxidative stress caused accumulation of Chl catabolites, which in turn induced photodynamic reactions causing membrane lipid peroxidation that resulted in accumulation of increased amounts of MDA in leaf tissues of WT and *pao* plants. In *PAO/RCCRx* plants due to reduced lipid peroxidation less, MDA was accumulated. Minimal amount of MDA was observed in *PAO/RCCRx* plants.

Our results clearly demonstrate the role of chlorophyll catabolic enzymes, i.e. PAO and RCCR in the efficient mobilization of the photodynamic Chl catabolites to non-photodynamic compounds, i.e., fluorescent chlorophyll catabolites to protect plants from oxidative stress. During stress conditions, the degradation of Chl increases that result in increased production of Chl catabolite pheophorbide a. Plants upregulate the PAO, a gene that is normally induced during senescence, for the safe disposal of photodynamic Chl catabolites to protect them from highly reactive $^1\text{O}_2$.

Double overexpressors were able to tolerate light stress better than single overexpressor (*PAOx*) plants. This is because both PAO and RCCR work in concert to degrade photodynamic pheophorbide a to non-photodynamic FCC.

Summary

Tetrapyrrole synthesis and degradation are highly regulated processes as some of the intermediates involved in the process are phototoxic in nature. During the chlorophyll biosynthesis, the evolution of light-dependent protochlorophyllide oxidoreductase c in higher plants allowed light-mediated conversion of photodynamic protochlorophyllide to chlorophyllide. Exposure of plants to high irradiance induces the formation of intermediate derived singlet oxygen by type II photosensitization reaction that causes photooxidative stress and thus reduced photosynthetic efficiency and the overall growth of the plant. Overexpression of PORC enzyme in *Arabidopsis* provides tolerance to plants against high light stress. Conversely, PORC knock-down that accumulate Pchlde generated more singlet oxygen in light.

The analysis of chlorophyll fluorescence parameters suggested that PORCx overexpressor were least affected by the singlet oxygen-induced photooxidative stress. On the other hand, *porC-2* mutant was severely affected by the high light stress. The singlet oxygen level after ALA treatment rapidly increased the SOSG fluorescence in the *porC-2* mutant after light exposure. Conversely, minimum SOSG fluorescence was observed in the PORC overexpressor. The singlet oxygen caused severe damage to the quantum yield of photosystem II, and the electron transport rates demonstrated that the accumulation of Pchlde derived singlet oxygen in the *porC-2* mutant damaged the photosynthetic apparatus. Presence of surplus PORC enzyme in the PORC overexpressor could efficiently photo-converted the dark accumulated Pchlde to Chlide, thereby reducing the concentration of the former. The reduced presence of the photosensitizer Pchlde in overexpressors generated lower amounts of singlet oxygen that caused smaller damage to the photosynthetic apparatus and cell death.

In the chlorophyll degradation pathway, the opening of the macrocyclic backbone of chlorine ring generated green colored photodynamic intermediate, pheophorbide a. It is the direct precursor of another photosensitizer, red chlorophyll catabolite. Their accumulation in plants causes severe necrotic lesions that follow runaway cell death phenotype. To reduce the severity of the stress, the overexpression of the enzymes that catalyze their conversion into a non-photodynamic form provided a solution to reduce the extent of photosensitizer-induced singlet oxygen production

in plants. The enzyme pheophorbide a oxygenase is a nuclear-encoded protein which is localized in the inner membrane of the chloroplast. It converts the chlorophyll a degradation product pheophorbide a to red chlorophyll catabolite (RCC) which is also photodynamic in nature. The RCCR, i.e., red chlorophyll catabolite reductase, generate primary fluorescent chlorophyll catabolite (pFCC) that is not photodynamic in nature. During stress conditions, extensive degradation of Chl a occurs that converts it to pheophorbide a that has to be immediately degraded to non-photodynamic compounds to prevent the generation of singlet oxygen.

In the present study, it is demonstrated that the genetic manipulation of the chlorophyll catabolic enzyme had no effect on the phenotype of the plants in control conditions. In high light stress conditions, the *pao* mutant had maximal damage to the photosynthetic apparatus, i.e., severe impairment of PSII and photosynthetic electron transport. The over-expression of PAO alone that converted pheophorbide a to RCC had reduced production of singlet oxygen and caused less damage to the photosynthetic apparatus. Better protection from photo-oxidative stress was obtained when both the enzymes involved in chlorophyll catabolism, i.e., *pao* and RCCR were overexpressed together. Exposure of these double over expressers to high light for 16 h caused marginal impairment of on the quantum yield and electron transport rates. This was effectively due to reduced accumulation of photodynamic chlorophyll catabolic products in the double overexpressors. On the contrary, *pao* mutant exhibited prominent photobleaching of leaves after high light stress. Further investigations suggested that *pao* mutant accumulated higher level of singlet oxygen than any other plant type. The excess singlet oxygen is generated due to limited availability of PAO enzyme, which catalyzes the key step in the chlorophyll degradation pathway. The opening of the macrocyclic ring by the PAO enzyme provides a characteristic structural basis for further downstream degradation events. In the absence of PAO enzyme, the accumulation of photodynamic photosensitizer induced singlet oxygen formation upon exposure to high light stress. The decrease in the electron transport rates and quantum yield of PSII correlate that singlet oxygen produced through the photodynamic intermediate readily attacks the PSII machinery and impair its function. Further analysis of the chlorophyll fast fluorescence parameters suggested that the accumulation of singlet oxygen in response to high light majorly target the membrane-bound lipids and proteins. Intensive peroxidation of the

membrane lipids severely altered the integrity of the membrane and caused cell death that allowed the inclusion of Evans blue dye in the *pao* mutant. In this study, we have observed that overexpression of both PAO and RCCR was necessary to tolerate high light-induced singlet oxygen stress and thus reduced cell death in the transgenic plants.

Together from this study, we demonstrate that reduction in the level of chlorophyll anabolic and catabolic photodynamic intermediates can be achieved by overexpressing their respective enzymes which enable the plants to tolerate the singlet oxygen-induced photooxidative stress. Therefore, implementation of this strategy could be applied to the crop plants to minimize singlet oxygen generation and cell death to protect photosynthesis and crop productivity.

References

- Ambastha V, Sopory SK, Tiwari BS, Tripathy BC (2017) Photo-modulation of programmed cell death in rice leaves triggered by salinity. *Apoptosis* 22:41–56. doi: 10.1007/s10495-016-1305-7
- Armstrong GA, Runge S, Frick G, et al (1995a) Identification of NADPH:Protochlorophyllide Oxidoreductases A and B: A Branched Pathway for Light-Dependent Chlorophyll Biosynthesis in *Arabidopsis thaliana*. *Plant Physiol* 108:1505–1517. doi: 10.1104/pp.108.4.1505
- Armstrong GA, Runge S, Frick G, et al (1995b) Identification of NADPH:protochlorophyllide oxidoreductases A and B: a branched pathway for light-dependent chlorophyll biosynthesis in *Arabidopsis thaliana*. *Plant Physiol* 108:1505–1517. doi: 10.1104/pp.108.4.1505
- Aro EM, Virgin I, Andersson B (1993) Photoinhibition of Photosystem II. Inactivation, protein damage and turnover. *BBA - Bioenerg* 1143:113–134. doi: 10.1016/0005-2728(93)90134-2
- Asada K (2006) Production and Scavenging of Reactive Oxygen Species in Chloroplasts and Their Functions 1. 141:391–396. doi: 10.1104/pp.106.082040.Several
- Asada K (1984) Chloroplasts: Formation of Active Oxygen and Its Scavenging. *Methods Enzymol* 105:422–429. doi: 10.1016/S0076-6879(84)05059-X
- Baker NR (2008) Chlorophyll Fluorescence: A Probe of Photosynthesis In Vivo. *Annu Rev Plant Biol* 59:89–113. doi: 10.1146/annurev.arplant.59.032607.092759
- Baroli I, Melis A (1998) Photoinhibitory damage is modulated by the rate of photosynthesis and by the photosystem II light-harvesting chlorophyll antenna size. *Planta* 205:288–296. doi: 10.1007/s004250050323
- Baroli I, Niyogi KK, Barber J, Heifetz P (2000) Molecular genetics of xanthophyll-dependent photoprotection in green algae and plants. *Philos Trans R Soc B Biol Sci* 355:1385–1394. doi: 10.1098/rstb.2000.0700

- Birtic S, Ksas B, Genty B, et al (2011) Using spontaneous photon emission to image lipid oxidation patterns in plant tissues. *Plant J* 67:1103–1115. doi: 10.1111/j.1365-313X.2011.04646.x
- Björkman O, Demmig B (1987) Photon yield of O₂ evolution and chlorophyll fluorescence characteristics at 77 K among vascular plants of diverse origins. *Planta* 170:489–504. doi: 10.1007/BF00402983
- Bradford M (1976) A rapid and sensitive method for the quantitation of microgram quantities of protein utilizing the principle of protein-dye binding. *Anal Biochem* 72:248–254. doi: 10.1016/0003-2697(76)90527-3
- Burke JJ (2008) Variation among Species in the Temperature Dependence of the Reappearance of Variable Fluorescence following Illumination. *Plant Physiol* 93:652–656. doi: 10.1104/pp.93.2.652
- Busch TM, Cengel KA, Finlay JC (2009) Pheophorbide a as a photosensitizer in photodynamic therapy: In vivo considerations. *Cancer Biol Ther* 8:540–542. doi: 10.4161/cbt.8.6.8067
- Chakraborty N, Tripathy BC (1992) Involvement of Singlet Oxygen in 5-Aminolevulinic Acid-Induced Photodynamic Damage of Cucumber (*Cucumis sativus* L.) Chloroplasts. *Plant Physiol* 98:7–11. doi: 10.1104/pp.98.1.7
- Chakraborty N, Tripathy BC (1991) Involvement of Singlet Oxygen in 5-Aminolevulinic Acid-Induced Photodynamic Damage of Cucumber (*Cucumis sativus* L.) Chloroplasts. *Plant Physiol* 98:7–11. doi: 10.1104/pp.98.1.7
- Curty C, Engel N, Gossauer A (1995) Evidence for a monooxygenase-catalyzed primary process in the catabolism of chlorophyll. *FEBS Lett* 364:41–44. doi: 10.1016/0014-5793(95)00348-D
- D'Alessandro S, Havaux M (2019) Sensing β - carotene oxidation in photosystem II to master plant stress tolerance. *New Phytol*. doi: 10.1111/nph.15924
- Dahlin C, Aronsson H, Timko M (2002) The importance of protein surface charge for catalytic activity and the interaction of NADPH:Pchlide oxidoreductase (POR) with chloroplast membranes as revealed by alanine scanning. *Entomol Exp Appl*

103:239–248. doi: 10.1023/A

- Dall'Osto L, Holt NE, Kaligotla S, et al (2012) Zeaxanthin protects plant photosynthesis by modulating chlorophyll triplet yield in specific light-harvesting antenna subunits. *J Biol Chem* 287:41820–41834. doi: 10.1074/jbc.M112.405498
- Dat J, Vandenameele S, Vranova' E, et al (2000) Dual action of the active oxygen species during plant stress responses. *Cell Mol Life Sci* 57:779–795. doi: 10.1176/ajp.88.1.103
- Dehesh K, Ryberg M (1985) The NADPH-protochlorophyllide oxidoreductase is the major protein constituent of prolamellar bodies in wheat (*Triticum aestivum* L.). *Planta* 164:396–399. doi: 10.1007/BF00402952
- Duggan J, Gassman M (2008) Induction of Porphyrin Synthesis in Etiolated Bean Leaves by Chelators of Iron. *Plant Physiol* 53:206–215. doi: 10.1104/pp.53.2.206
- Edelman M, Mattoo AK (2008) D1-protein dynamics in photosystem II: The lingering enigma. *Photosynth Res* 98:609–620. doi: 10.1007/s11120-008-9342-x
- Farmer EE, Mueller MJ (2013) ROS-Mediated Lipid Peroxidation and RES-Activated Signaling. *Annu Rev Plant Biol* 64:429–450. doi: 10.1146/annurev-arplant-050312-120132
- Fischer BB, Ledford HK, Wakao S, et al (2012) SINGLET OXYGEN RESISTANT 1 links reactive electrophile signaling to singlet oxygen acclimation in *Chlamydomonas reinhardtii*. *Proc Natl Acad Sci* 109:E1302–E1311. doi: 10.1073/pnas.1116843109
- Foote CS (1991) Definition of Type I and Type II. *Photochem Photobiol* 54:659. doi: 10.1111/j.1751-1097.1991.tb02071.x
- Foyer CH, Shigeoka S (2011) Understanding Oxidative Stress and Antioxidant Functions to Enhance Photosynthesis. *Plant Physiol* 155:93–100. doi: 10.1104/pp.110.166181
- Gamborg OL, Miller RA, Ojima K (1968) Nutrient requirements of suspension cultures of soybean root cells. *Exp Cell Res* 50:151–158. doi: 10.1016/0014-

4827(68)90403-5

Gorman AA, Rodgers MAJ (1992) New trends in photobiology. Current perspectives of singlet oxygen detection in biological environments. *J Photochem Photobiol* 14:159–176. doi: 10.1016/1011-1344(92)85095-C

Gray J, Close PS, Briggs SP, Johal GS (1997) A novel suppressor of cell death in plants encoded by the *Lls1* gene of maize. *Cell* 89:25–31. doi: 10.1016/S0092-8674(00)80179-8

Gutiérrez J, González-pérez S, García-garcía F, et al (2014) Programmed cell death activated by Rose Bengal in *Arabidopsis thaliana* cell suspension cultures requires functional chloroplasts. *J Exp Bot* 65:3081–3095. doi: 10.1093/jxb/eru151

Gutiérrez J, González-Pérez S, García-García F, et al (2011) Does singlet oxygen activate cell death in *Arabidopsis* cell suspension cultures? Analysis of the early transcriptional defence responses to high light stress. *Plant Signal Behav* 6:1937–42. doi: 10.4161/psb.6.12.18264

Hamdani S, Qu M, Xin CP, et al (2015) Variations between the photosynthetic properties of elite and landrace Chinese rice cultivars revealed by simultaneous measurements of 820nm transmission signal and chlorophyll a fluorescence induction. Elsevier GmbH.

Hankamer B, Barber J, Boekema EJ (1997) Structure and membrane organization of photosystem II in green plants. *Annu Rev Plant Physiol Plant Mol Biol* 48:641–71

Hirashima M, Tanaka R, Tanaka A (2009) Light-independent cell death induced by accumulation of pheophorbide a in *arabidopsis thaliana*. *Plant Cell Physiol* 50:719–729. doi: 10.1093/pcp/pcp035

Hodges DM, DeLong JM, Forney CF, Prange RK (1999) Improving the thiobarbituric acid-reactive-substances assay for estimating lipid peroxidation in plant tissues containing anthocyanin and other interfering compounds. *Planta* 207:604–611. doi: 10.1007/s004250050524

- Hörtensteiner S, Kräutler B (2011) Biochimica et Biophysica Acta Chlorophyll breakdown in higher plants ☆. *BBA - Bioenerg* 1807:977–988. doi: 10.1016/j.bbabi.2010.12.007
- Hörtensteiner S, Vicentini F, Matile P (1995) Chlorophyll breakdown in senescent cotyledons of rape, *Brassica napus* L.: Enzymatic cleavage of phaeophorbide a in vitro. *New Phytol* 129:237–246. doi: 10.1111/j.1469-8137.1995.tb04293.x
- Hörtensteiner S, Wüthrich KL, Matile P, et al (2002) The Key Step in Chlorophyll Breakdown in Higher Plants. *J Biol Chem* 273:15335–15339. doi: 10.1074/jbc.273.25.15335
- Hukmani P, Tripathy BC (1992) Spectrofluorometric estimation of intermediates of chlorophyll biosynthesis: Protoporphyrin IX, Mg-protoporphyrin, and protochlorophyllide. *Anal Biochem* 206:125–130. doi: 10.1016/S0003-2697(05)80021-1
- Kandoi D, Mohanty S, Govindjee, Tripathy BC (2016) Towards efficient photosynthesis: overexpression of *Zea mays* phosphoenolpyruvate carboxylase in *Arabidopsis thaliana*. *Photosynth Res* 130:47–72. doi: 10.1007/s11120-016-0224-3
- Kim C, Meskauskiene R, Zhang S, et al (2012) Chloroplasts of *Arabidopsis* Are the Source and a Primary Target of a Plant-Specific Programmed Cell Death Signaling Pathway. *Plant Cell* 24:3026–3039. doi: 10.1105/tpc.112.100479
- Krautler B (2008) Chlorophyll breakdown and chlorophyll catabolites in leaves and fruit †. *Photochem Photobiol Sci* 7:. doi: 10.1039/b802356p
- Krautler B, Miihlecker W, Anderl M (1997) Breakdown of Chlorophyll, Partial Synthesis of a Putative Intermediary Catabolite. 80:1355–1362
- Kwon CT, Kim SH, Song G, et al (2017) Two NADPH: Protochlorophyllide Oxidoreductase (POR) Isoforms Play Distinct Roles in Environmental Adaptation in Rice. *Rice* 10:1–14. doi: 10.1186/s12284-016-0141-2
- Lee KP, Kim C, Landgraf F, Apel K (2007) EXECUTER1- and EXECUTER2-dependent transfer of stress-related signals from the plastid to the nucleus of

- Arabidopsis thaliana*. Proc Natl Acad Sci U S A 104:10270–10275. doi: 10.1073/pnas.0702061104
- León IP De, Montesano M (2013) Activation of Defense Mechanisms against Pathogens in Mosses and Flowering Plants. Int J Mol Sci 14:3178–3200. doi: 10.3390/ijms14023178
- Loll B, Kern J, Saenger W, et al (2005) Towards complete cofactor arrangement in the ρ resolution structure of photosystem II. Nat 438:0–4. doi: 10.1038/nature04224
- Lu T, Meng Z, Zhang G, et al (2017) Sub-high Temperature and High Light Intensity Induced Irreversible Inhibition on Photosynthesis System of Tomato Plant (*Solanum lycopersicum* L.). Front Plant Sci 8:1–16. doi: 10.3389/fpls.2017.00365
- Lu T, Yu H, Li Q, et al (2019) Improving Plant Growth and Alleviating Photosynthetic Inhibition and Oxidative Stress From Low-Light Stress With Exogenous GR24 in Tomato (*Solanum lycopersicum* L.) Seedlings. Front Plant Sci 10:1–13. doi: 10.3389/fpls.2019.00490
- Mach JM, Castillo AR, Hoogstraten R, Greenberg JT (2001) The *Arabidopsis*-accelerated cell death gene *ACD2* encodes red chlorophyll catabolite reductase and suppresses the spread of disease symptoms. Proc Natl Acad Sci 98:771–776. doi: 10.1073/pnas.98.2.771
- Makhadmeh GN, Abdul Aziz A (2018) Photodynamic application of protoporphyrin IX as a photosensitizer encapsulated by silica nanoparticles. Artif Cells, Nanomedicine Biotechnol 46:S1043–S1046. doi: 10.1080/21691401.2018.1528982
- Mamedov M, Govindjee, Nadtochenko V, Semenov A (2015) Primary electron transfer processes in photosynthetic reaction centers from oxygenic organisms. Photosynth Res 125:51–63. doi: 10.1007/s11120-015-0088-y
- Masuda T, Fusada N, Oosawa N, et al (2003) Functional Analysis of Isoforms of NADPH:Protochlorophyllide Oxidoreductase (POR), PORB and PORC, in *Arabidopsis thaliana*. Plant Cell Physiol 44:963–974. doi: 10.1093/pcp/pcg128

- Meskauskiene R, Nater, M. Goslings D, et al (2001) FLU: A negative regulator of chlorophyll biosynthesis in *Arabidopsis thaliana*. *Proc Natl Acad Sci* 98:12826–12831. doi: 10.1073/pnas.221252798
- Mohapatra A, Tripathy BC (2007) Differential distribution of chlorophyll biosynthetic intermediates in stroma, envelope and thylakoid membranes in *Beta vulgaris*. *Photosynth Res* 94:401–410. doi: 10.1007/s11120-007-9209-6
- Mohapatra A, Tripathy BC (2002) Detection of protoporphyrin IX in envelope membranes of pea chloroplasts. *Biochem Biophys Res Commun* 299:751–754. doi: 10.1016/S0006-291X(02)02703-1
- Moulin M, McCormac AC, Terry MJ, Smith AG (2008) Tetrapyrrole profiling in *Arabidopsis* seedlings reveals that retrograde plastid nuclear signaling is not due to Mg-protoporphyrin IX accumulation. *Proc Natl Acad Sci* 105:15178–15183. doi: 10.1073/pnas.0803054105
- Muchowicz A, Gabrysiak M, Winiarska M, et al (2011) Aminolevulinic Acid (ALA) as a Prodrug in Photodynamic Therapy of Cancer. *Molecules* 16:4140–4164. doi: 10.3390/molecules16054140
- Mueller MJ, Mène-Saffrané L, Grun C, et al (2006) Oxylipin analysis methods. *Plant J* 45:472–489. doi: 10.1111/j.1365-313X.2005.02614.x
- Murakami Y, Tsuyama M, Kobayashi Y, et al (2002) Trienoic fatty acids and plant tolerance of temperature. *Science* (80-) 287:476–479
- Muramoto T, Kohchi T, Yokota A, et al (1999) The *Arabidopsis* photomorphogenic mutant *hy1* is deficient in phytochrome chromophore biosynthesis as a result of a mutation in a plastid heme oxygenase. *Plant Cell* 11:335–48
- Nishiyama Y, Yamamoto H, Allakhverdiev SI, et al (2001) Oxidative stress inhibits the repair of photodamage.pdf. 20:1–8
- Niyogi KK (2002) PHOTOPROTECTION REVISITED: Genetic and Molecular Approaches . *Annu Rev Plant Physiol Plant Mol Biol* 50:333–359. doi: 10.1146/annurev.arplant.50.1.333
- Oosawa N, Masuda T, Awai K, et al (2000) Identification and light-induced

- expression of a novel gene of NADPH-protochlorophyllide oxidoreductase isoform in *Arabidopsis thaliana*. *FEBS Lett* 474:133–136. doi: 10.1016/S0014-5793(00)01568-4
- op den Camp RGL (2003) Rapid Induction of Distinct Stress Responses after the Release of Singlet Oxygen in *Arabidopsis*. *Plant Cell* 15:2320–2332. doi: 10.1105/tpc.014662
- Pattanayak GK, Tripathy BC (2002) Catalytic function of a novel protein protochlorophyllide oxidoreductase C of *Arabidopsis thaliana*. *Biochem Biophys Res Commun* 291:921–924. doi: 10.1006/bbrc.2002.6543
- Pattanayak GK, Tripathy BC (2011) Overexpression of Protochlorophyllide Oxidoreductase C Regulates Oxidative Stress in *Arabidopsis*. *PLoS One* 6:. doi: 10.1371/journal.pone.0026532
- Pintó-Marijuan M, Munné-Bosch S (2014) Photo-oxidative stress markers as a measure of abiotic stress-induced leaf senescence: Advantages and limitations. *J Exp Bot* 65:3845–3857. doi: 10.1093/jxb/eru086
- Pontier D, Albrieux C, Joyard J, et al (2007) Knock-out of the magnesium protoporphyrin IX methyltransferase gene in *Arabidopsis*: Effects on chloroplast development and on chloroplast-to-nucleus signaling. *J Biol Chem* 282:2297–2304. doi: 10.1074/jbc.M610286200
- Porra RJ, Thompson WA, Kriedemann PE (1989) Determination of accurate extinction coefficients and simultaneous equations for assaying chlorophylls a and b extracted with four different solvents: verification of the concentration of chlorophyll standards by atomic absorption spectroscopy. *BBA - Bioenerg* 975:384–394. doi: 10.1016/S0005-2728(89)80347-0
- Pospíšil P, Skotnica J, Nauš J (1998) Low and high temperature dependence of minimum F₀ and maximum F(M) chlorophyll fluorescence in vivo. *Biochim Biophys Acta - Bioenerg* 1363:95–99. doi: 10.1016/S0005-2728(97)00095-9
- Poulson R, Polglase WJ (1974) Aerobic and anaerobic coproporphyrinogenase activities in extracts from *Saccharomyces cerevisiae*. Purification and characterization. *J Biol Chem* 249:6367–6371

- Pruzinska A (2005) Chlorophyll Breakdown in Senescent Arabidopsis Leaves. Characterization of Chlorophyll Catabolites and of Chlorophyll Catabolic Enzymes Involved in the Degreening Reaction. *Plant Physiol* 139:52–63. doi: 10.1104/pp.105.065870
- Pruzinska A, Anders I, Aubry S, et al (2007) In Vivo Participation of Red Chlorophyll Catabolite Reductase in Chlorophyll Breakdown. *Plant Cell Online* 19:369–387. doi: 10.1105/tpc.106.044404
- Pruzinska A, Tanner G, Anders I, et al (2003) Chlorophyll breakdown: Pheophorbide a oxygenase is a Rieske-type iron-sulfur protein, encoded by the accelerated cell death 1 gene. *Proc Natl Acad Sci* 100:15259–15264. doi: 10.1073/pnas.2036571100
- Ramel F, Ksas B, Akkari E, et al (2013) Light-induced acclimation of the Arabidopsis chlorina1 mutant to singlet oxygen. *Plant Cell* 25:1445–1462. doi: 10.1105/tpc.113.109827
- Rebeiz CA, Zouhoor AM, Mayasich JM, et al (1988) Photodynamic herbicides . Recent developments and molecular basis of selectivity. *CRC Crit Rev Plant Sci* 6:385–436. doi: 10.1080/07352688809382256
- Reinbothe S, Gray J, Rustgi S, et al (2015) Cell growth defect factor 1 is crucial for the plastid import of NADPH:protochlorophyllide oxidoreductase A in Arabidopsis thaliana . *Proc Natl Acad Sci* 112:5838–5843. doi: 10.1073/pnas.1506339112
- Rodoni S, Mühlecker W, Anderl M, et al (1997) Chlorophyll Breakdown in Senescent Chloroplasts'. *Plant Physiol* 669–676
- Rossel JB, Wilson PB, Hussain D, et al (2007) Systemic and Intracellular Responses to Photooxidative Stress in Arabidopsis. 19:4091–4110. doi: 10.1105/tpc.106.045898
- Ruban A V., Johnson MP, Duffy CDP (2012) The photoprotective molecular switch in the photosystem II antenna. *Biochim Biophys Acta - Bioenerg* 1817:167–181. doi: 10.1016/j.bbabi.2011.04.007

- Sachar M, Anderson KE, Ma X (2016) Protoporphyrin IX: the Good, the Bad, and the Ugly. *J Pharmacol Exp Ther* 356:267–275. doi: 10.1124/jpet.115.228130
- Shao N, Duan GY, Bock R (2013) A mediator of singlet oxygen responses in *Chlamydomonas reinhardtii* and *Arabidopsis* identified by a luciferase-based genetic screen in algal cells.
- Shevela D, Eaton-rye JJ, Shen J (2012) Biochimica et Biophysica Acta Photosystem II and the unique role of bicarbonate : A historical perspective ☆. *BBA - Bioenerg* 1817:1134–1151. doi: 10.1016/j.bbabi.2012.04.003
- Shook, F. C., & Abakerli RB (1984). (1984) Characterization of Singlet Oxygen. *Methods* 105:36–47
- Shumbe L, Chevalier A, Legeret B, et al (2016a) Singlet Oxygen-Induced Cell Death in *Arabidopsis* under High-Light Stress Is Controlled by OXI1 Kinase 1. *Plant Physiol* 170:1757–1771. doi: 10.1104/pp.15.01546
- Shumbe L, Chevalier A, Legeret B, et al (2016b) Singlet Oxygen-Induced Cell Death in *Arabidopsis* under High Light Stress is Controlled by OXI1 Kinase. *Plant Physiol* 170:1757–1771. doi: 10.1104/pp.15.01546
- Sies H, Menck CFM (1992) Singlet oxygen induced DNA damage. *Mutat Res DNAging* 275:367–375. doi: 10.1016/0921-8734(92)90039-R
- Sperling U, Van Cleve B, Frick G, et al (1997) Overexpression of light-dependent PORA or PORB in plants depleted of endogenous POR by far-red light enhances seedling survival in white light and protects against photooxidative damage. *Plant J* 12:649–658. doi: 10.1046/j.1365-313X.1997.d01-11.x
- Stemler A (1973) Bicarbonate Ion as Oxygen Evolution ' Critical Factor in Photosynthetic. 119–123
- Stirbet A, Lazár D, Kromdijk J, Govindjee (2018) Chlorophyll a fluorescence induction: Can just a one-second measurement be used to quantify abiotic stress responses? *Photosynthetica* 56:86–104. doi: 10.1007/s11099-018-0770-3
- Strand A, Asami T, Ecker JR (2003) Chloroplast communication triggered by accumulation of Mg-protoporphyrin. *Nature* 421:79–83. doi:

10.1038/nature01250.1.

Strasser R, Tsimilli-Michael M, Srivastava A (2005) Analysis of the Fluorescence Transient Reto

Stratton SP, Liebler DC (1997) Determination of Singlet Oxygen-Specific versus Radical-Mediated Lipid Peroxidation in Photosensitized Oxidation of Lipid Bilayers : Effect of -Carotene. *Biochemistry* 36:12911–12920. doi: 10.1021/bi9708646

Stroebel D, Choquet Y, Popot J, Picot D (2003) An atypical haem in the cytochrome b 6 f complex. 413–418

Su Q, Armstrong G, Apel K (2001) POR C of *Arabidopsis thaliana* : a third light- and NADPH-dependent protochlorophyllide oxidoreductase that is differentially regulated by light. *Plant Mol Biol* 47:805–813

Suh H, Kim CS, Jung J (2000) Cytochrome b 6 / f Complex as an Indigenous Photodynamic Generator of Singlet Oxygen in Thylakoid Membranes. *Photochem Photobiol* 71:103–109

Tanaka R, Hirashima M, Satoh S, Tanaka A (2003) The *Arabidopsis*-accelerated cell death Gene *ACD1* is Involved in Oxygenation of Pheophorbide a: Inhibition of the Pheophorbide a Oxygenase Activity does not Lead to the “Stay-Green” Phenotype in *Arabidopsis*. *Plant Cell Physiol* 44:1266–1274. doi: 10.1093/pcp/pcg172

Triantaphylides C, Krischke M, Hoerberichts FA, et al (2008a) Singlet Oxygen Is the Major Reactive Oxygen Species Involved in Photooxidative Damage to Plants. *Plant Physiol* 148:960–968. doi: 10.1104/pp.108.125690

Triantaphylides C, Krischke M, Hoerberichts FA, et al (2008b) Singlet Oxygen Is the Major Reactive Oxygen Species Involved in Photooxidative Damage to Plants. *Plant Physiol* 148:960–968. doi: 10.1104/pp.108.125690

Tripathy BC, Chakraborty N (1991) 5-Aminolevulinic Acid Induced Photodynamic Damage of the Photosynthetic Electron Transport Chain of Cucumber (*Cucumis sativus* L.) Cotyledons. *Plant Physiol* 96:761–767. doi: 10.1104/pp.96.3.761

- Tripathy BC, Mohapatra A, Gupta I (2007) Impairment of the photosynthetic apparatus by oxidative stress induced by photosensitization reaction of protoporphyrin IX. *Biochim Biophys Acta - Bioenerg* 1767:860–868. doi: 10.1016/j.bbabi.2007.03.008
- Tripathy BC, Pattanayak G (2010) Singlet Oxygen-Induced Oxidative Stress in Plants. In: Rebeiz CA, Benning C, Bohnert HJ, et al. (eds) *The Chloroplast: Basics and Applications*. Springer Netherlands, Dordrecht, pp 397–412
- Valdes P, Bekelis K, Harris B, et al (2014) NIH Public Access. *Neurosurgery* 10:74–83. doi: 10.1227/NEU.000000000000117.5-Aminolevulinic
- Vass I (2011) Role of charge recombination processes in photodamage and photoprotection of the photosystem II complex. *Physiol Plant* 142:6–16. doi: 10.1111/j.1399-3054.2011.01454.x
- von Caemmerer S, Farquhar GD (1981) Some relationships between the biochemistry of photosynthesis and the gas exchange of leaves. *Planta* 153:376–387. doi: 10.1007/BF00384257
- Wagner D, Przybyla D, Camp R Den, et al (2004) The Genetic Basis of Singlet Oxygen – Induced Stress Responses of *Arabidopsis thaliana*. 1183–1186
- Wellburn AR, Lichtenthaler H (1984) Formulae and Program to Determine Total Carotenoids and Chlorophylls A and B of Leaf Extracts in Different Solvents. *Adv Photosynth Res* II:9–12. doi: 10.1007/978-94-017-6368-4_3
- Wu FH, Shen SC, Lee LY, et al (2009) Tape-arabidopsis sandwich - A simpler arabidopsis protoplast isolation method. *Plant Methods* 5:1–10. doi: 10.1186/1746-4811-5-16
- Wüthrich KL, Bovey L, Hunziker PE, et al (2000) Molecular cloning, functional expression and characterisation of RCC reductase involved in chlorophyll catabolism. *Plant J* 21:189–198. doi: 10.1046/j.1365-3113.2000.00667.x
- Yao N, Greenberg JT (2006) *Arabidopsis ACCELERATED CELL DEATH2* Modulates Programmed Cell Death. 18:397–411. doi: 10.1105/tpc.105.036251.1
- Zhan W, Liu J, Pan Q, et al (2019) An allele of *Zm <scp>PORB</scp> 2* encoding

a protochlorophyllide oxidoreductase promotes tocopherol accumulation in both leaves and kernels of maize. *Plant J* tpj.14432. doi: 10.1111/tpj.14432

Appendix

Research publication and Conferences attended

Research article

1. Chauhan G, Tripathy B. C. **Role of Protochlorophyllide Oxidoreductase C in Protection of Plants from Singlet Oxygen-Induced Oxidative Stress.** Biosc.Biotech.Res.Comm. 2019;12(2).

Conferences attended

1. **National Conference on ‘Impact of Climate Change on Indian Agriculture and plant productivity’ organised by School of Life Sciences, Jawaharlal Nehru University, New Delhi**
2. **International Conference on Plant Genetics and Genomics ‘Next Gen Crops for Sustainable Agriculture’ held in Chandigarh, India**

WT

PORCx

porC-2



Figure 1. Phenotype of *Arabidopsis* WT, Protochlorophyllide C oxidoreductase C overexpressor (PORCx) and known-down mutant of PORC (*porC-2*) plants. Plants were grown at 21⁰C under 10h L and 14h D photoperiod in cool-white-fluorescent light (100 $\mu\text{mol photons m}^{-2} \text{s}^{-1}$) for 5 weeks.

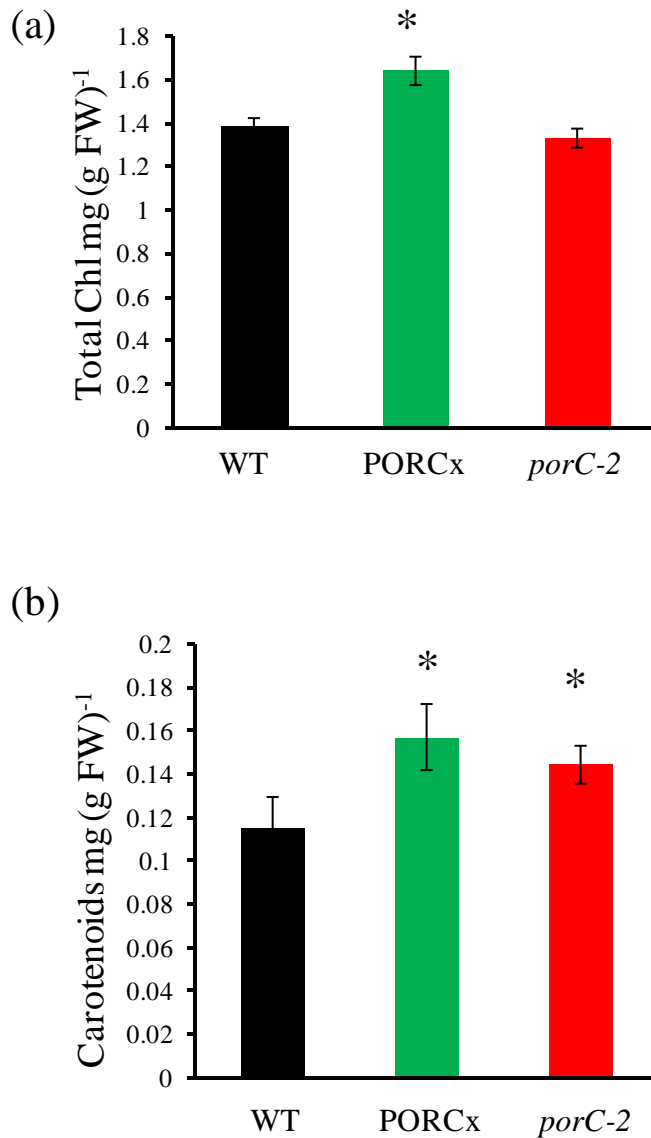


Figure 2. Pigment content of *Arabidopsis* WT, PORCx and *porC-2* mutant plants. Plants were grown at 21⁰C under 10h L and 14h D photoperiod in cool-white-fluorescent light (100 $\mu\text{mol photons m}^{-2} \text{s}^{-1}$) for three weeks and their (a) Chlorophyll and (b) Carotenoids contents were measured. Each data point is an average of six replicates. The error bar represent standard error ($\pm\text{SE}$). Asterisk indicate significant difference determined by *t* test (* $P < 0.05$).

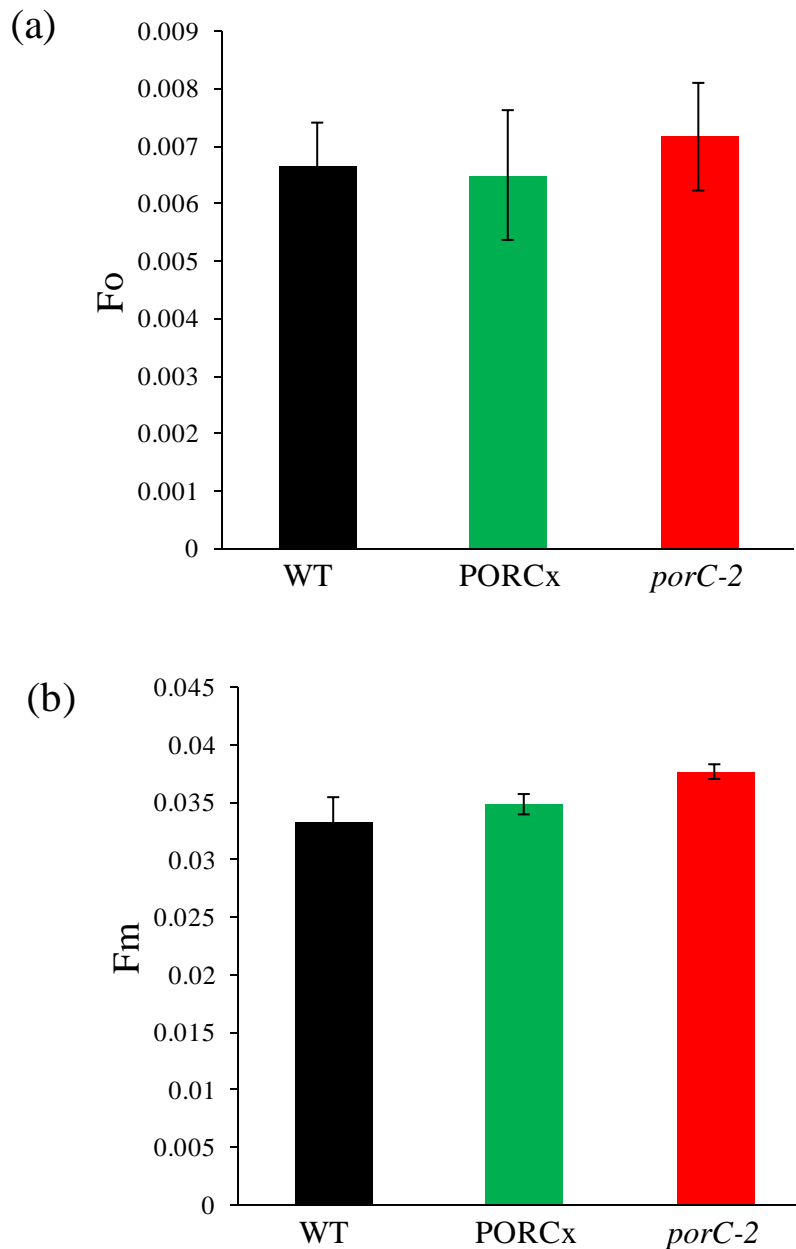


Figure 3. Chlorophyll a fluorescence yield of WT, PORCx and *porC-2* plants. Plants were grown at 21⁰C under 10h L and 14h D photoperiod in cool-white-fluorescent light (100 $\mu\text{mol photons m}^{-2} \text{s}^{-1}$) for 5 weeks. Plants were dark-adapted for 20 min. The chlorophyll a fluorescence parameters (a) Minimum fluorescence (F_o) (b) Maximum fluorescence (F_m) were calculated using Dual-PAM 100 fluorometer (Walz, Germany). Each data point is the average of six replicates and error bar represents $\pm\text{SE}$.

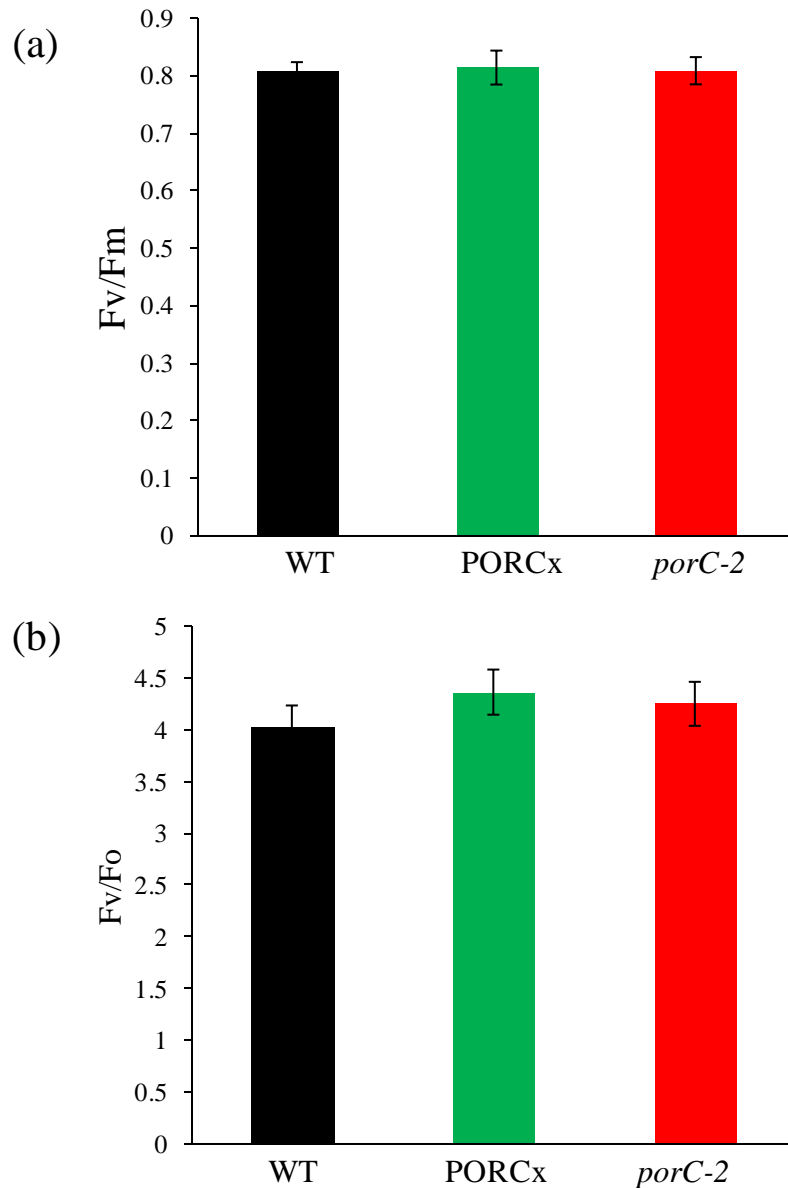


Figure 4. Chlorophyll a fluorescence parameters of WT, PORCx and *porC-2* plants. Plants were grown at 21°C under 10h L and 14h D photoperiod in cool-white-fluorescent light (100 $\mu\text{mol photons m}^{-2} \text{s}^{-1}$) for 5 weeks. Plants were dark-adapted for 20 min. The chlorophyll a fluorescence parameters (a) the ratio of variable fluorescence to maximum fluorescence (F_v/F_m), and (b) the ratio of variable to minimum chlorophyll fluorescence (F_v/F_o) were measured using Dual-PAM 100 fluorometer (Walz, Germany). Each data point is the average of six replicates and error bar represents $\pm\text{SE}$.

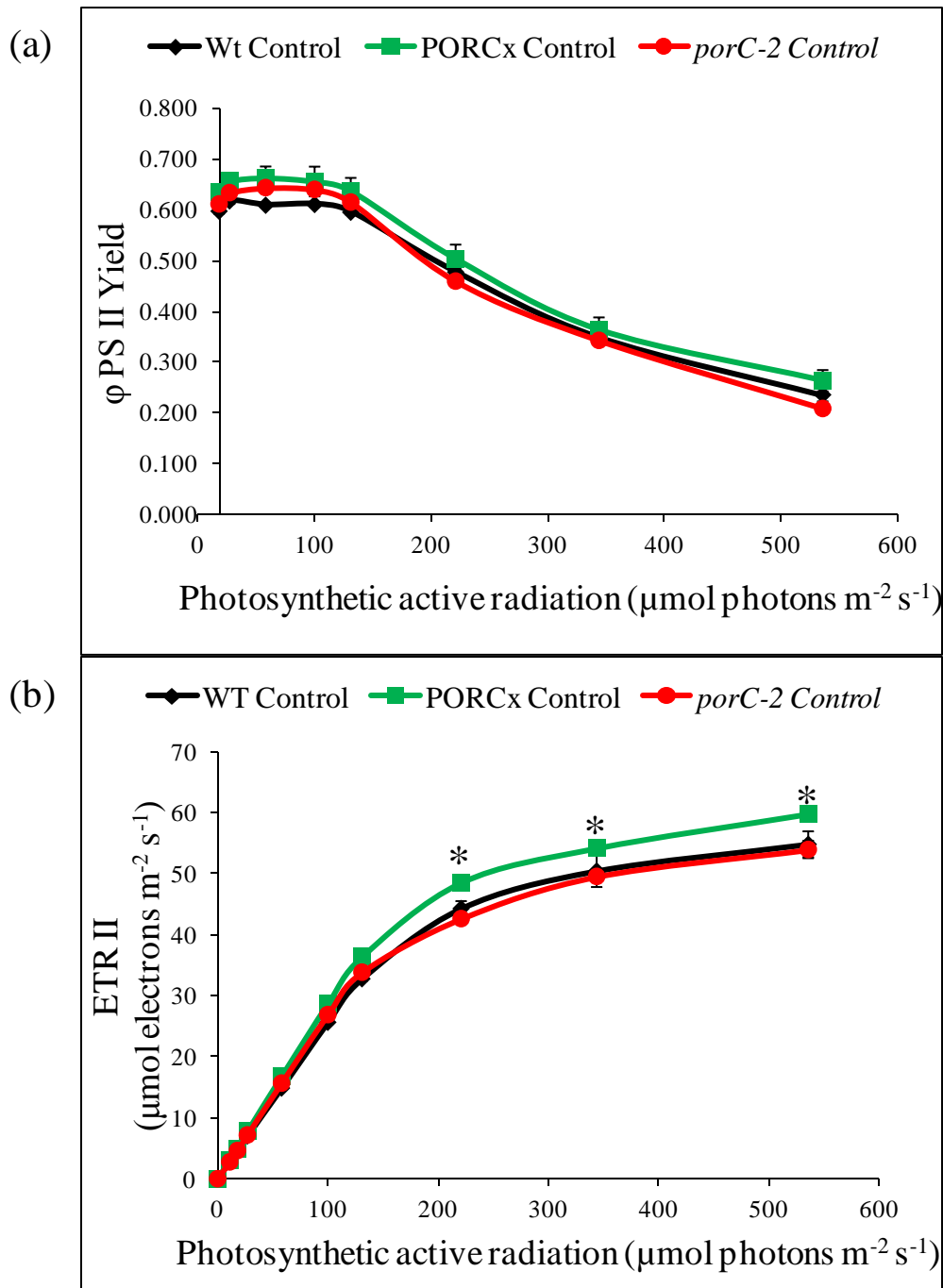


Figure 5. Quantum yield of PSII (ϕ PSII) and Electron transport rate (ETR) in WT, PORCx and *porC-2* mutant plants. Plants were grown at 21°C under 10h L and 14h D photoperiod in cool-white-fluorescent light ($100 \mu\text{mol photons m}^{-2} \text{s}^{-1}$) for 5 weeks. Plants were dark-adapted for 20 min. The chlorophyll a fluorescence parameters (a) Quantum yield of PSII (ϕ PSII), and (b) PSII-dependent electron transport rates were determined by using Dual PAM 100 fluorometer as in materials and methods. Each data point is the average of six replicates and error bar represents \pm SE. Asterisk indicate significant difference determined by *t* test (* $P < 0.05$).

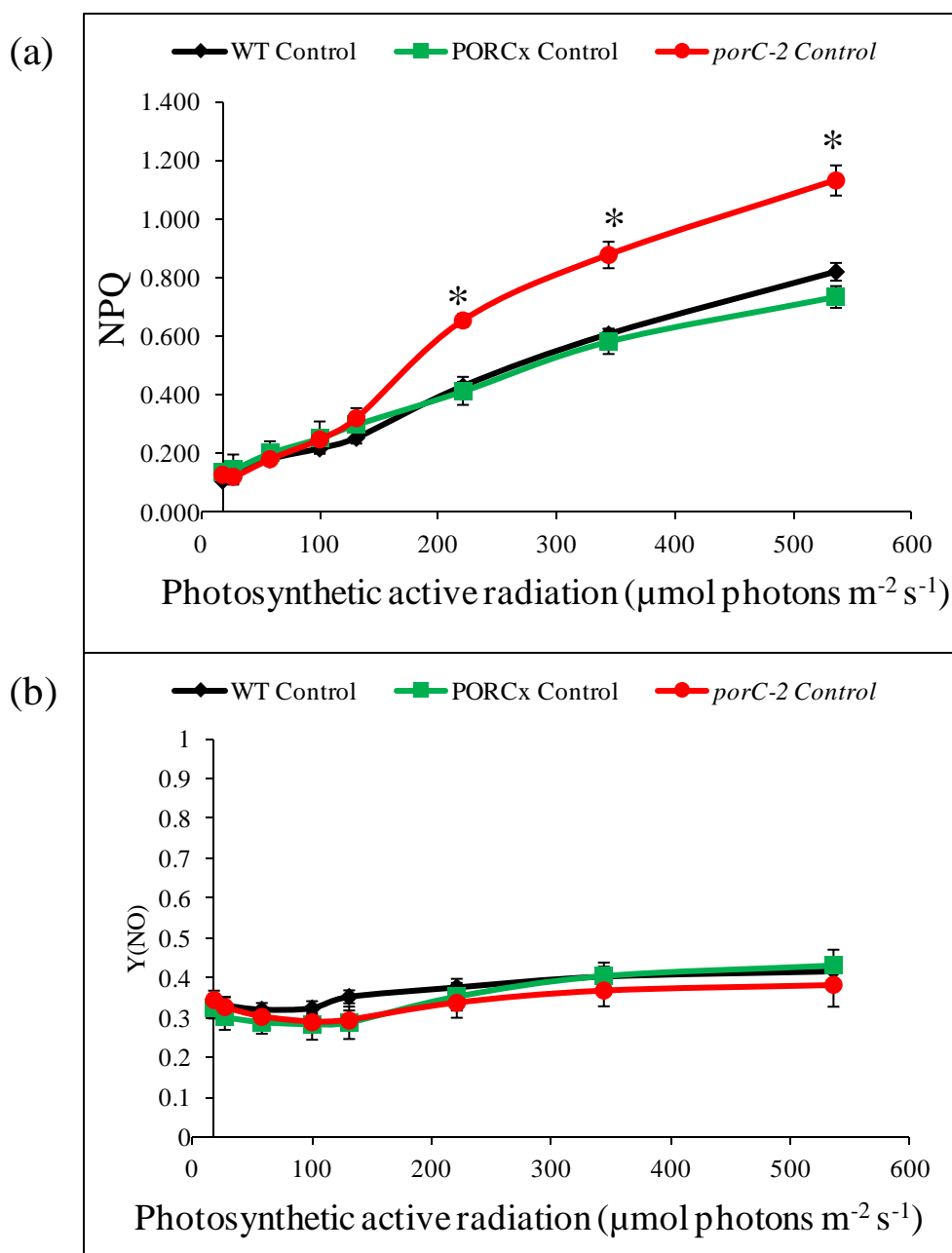


Figure 6. Analysis of (a) Non-photochemical quenching (NPQ), and (b) Quantum yield of non-regulated heat dissipation Y(NO) in WT, PORCx and its mutant (*porC-2*). Plants were grown at 21°C under 10h L and 14h D photoperiod in cool-white-fluorescent light ($100 \mu\text{mol photons m}^{-2} \text{s}^{-1}$) for 5 weeks. Plants were dark-adapted for 20 min. Chlorophyll a fluorescence parameters were determined by using Dual PAM 100 fluorometer. Each data point is the average of six replicates and error bar represents \pm SE. Asterisk indicate significant difference determined by *t* test (* $P < 0.05$).

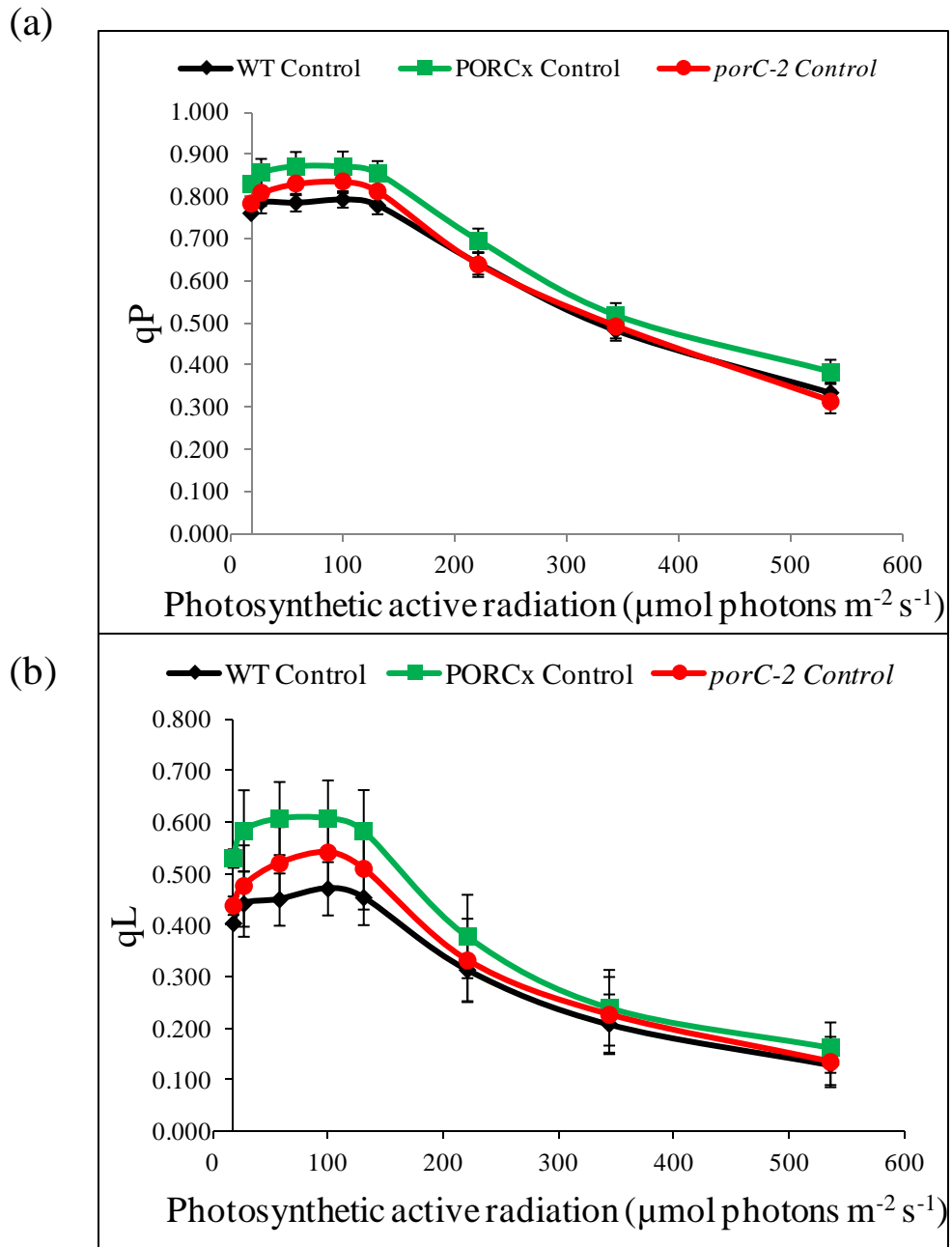


Figure 7. Analysis of (a) coefficient of photochemical quenching ‘puddle model’ (qP) and, (b) coefficient of photochemical quenching ‘lake model’ (qL) of chlorophyll a fluorescence in WT, PORCx and its mutant (*porC-2*). Plants were grown at 21°C under 10h L and 14h D photoperiod in cool-white-fluorescent light ($100 \mu\text{mol photons m}^{-2} \text{s}^{-1}$) for 5 weeks. Chlorophyll a fluorescence parameters were determined by using Dual PAM 100 fluorometer. Each data point is the average of six replicates and error bar represents $\pm\text{SE}$.

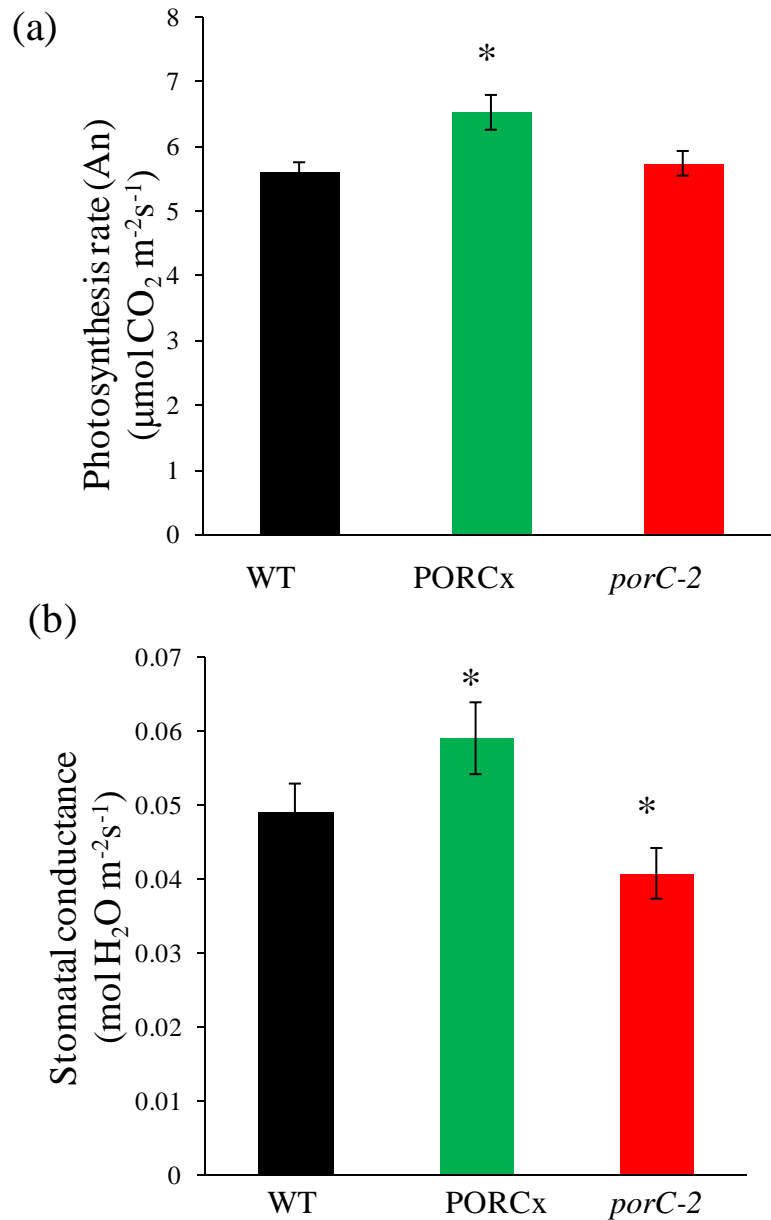


Figure 8. Measurement of (a) photosynthetic carbon dioxide assimilation (An), and (b) Stomatal conductance (g_s) in WT, PORCx and its mutant (*porC-2*). Plants were grown at 21⁰C under 10h L and 14h D photoperiod in cool-white-fluorescent light ($100 \mu\text{mol photons m}^{-2} \text{ s}^{-1}$) for 5 weeks. Before measurements, leaves were pre-illuminated at $400 \mu\text{mol photons m}^{-2} \text{ s}^{-1}$ for 20 min. The photosynthesis and stomatal conductance were monitored in the same light intensity and $400 \mu\text{mol (mol)}^{-1}$ of CO_2 at the leaf temperature of 25⁰C using LiCOR (6400) Infrared gas analyzer. Each data point is the average of six replicates and error bar represents $\pm\text{SE}$. Asterisk indicate significant difference determined by *t* test ($*P < 0.05$)

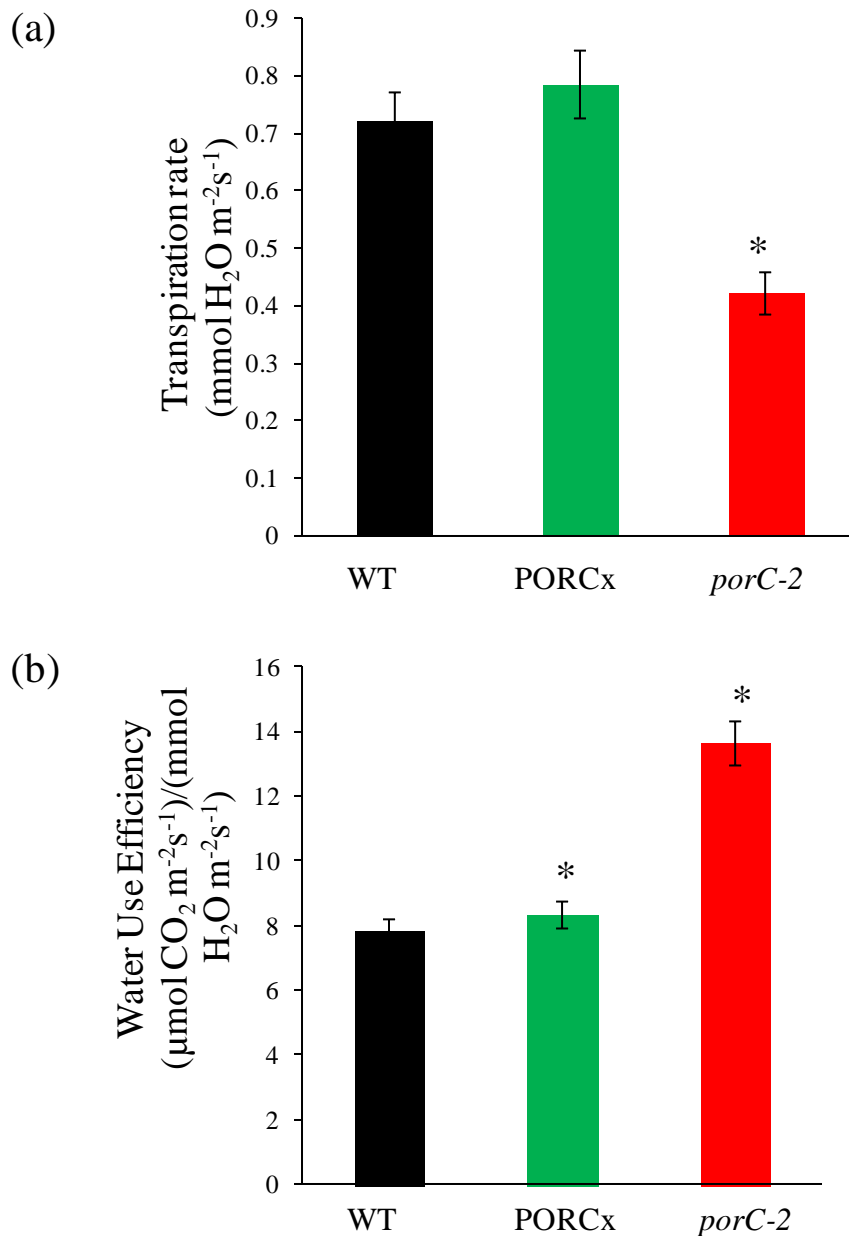


Figure 9. Measurement of (a) Transpiration rate, and (b) Water use efficiency (WUE) in WT, PORCx and its mutant (*porC-2*). Plants were grown at 21^oC under 10h L and 14h D photoperiod in cool-white-fluorescent light (100 μmol photons m⁻² s⁻¹) for 5 weeks. Other experimental details are as in figure-8. Each measurement is the average of six replicates and error bar represents ±SE. Asterisk indicate significant difference determined by *t* test (*P<0.05)

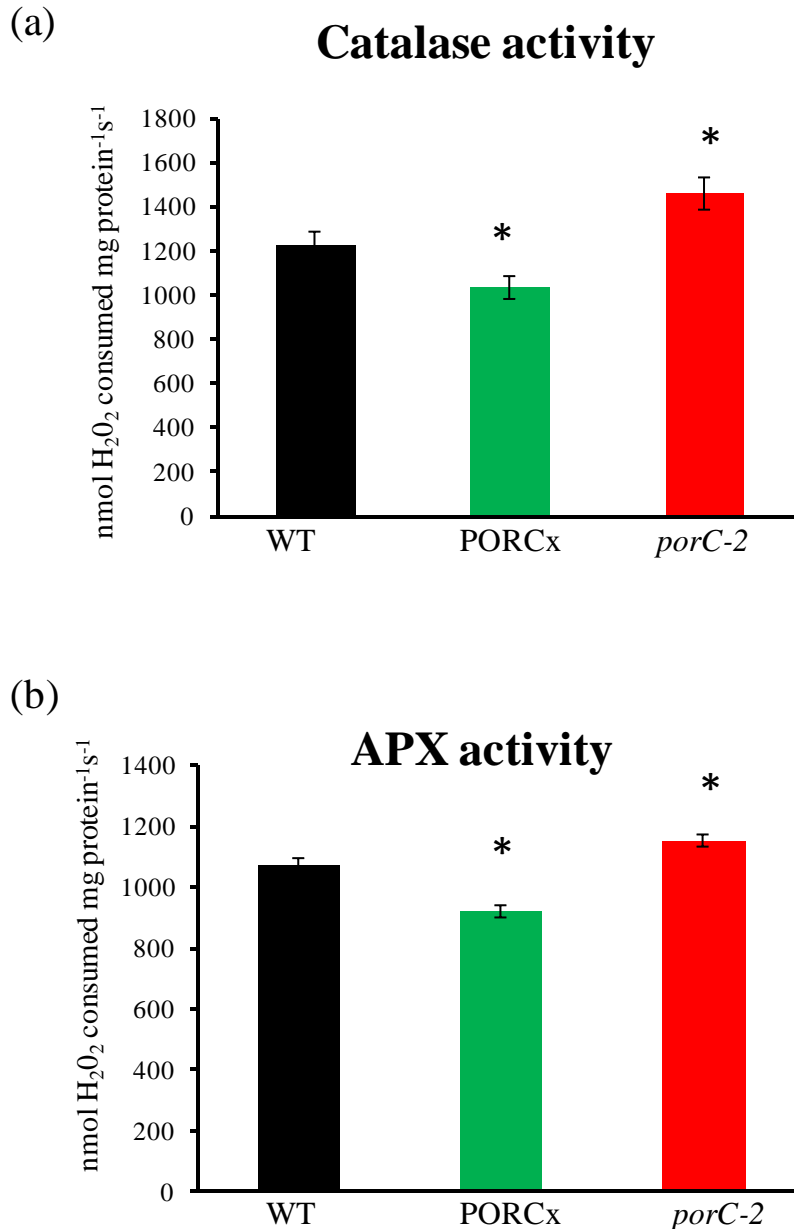


Figure 10. Measurement of antioxidative enzyme activities (a) Catalase and (b) Ascorbate Peroxidase activity in WT, PORCx and its mutant (*porC-2*). Plants were grown at 21^oC under 10h L and 14h D photoperiod in cool-white-fluorescent light (100 μ mol photons m⁻² s⁻¹) for 5 weeks. Their antioxidant enzyme activities were measured as described in materials and methods. Asterisk indicate significant difference determined by *t* test (*P<0.05)

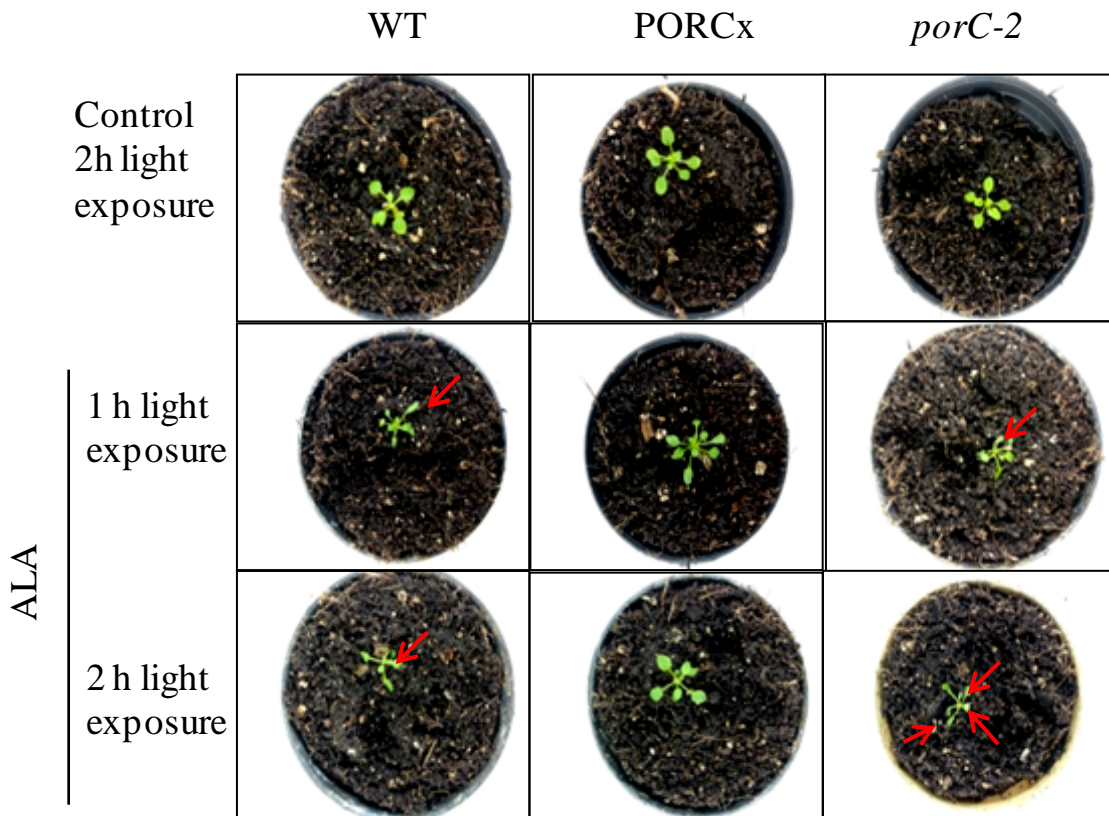


Figure 11. Morphological changes in WT, PORCx and its mutant (*porC-2*) in response to ALA treatment. Plants were grown at 21°C under 10h L and 14h D photoperiod in cool-white-fluorescent light (100 $\mu\text{mol photons m}^{-2} \text{s}^{-1}$). Three-week old plants were sprayed with distilled water or 1 mM ALA and incubated for 12 h to accumulate the photosensitizer protochlorophyllide. Pictures were captured after 1 h and 2 h of low light exposure (75 $\mu\text{mol photons m}^{-2} \text{s}^{-1}$). Red arrow indicate wilted leaves.

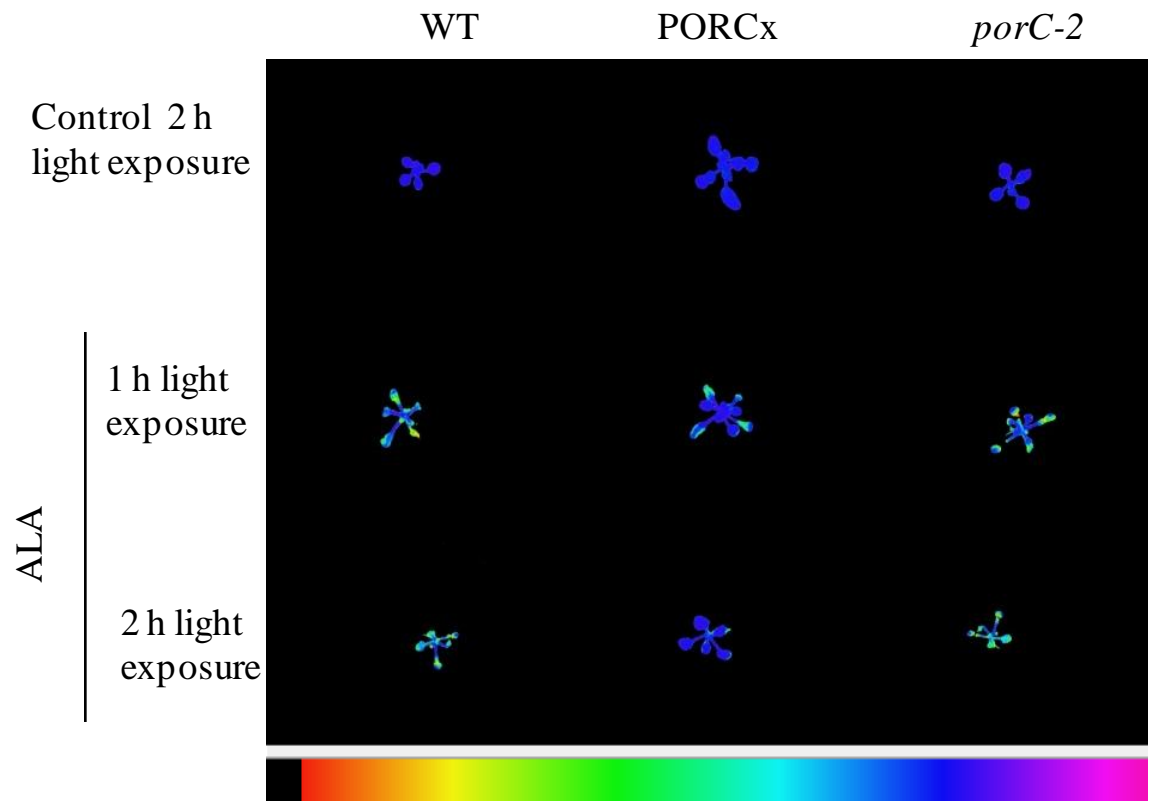


Figure 12. Exogenous application of ALA induces photooxidative damage to plants. Plants were grown at 21⁰C under 10h L and 14h D photoperiod in cool-white-fluorescent light (100 $\mu\text{mol photons m}^{-2} \text{s}^{-1}$). Three-week-old *Arabidopsis thaliana* plants were sprayed with water or 1mM ALA, dark incubated for 12 h and exposed to light (75 $\mu\text{mol photons m}^{-2} \text{s}^{-1}$) for 1-2 h. The false color images of Fv/Fm of control and ALA-treated-light-exposed plants captured by Imaging-PAM. The colored scale bar shows the Fv/Fm increasing in value from left (green) to right (blue).

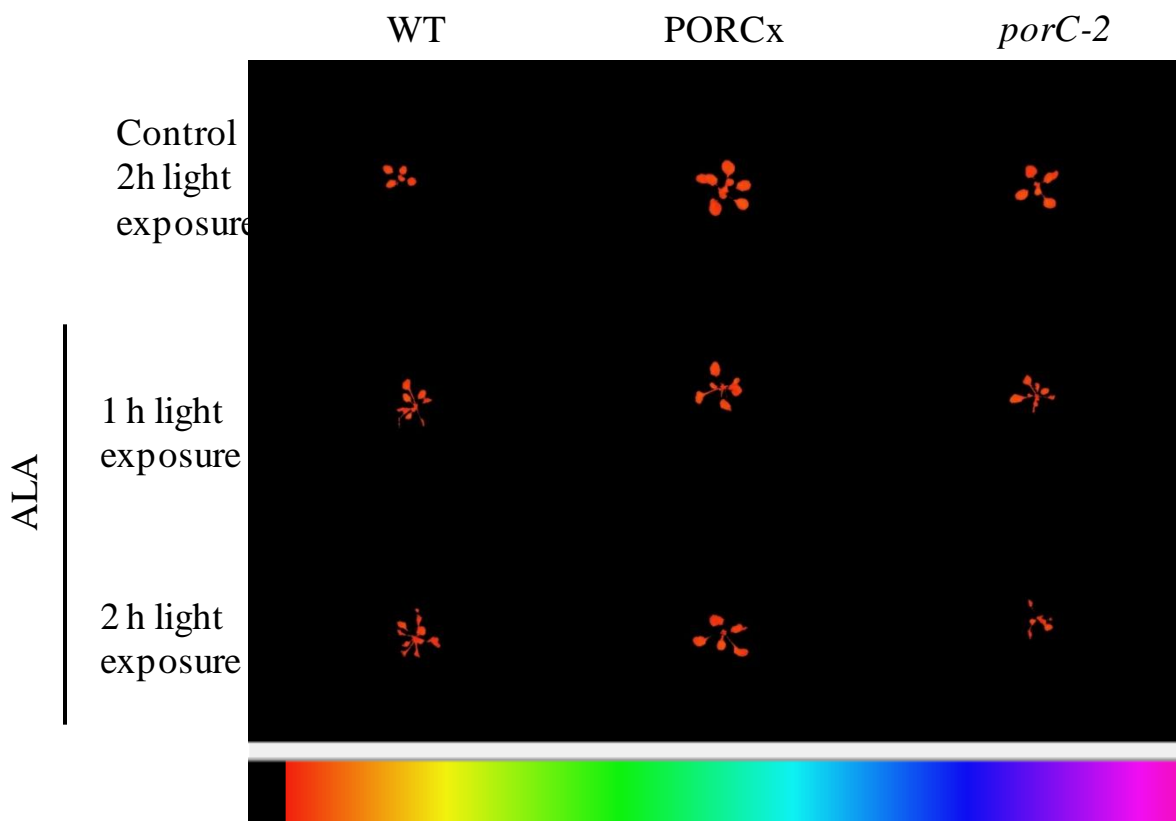


Figure 13. Overexpression of PORC protect plants from 5-Aminolevulinic acid (ALA) induced oxidative stress. Three-week-old WT, PORC overexpressor and its knock-down mutant (*porC-2*) plants were sprayed with 1mM ALA or distilled water and kept in the dark for 12 h to accumulate photosensitizer Pchl_a. Chlorophyll a fluorescence images at time t (F_t) were analysed by using Imaging-PAM (Walz, Germany) after 1 h and 2 h of light (75 $\mu\text{mol photons m}^{-2} \text{s}^{-1}$) exposure. The color code beneath the image depict values from 0 to 1.

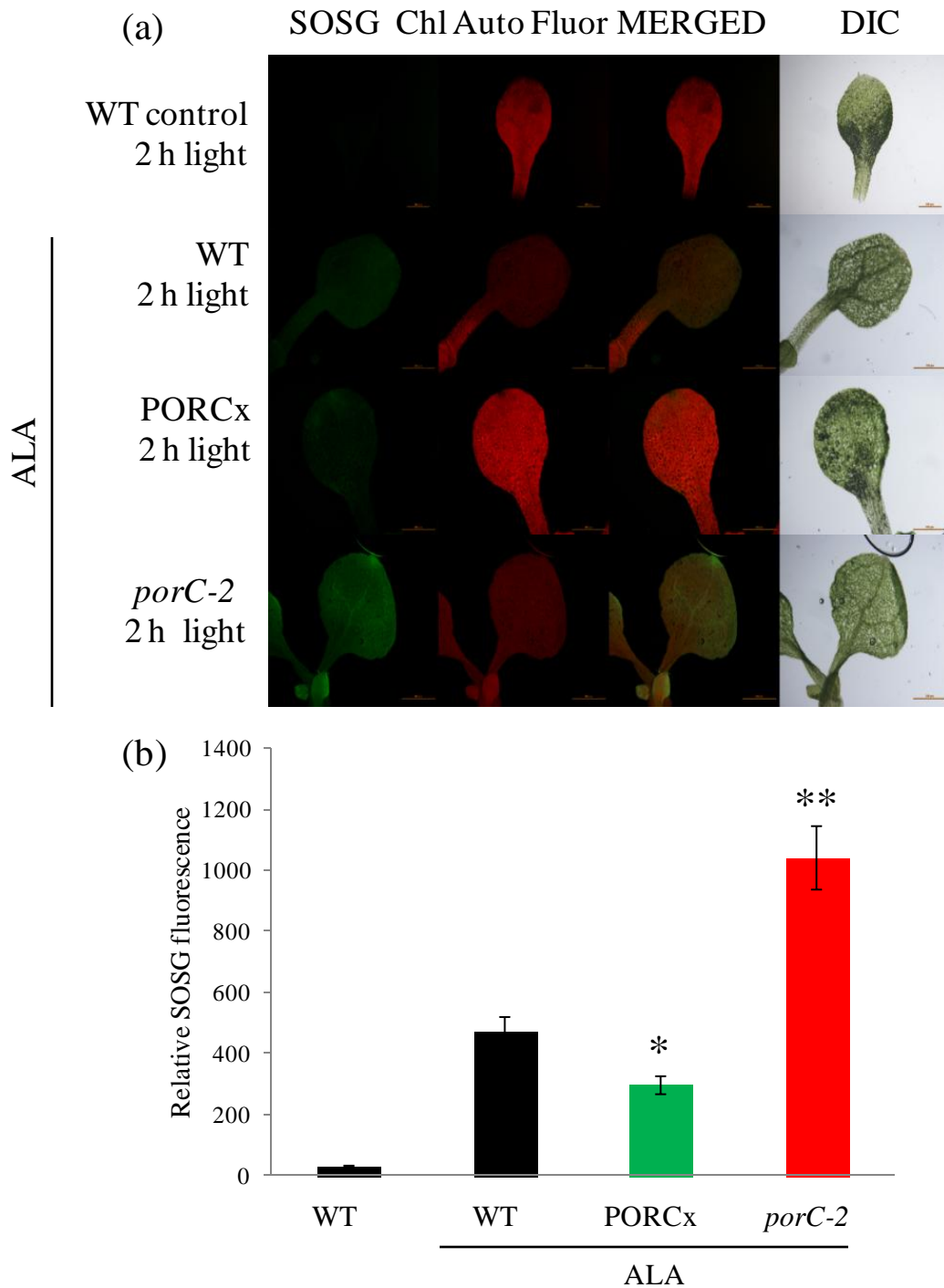


Figure 14. Overaccumulation of Pchlide induces singlet oxygen production in low light. Three-week-old *Arabidopsis thaliana* plants were sprayed with water or 1mM ALA and incubated in dark for 12 h (a) Analysis of singlet oxygen level in leaves by SOSG staining after 1-2 h of light ($75 \mu\text{mol photons m}^{-2} \text{s}^{-1}$) exposure, (b) Quantification of relative SOSG fluorescence intensity. Asterisks indicate significant differences determined by Student's *t* test compared with ALA-treated WT (* $P < 0.05$, ** $P < 0.01$).

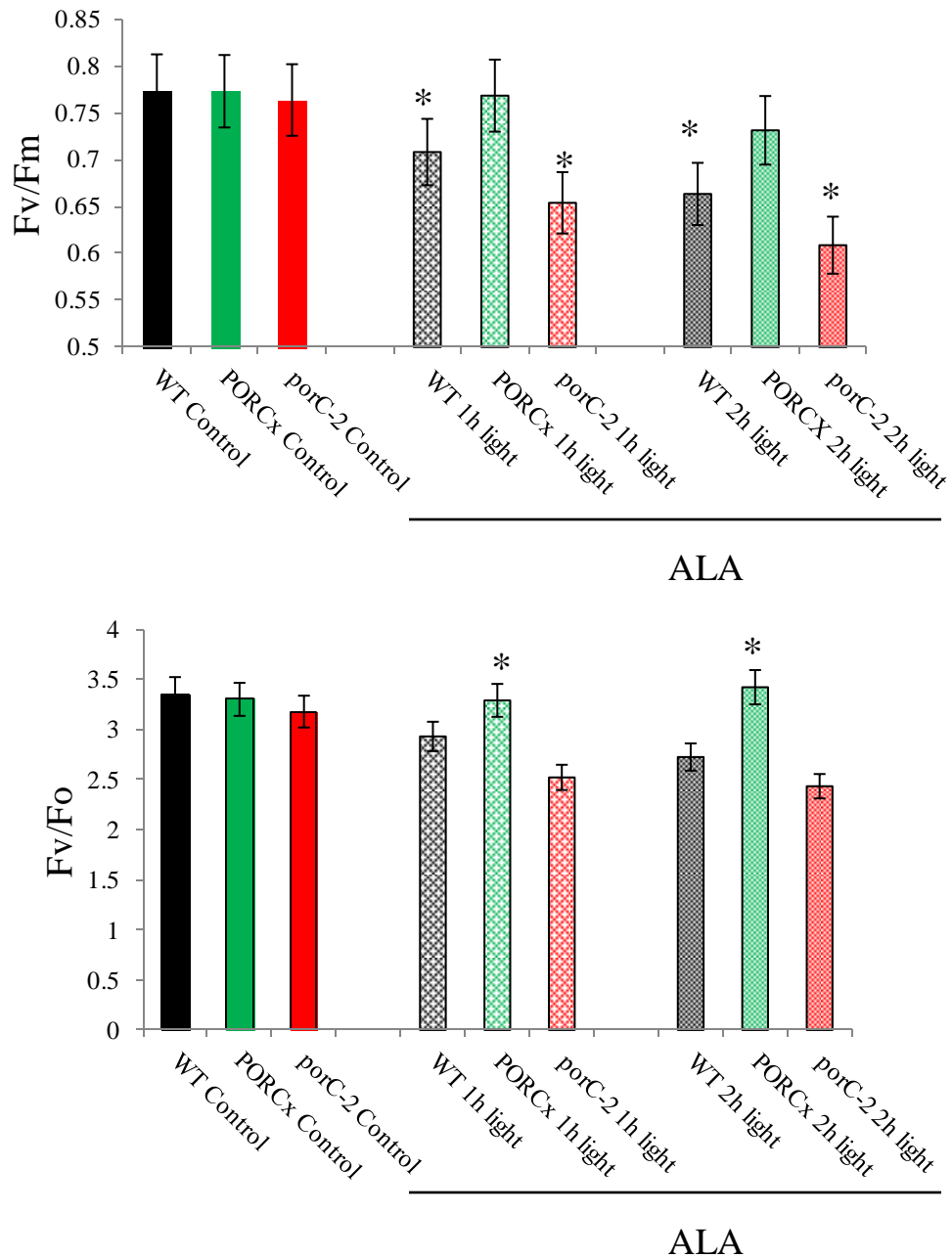


Figure 15. Pchlide derived singlet oxygen decreased chlorophyll a fluorescence parameters. To understand the effect of accumulated singlet oxygen due to ALA treatment on the photosynthetic parameters, the chlorophyll a fluorescence were measured in ALA or distilled water treated and dark incubated (12 h) WT, PORCx and *porC-2* mutant plants after 1h or 2h light ($75 \mu\text{mol photons m}^{-2} \text{s}^{-1}$) exposure. (a) The ratio of variable to maximum fluorescence (F_v/F_m), and (b) the ratio of variable to minimum fluorescence (F_v/F_o). Each data point is the average of 5 replicates and error bars represent $\pm\text{SE}$. Asterisks indicate significant differences determined by t test ($*P < 0.05$).

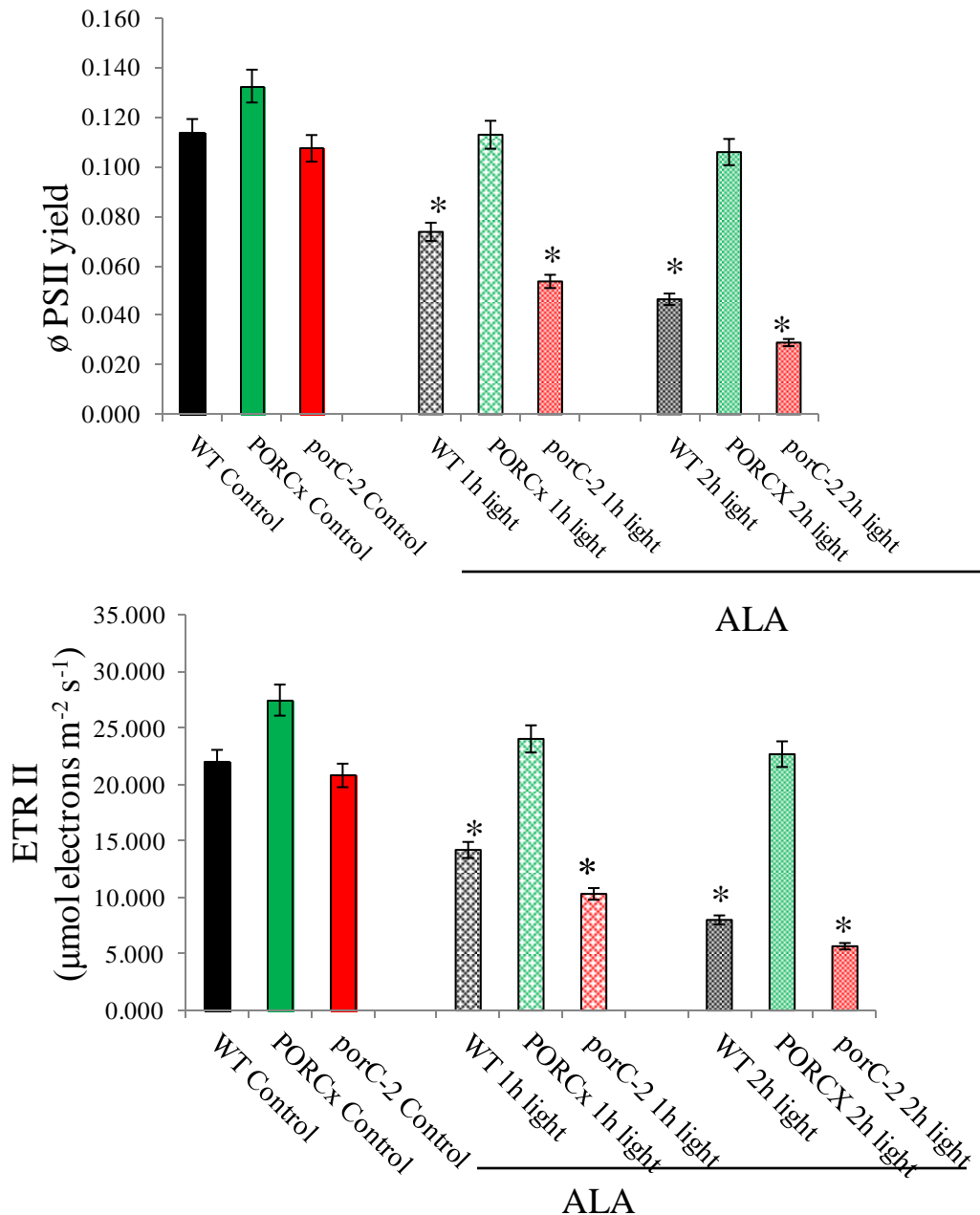


Figure 16. Impact of exogenous application of ALA to the quantum yield and electron transport rates (measured in 530 μmol photons m⁻² s⁻¹) of WT, PORC and *porC-2* mutant. Pulse amplitude modulated chlorophyll a fluorescence parameters were analyzed from ALA or distilled water treated samples. (a) Quantum yield of photosystem II (b) Electron transport rate of photosystem II was calculated using Imaging Win Software. Each data point is the average of 5 replicates and error bars represent ±SE. Asterisks indicate significant differences determined by t test (*P<0.05, **P<0.01).

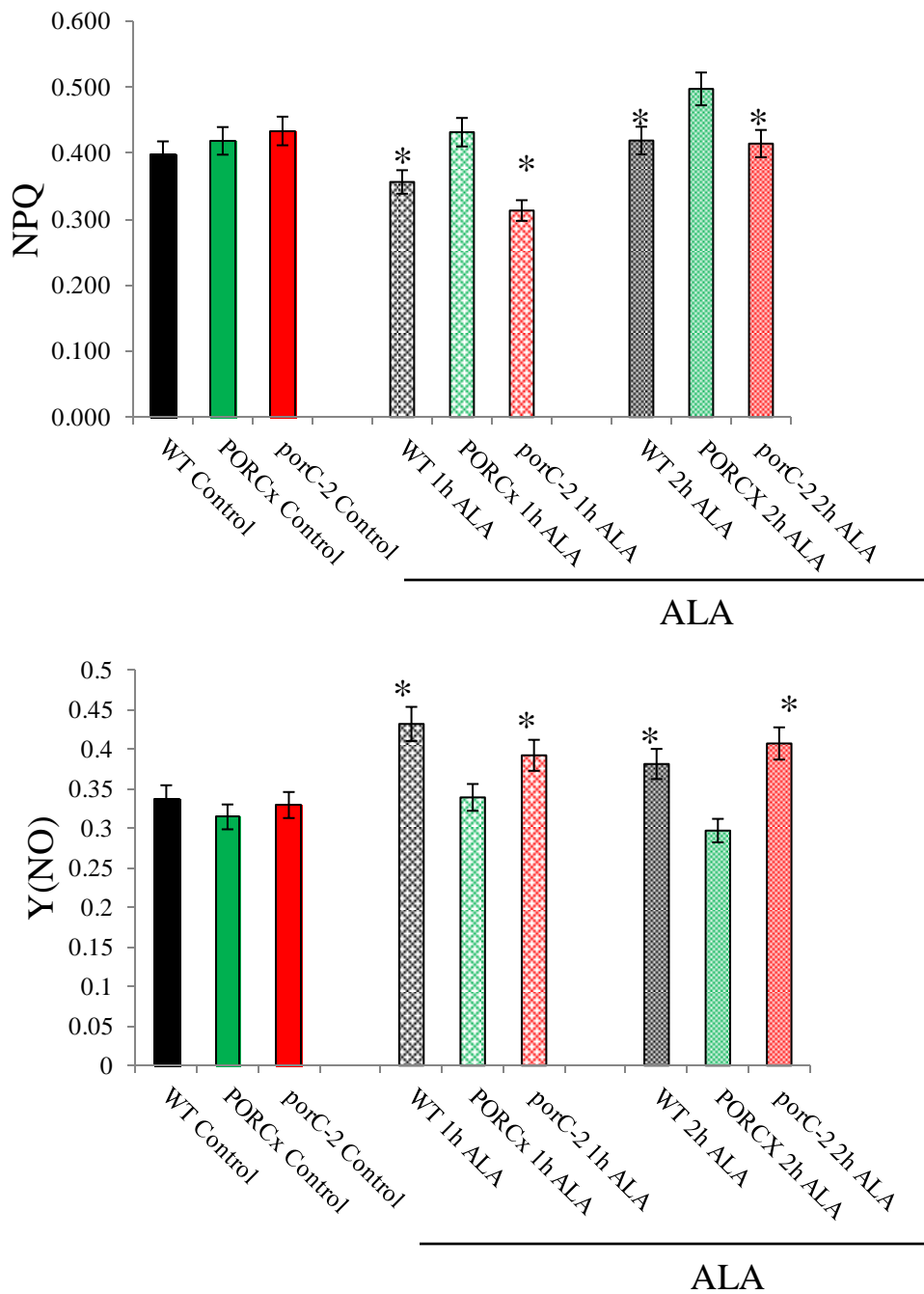


Figure 17. Activation of heat dissipation machinery in PORCx in response to ALA-induced oxidative stress. Pulse amplitude modulated Chlorophyll a fluorescence parameters in ALA or distilled water treated samples were determined by Imaging PAM. (a) Non photochemical quenching (NPQ) (b) Quantum yield of non-regulated energy dissipation in PSII (Y(NO)). Each data point is the average of 5 replicates and error bars represent \pm SE. Asterisks indicate significant differences determined by t test (*P<0.05).

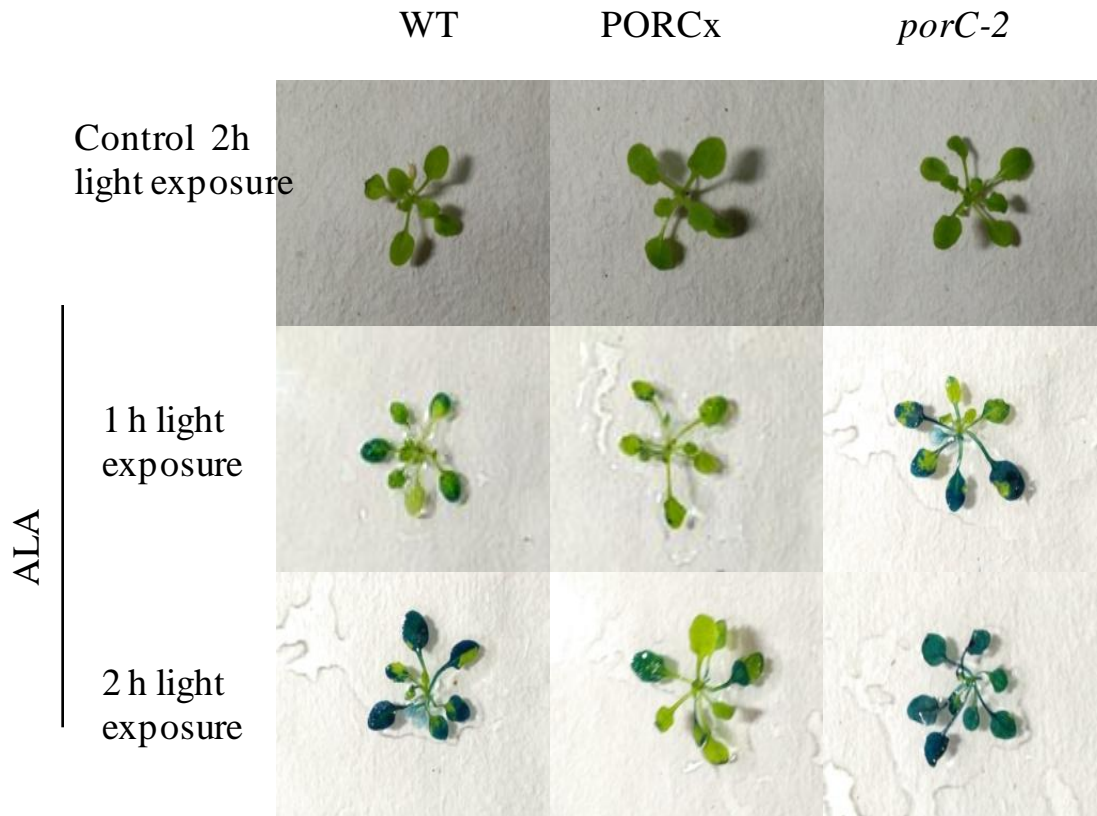


Figure 18. Cell death in photooxidative stress. Three-week-old WT, PORC_x and *porC-2* plants were sprayed with distilled water or 1 mM ALA and incubated overnight to accumulate the photo-sensitizer protochlorophyllide. Pictures were captured after 1 h and 2 h of low light exposure ($75 \mu\text{mol photons m}^{-2} \text{s}^{-1}$). After image capture, plants were stained with Evans blue dye to detect cell death in the affected leaves.

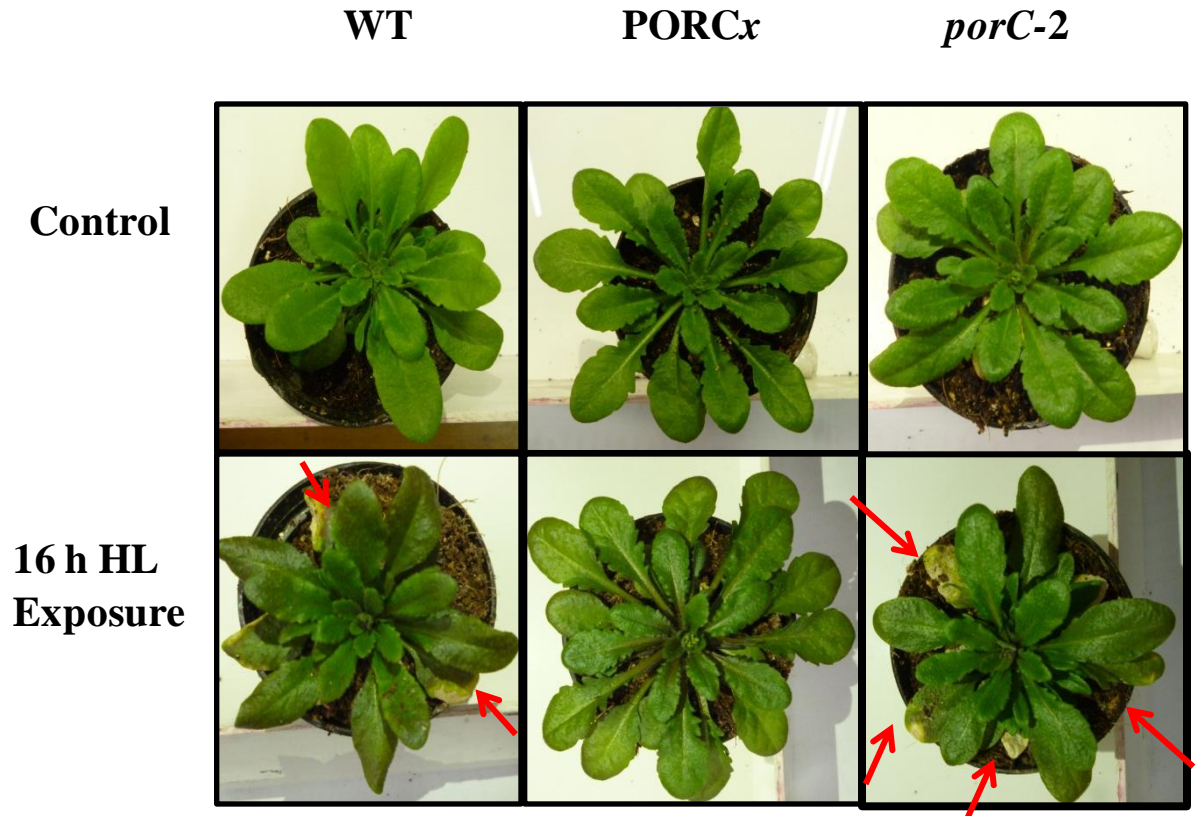


Figure 19. Morphological changes in WT, PORC x and *porC-2* mutant plants before and after high light treatment ($800 \mu\text{mol photons m}^{-2}\text{s}^{-1}$) for 16 h. Plants were grown at 21°C under 10h L and 14h D photoperiod in cool-white-fluorescent light ($100 \mu\text{mol photons m}^{-2} \text{s}^{-1}$) for 5 weeks. Well hydrated plants were kept under high light ($800 \mu\text{mol photons m}^{-2} \text{s}^{-1}$) for 16 h in the plant growth chamber maintained at 21°C . Minimum 6 plants from each type was used in the study. Red arrows indicate photo-bleached leaves due to high light stress.

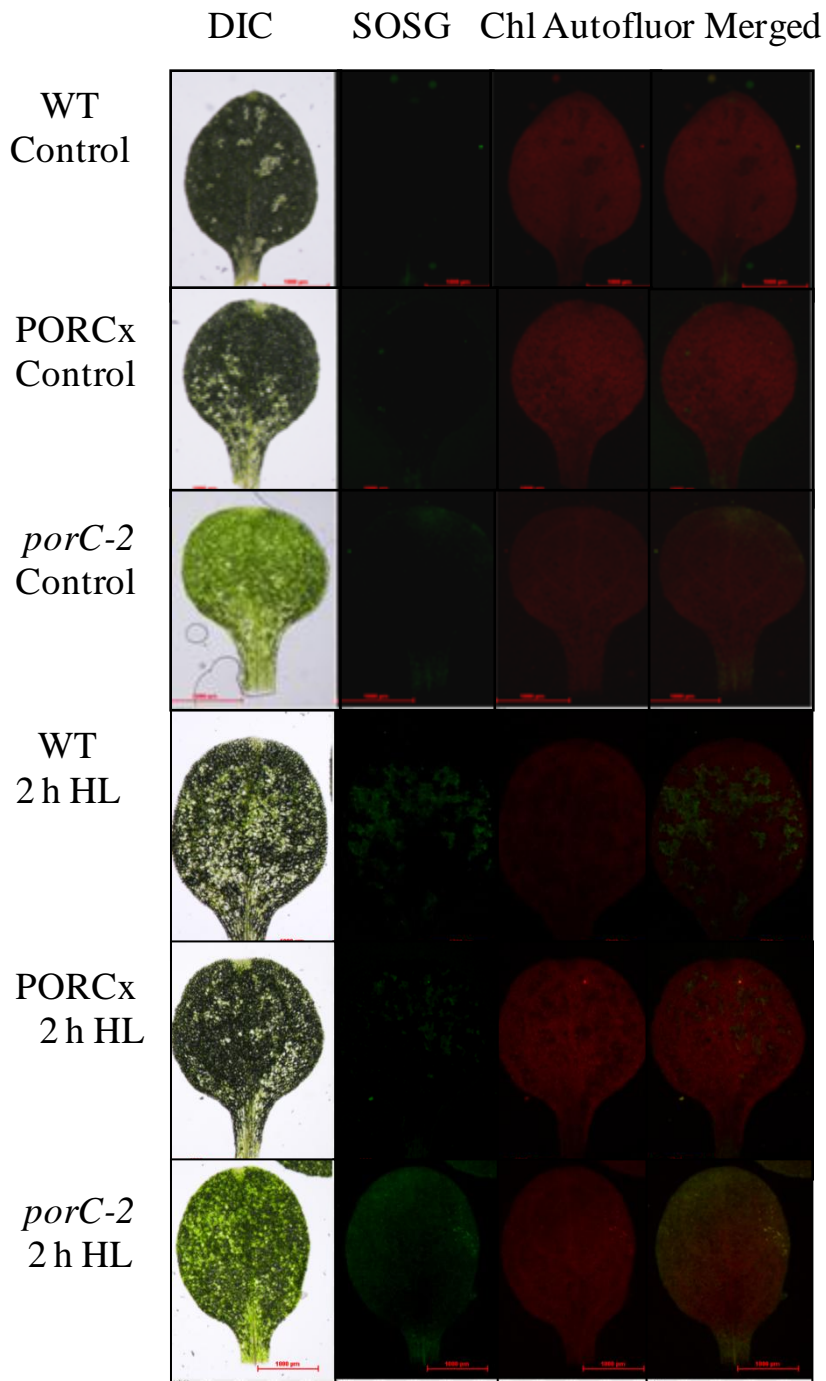


Figure 20. Monitoring of singlet oxygen level in WT, PORCx and *porC-2* plants by Singlet oxygen sensor green (SOSG). Three-week-old plants were kept under growth light ($100 \mu\text{mol photons m}^{-2}\text{s}^{-1}$) or high light ($800 \mu\text{mol photons m}^{-2}\text{s}^{-1}$) for 2 h. SOSG stained leaves were observed under 1.5X magnification using different fluorescent channels.

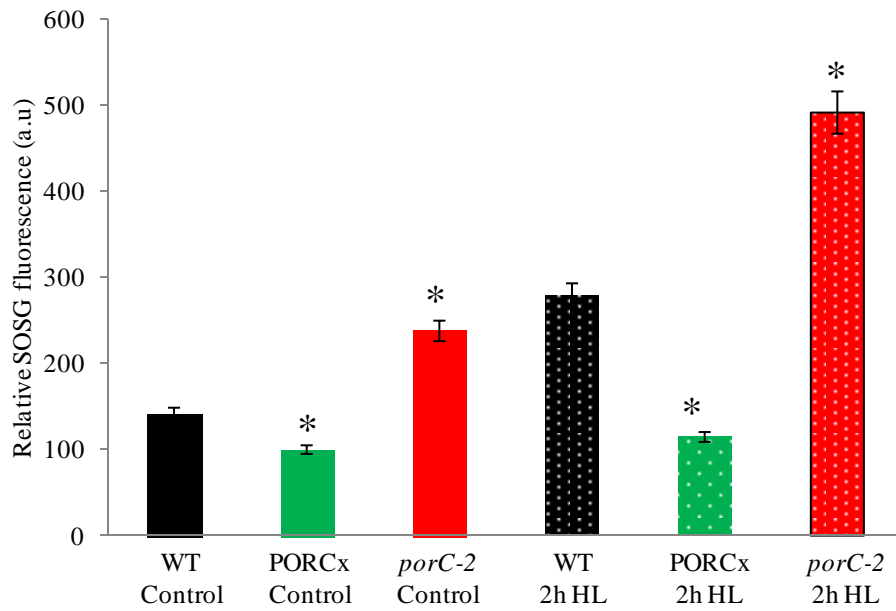


Figure 21. Estimation SOSG fluorescence emanating from light treated leaves. The captured images were analyzed using ImageJ software. Each data point is the average of six replicates and error bar represents \pm SE. Asterisk indicate significant difference determined by *t* test (* $P < 0.05$)

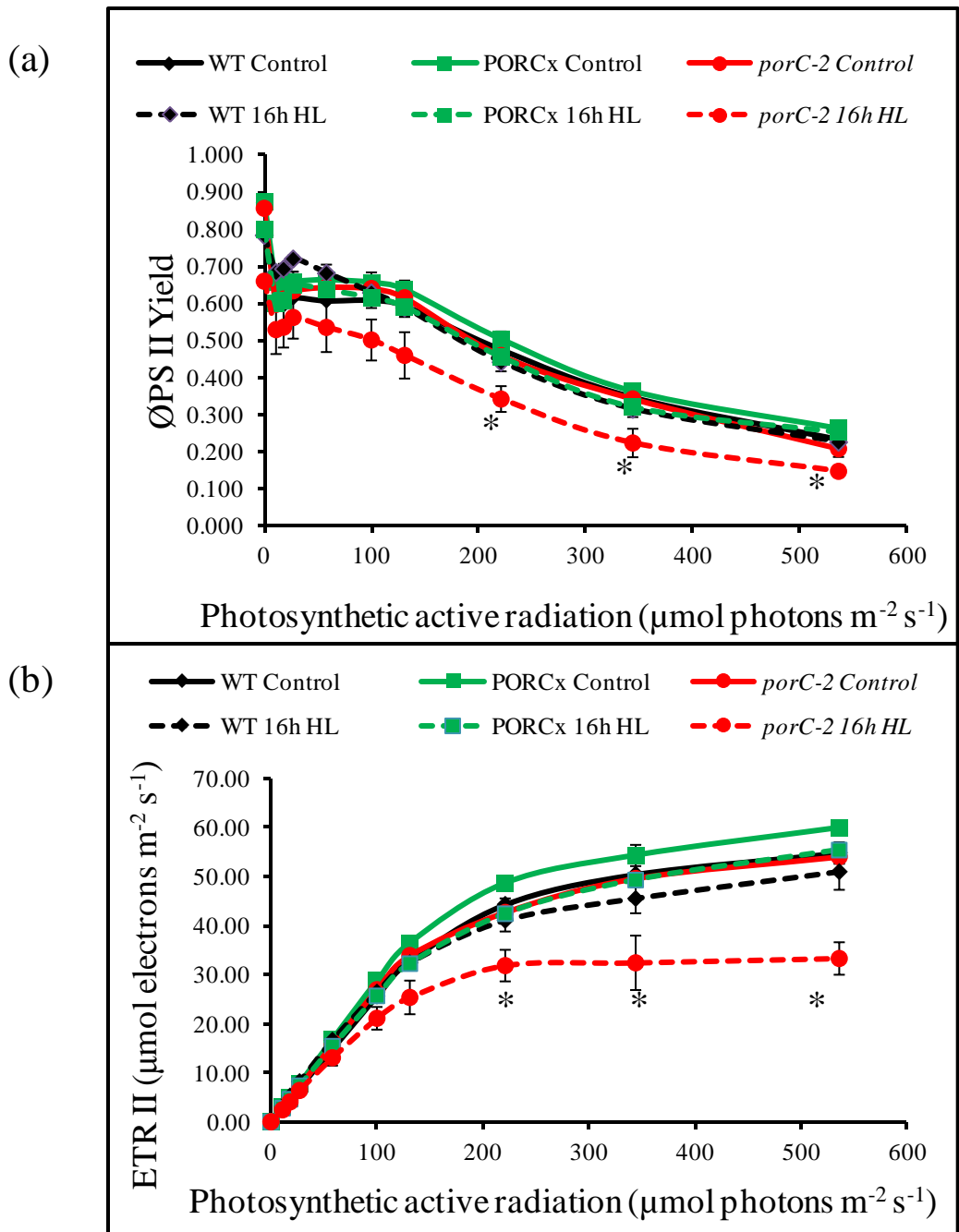


Figure 22. High-light-induced damage to the photosynthetic apparatus. (a) Quantum yield of PSII (b) PSII-dependent electron transport rate (ETR) of WT, PORCx and its mutant (*porC-2*) plants. Well hydrated plants were kept under high light ($800 \mu\text{mol photons m}^{-2} \text{s}^{-1}$) for 16 h in the plant growth chamber maintained at 21°C . Chl a fluorescence parameters were determined by using Dual PAM 100 fluorometer (Walz, Germany) as in materials and methods. Each data point is the average of six replicates and error bar represents $\pm\text{SE}$. Asterisk indicate significant difference determined by *t* test ($*P < 0.05$)

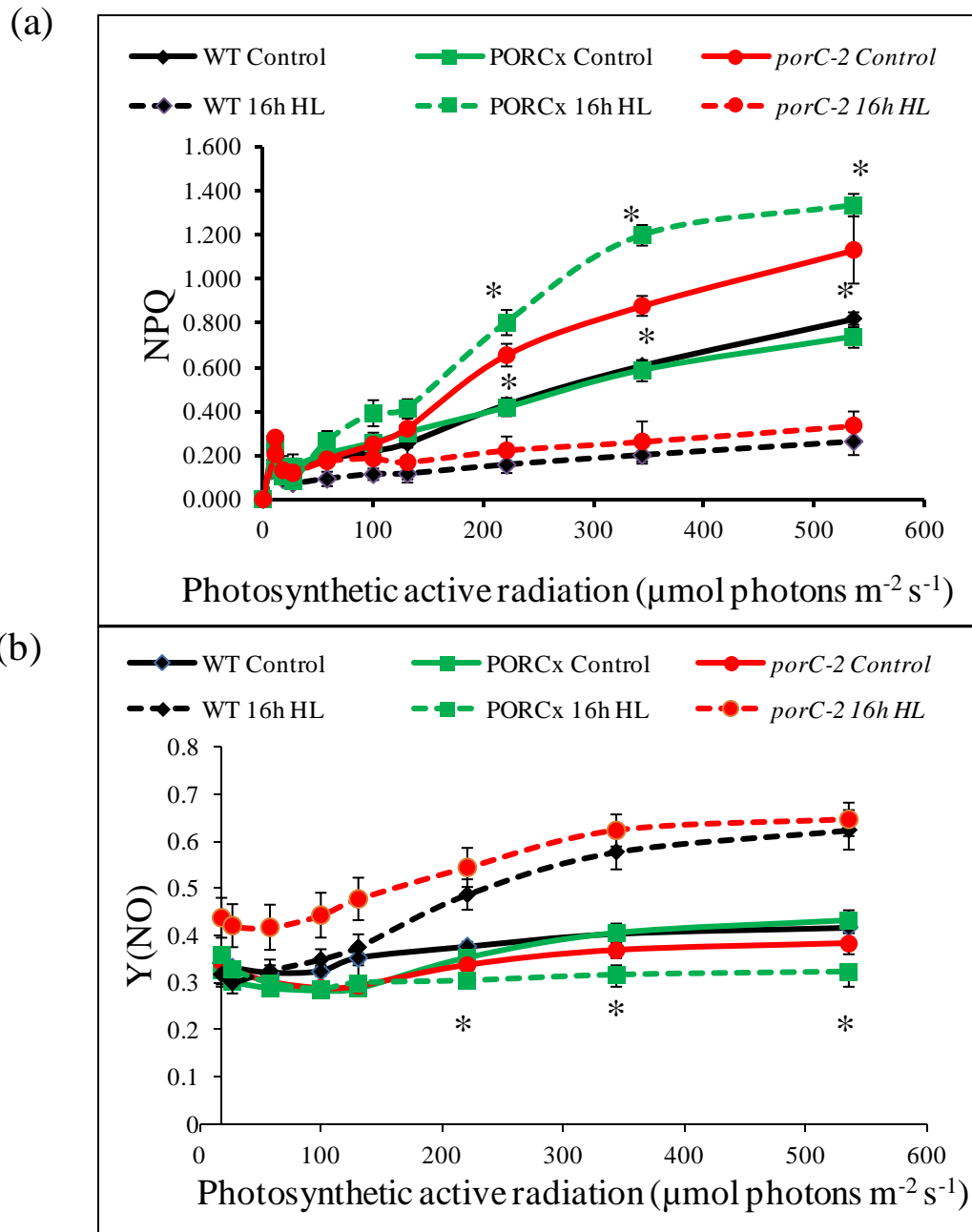


Figure 23. Impact of high light on energy dissipation in WT, PORCx and *porC-2* plants. (a) Non-photochemical quenching (NPQ) and (b) quantum yield of light regulated energy dissipation of PSII Y(NO). Well hydrated plants grown in $100 \mu\text{mol photons m}^{-2} \text{s}^{-1}$ were exposed to high light ($800 \mu\text{mol photons m}^{-2} \text{s}^{-1}$) for 16 h in the plant growth chamber maintained at 21°C . Chl a fluorescence parameters were determined by using Dual PAM 100 fluorometer (Walz, Germany) as in materials and methods. Each data point is the average of six replicates and error bar represents $\pm\text{SE}$. Asterisk indicate significant difference determined by *t* test ($*P < 0.05$)

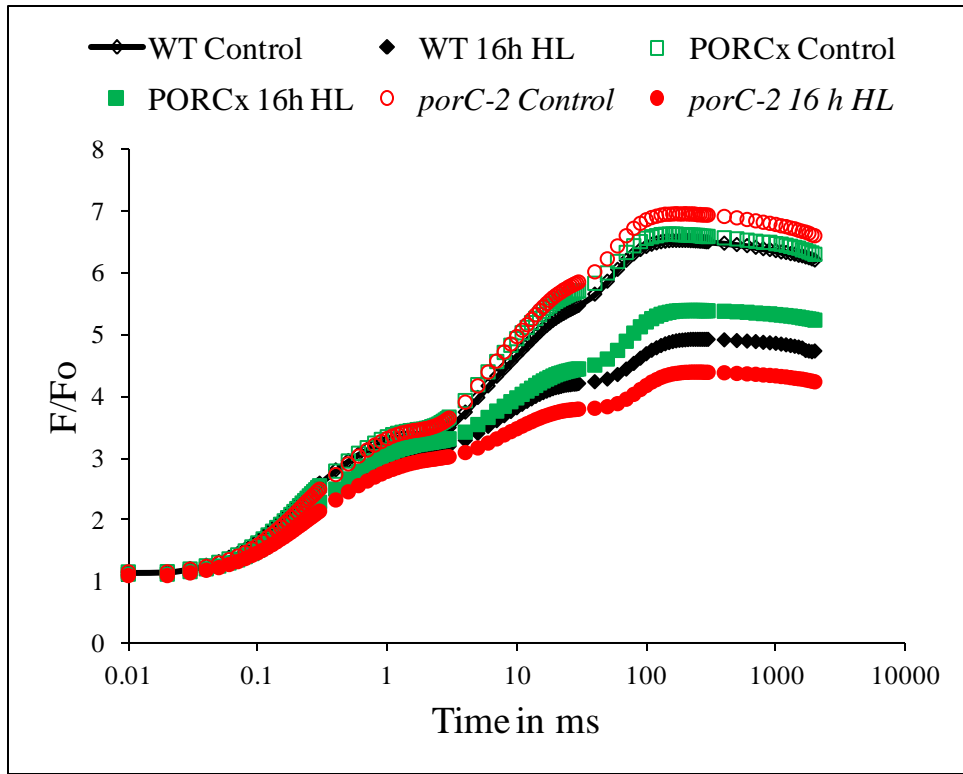


Figure 24. Analysis of chlorophyll a fluorescence induction curve in WT, PORCx and its mutant (*porC-2*) plants. Well hydrated plants grown in $100 \mu\text{mol photons m}^{-2} \text{s}^{-1}$ were exposed to high light ($800 \mu\text{mol photons m}^{-2} \text{s}^{-1}$) for 16 h in the plant growth chamber maintained at 21°C . Control plants were kept under growth light. After light treatment, plants were dark adapted for 20 min. Chlorophyll a fluorescence transient were determined by using photosynthetic efficiency analyzer, Handy- PEA fluorometer. Data was normalized at F_0 where F denotes fluorescence at time t (F_t).

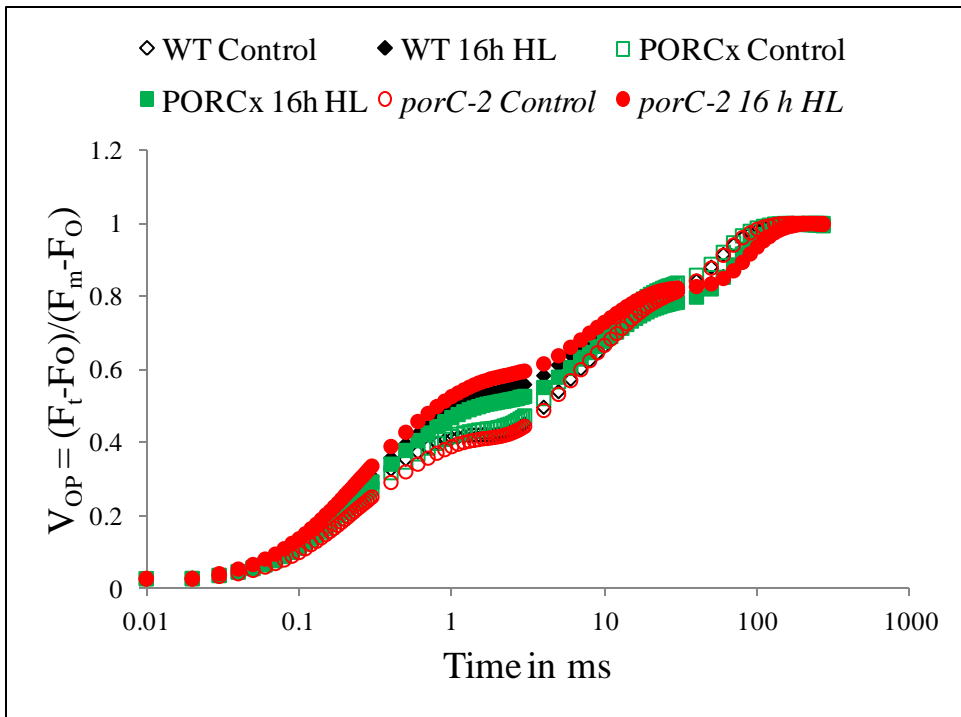


Figure 25. Analysis of chlorophyll a fluorescence induction curve double normalized at O and P level. Well hydrated plants grown in $100 \mu\text{mol photons m}^{-2} \text{s}^{-1}$ were exposed to high light ($800 \mu\text{mol photons m}^{-2} \text{s}^{-1}$) for 16 h in the plant growth chamber maintained at 21°C . Control plants were kept under growth light ($100 \mu\text{mol photons m}^{-2} \text{s}^{-1}$). After light treatment, plants were dark adapted for 20 min. Chlorophyll a fluorescence transient were determined by using photosynthetic efficiency analyzer, Handy- PEA fluorometer. Chlorophyll fluorescence transient were plotted against logarithmic time scale.

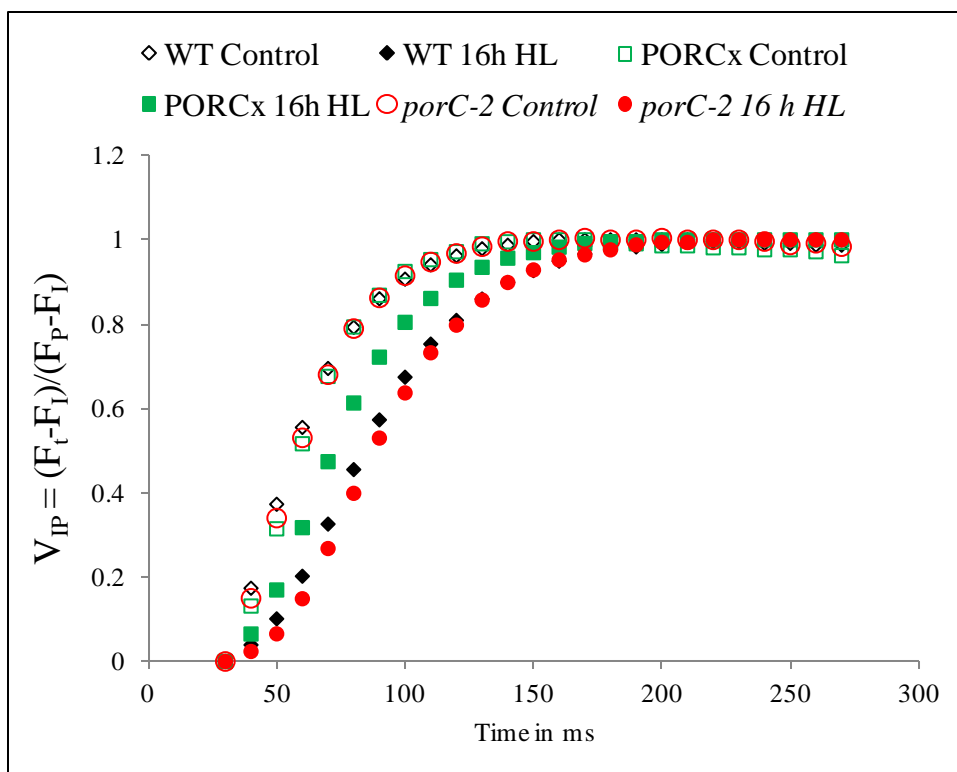


Figure 26. I to P rise transient normalized at both at I and P, deduced from the OJIP curves of figure-23. Variable fluorescence transients from the I to the P double normalized between I (F_I) and P (F_P) phases. Measurement was performed by photosynthetic efficiency analyzer, Handy-PEA.

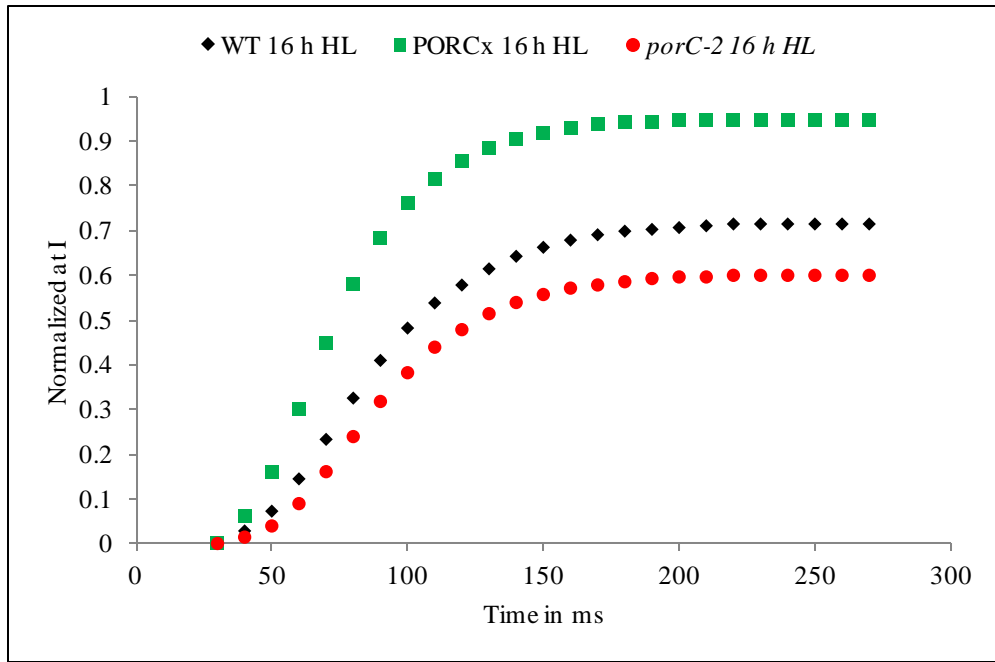


Figure 27. I to P rise normalized at I deduced from the analysis of chlorophyll a fluorescence transient. Variable fluorescence transients from the I to the P single normalized at I phase (30ms). Measurement was performed by photosynthetic efficiency analyzer, Handy-PEA

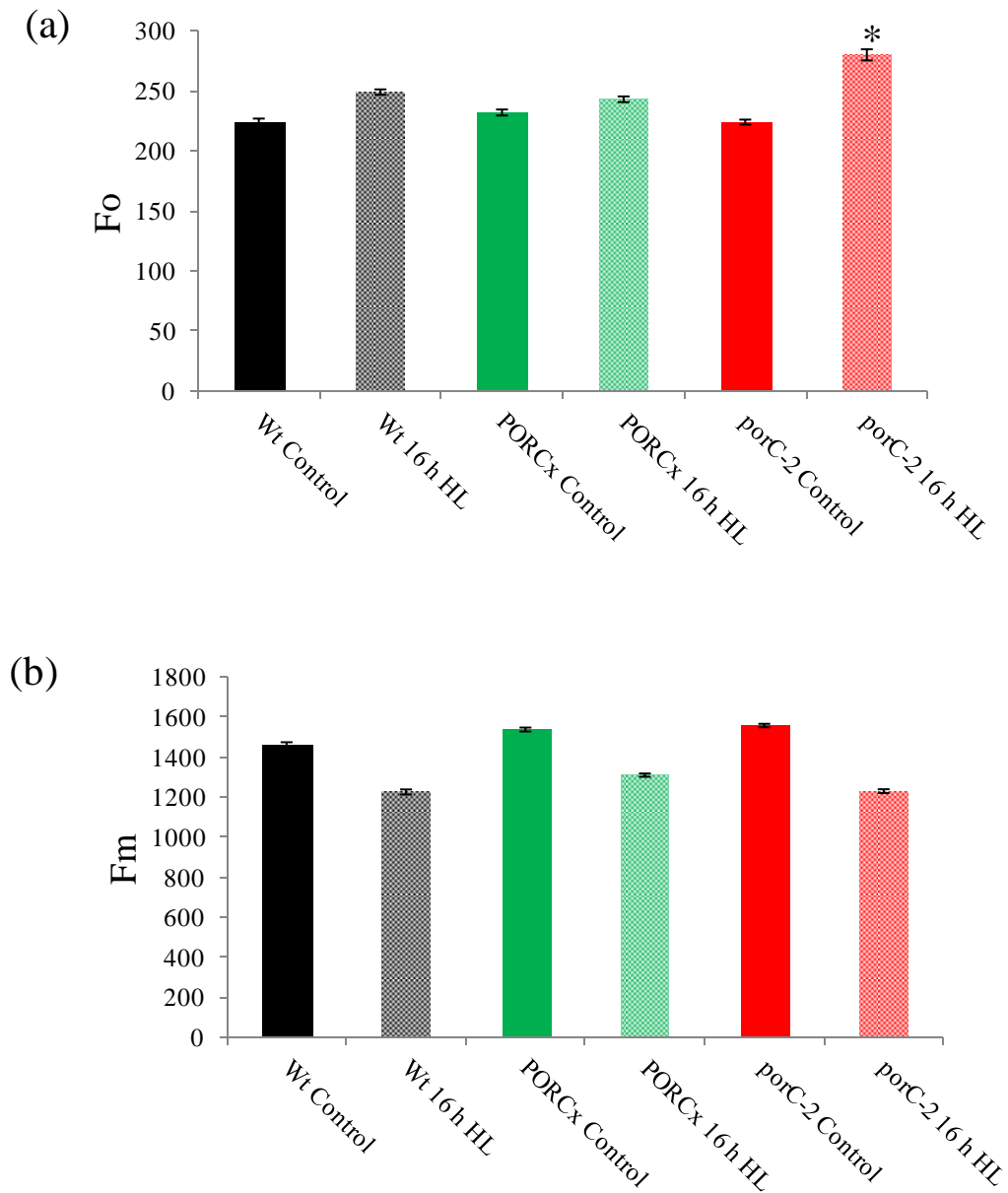


Figure 28. Chlorophyll a fluorescence yield measurements in plants exposed to high light. The WT, PORCx and *porC-2* plants were exposed to the growth light ($100 \mu\text{mol photons m}^{-2} \text{s}^{-1}$) or high light ($800 \mu\text{mol photons m}^{-2} \text{s}^{-1}$) for 16 h in the plant growth chamber maintained at 21°C . (a) Dark fluorescence yield (F_o) (b) Maximum fluorescence yield (F_m) were measured from Handy-PEA in dark-adapted (20 min) plants. The data points are average of 30 replicates and error bars represent $\pm\text{SE}$. Asterisk indicate significant difference determined by *t* test ($*P < 0.05$)

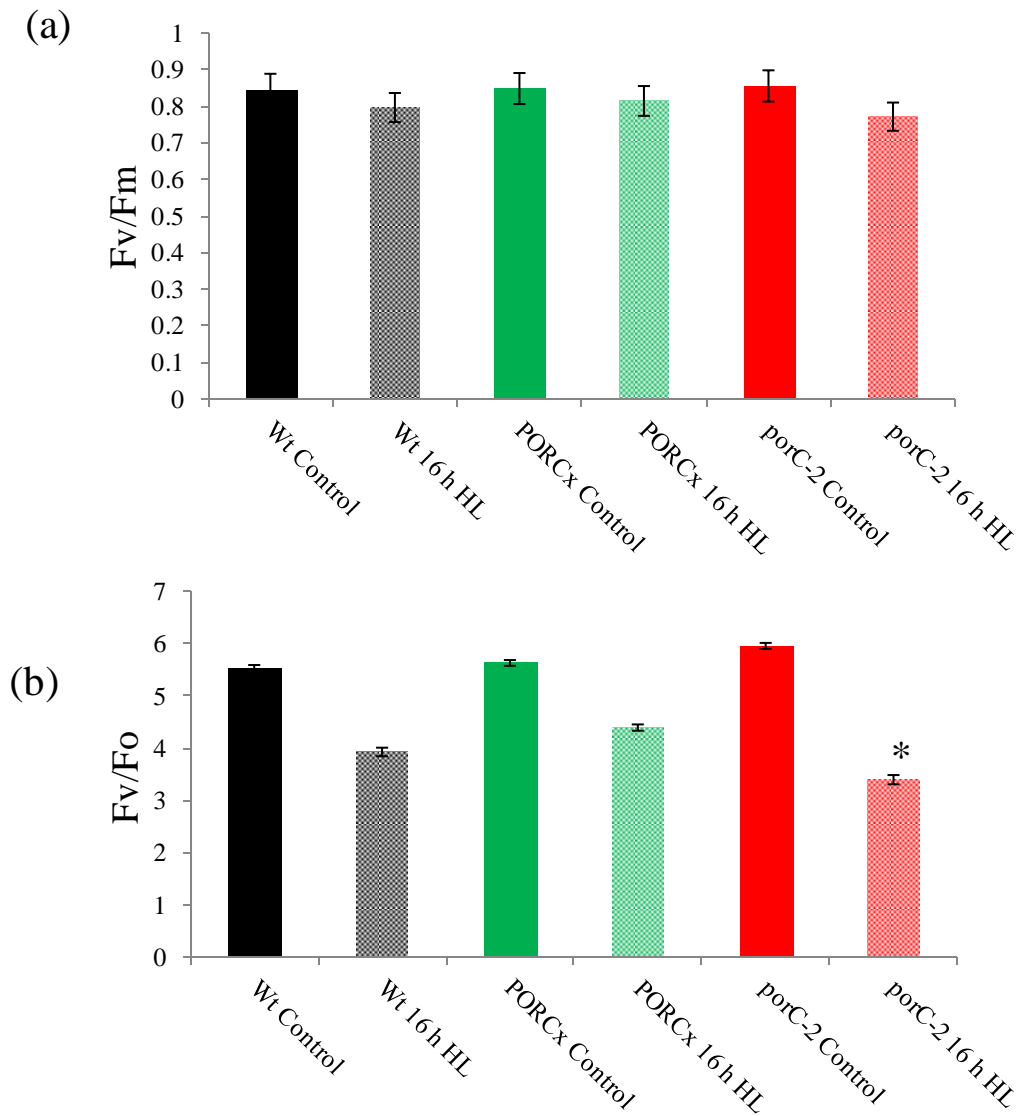


Figure 29. Chlorophyll a fluorescence parameter in WT, PORCx and *porC-2* mutant. Plants were kept in growth light ($100 \mu\text{mol photons m}^{-2} \text{s}^{-1}$) and high light ($800 \mu\text{mol photons m}^{-2} \text{s}^{-1}$) for 16 h in the plant growth chamber maintained at 21°C . (a) Ratio of variable to maximum fluorescence (F_v/F_m), (b) Ratio of variable to minimum fluorescence (F_v/F_o) were measured from photosynthetic efficiency analyzer Handy-PEA. The data points are average of 30 replicates and error bars represent $\pm\text{SE}$. Asterisk indicate significant difference determined by *t* test (* $P < 0.05$)

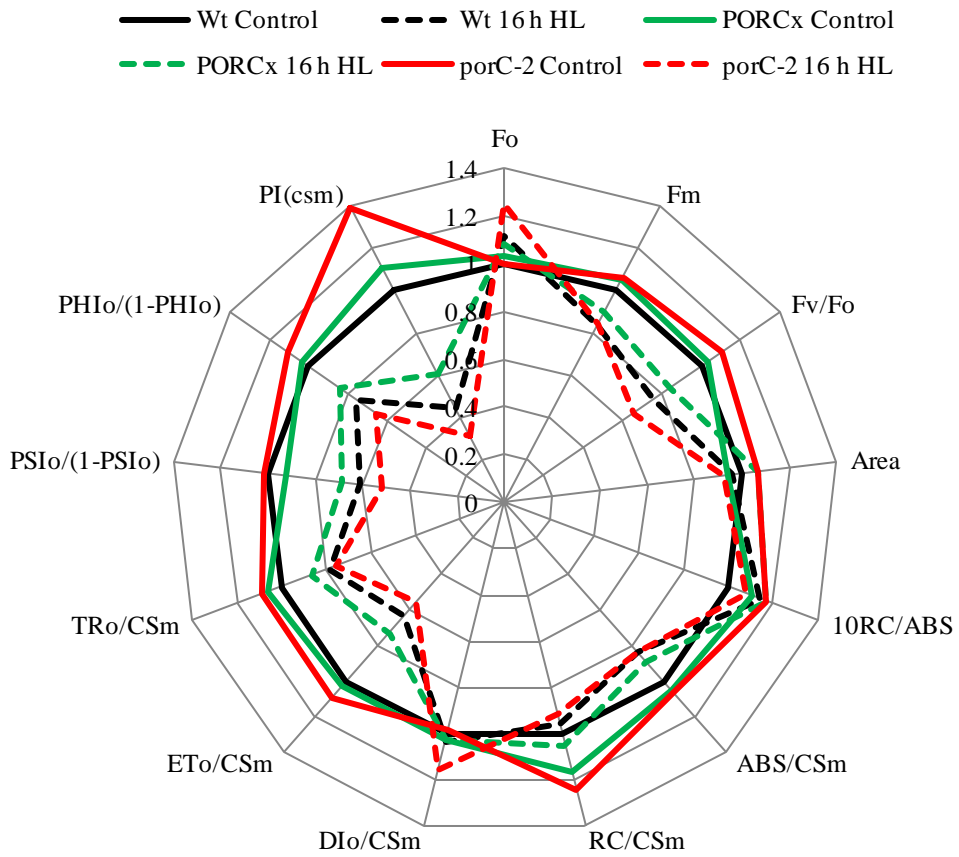


Figure. 30 Radar plot depicting parameters derived from OJIP transient curve. After analysis of OJIP curve, different parameters were interpreted from Biolyzer software. WT control was taken as reference.

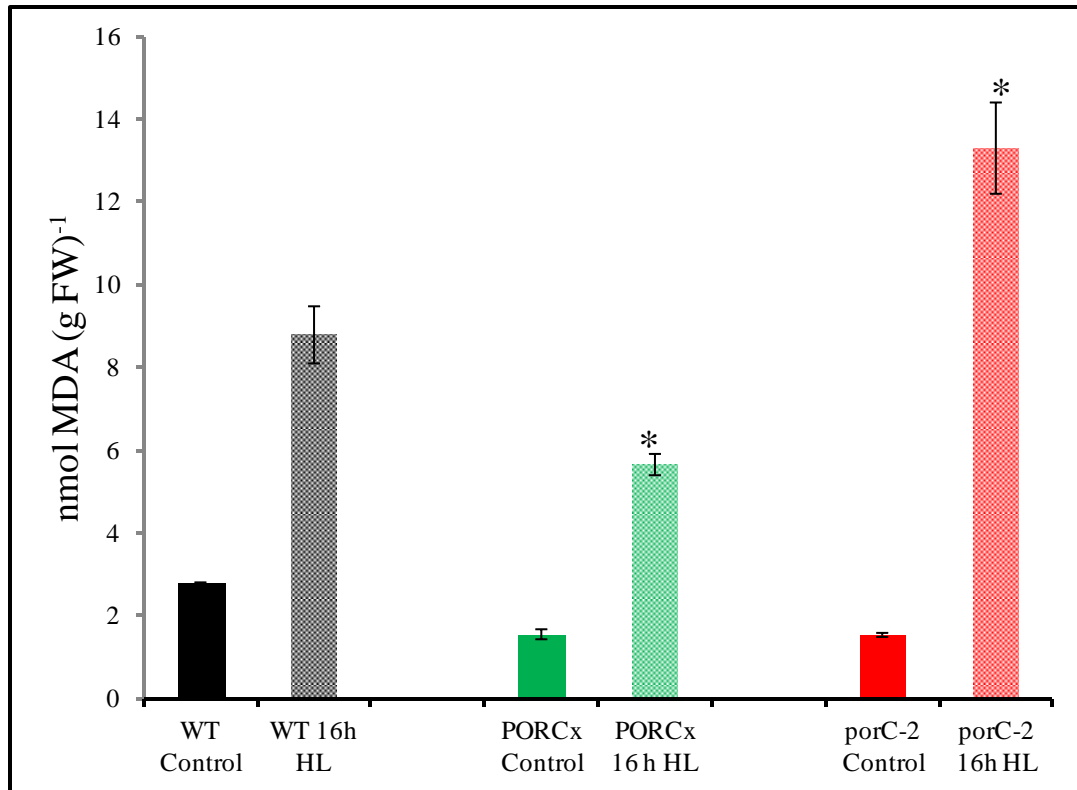


Figure 31. MDA assay to detect lipid peroxidation in WT, PORCx and *porC-2* plants. The WT, PORCx and *porC-2* plants were exposed to high light (800 $\mu\text{mol photons m}^{-2} \text{s}^{-1}$) for 16 h in the plant growth chamber maintained at 21°C. The MDA (Thiobarbituric acid reactive substance-TBARS) content was measured from the leaves as in materials and methods. Each data point is an average of six replicates. The error bar represent standard error ($\pm\text{SE}$). Asterisk indicate significant difference determined by *t* test (* $P < 0.05$)

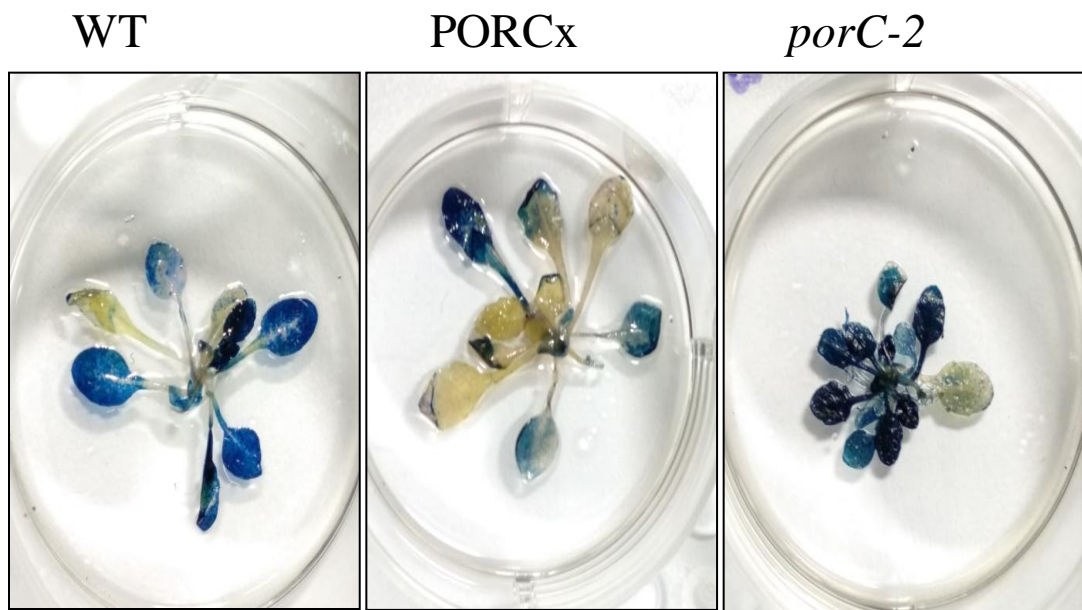


Figure 32. Detection of high-light-induced cell death by Evans blue staining. Three-week-old arabidopsis plants kept under high light ($800 \mu\text{mol photons m}^{-2} \text{s}^{-1}$) in the plant growth chamber maintained at 21°C . After high light treatment, plants were stained with Evan's blue dye to monitor cell death.

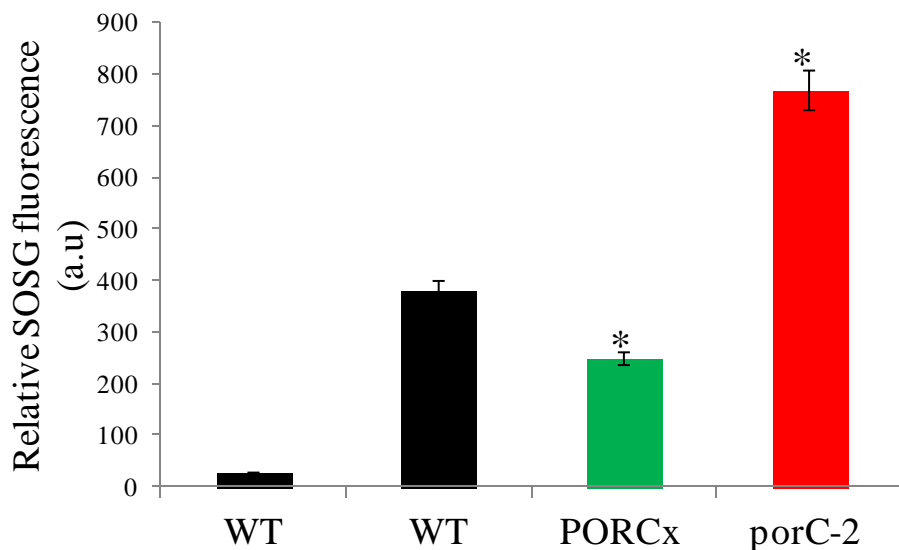
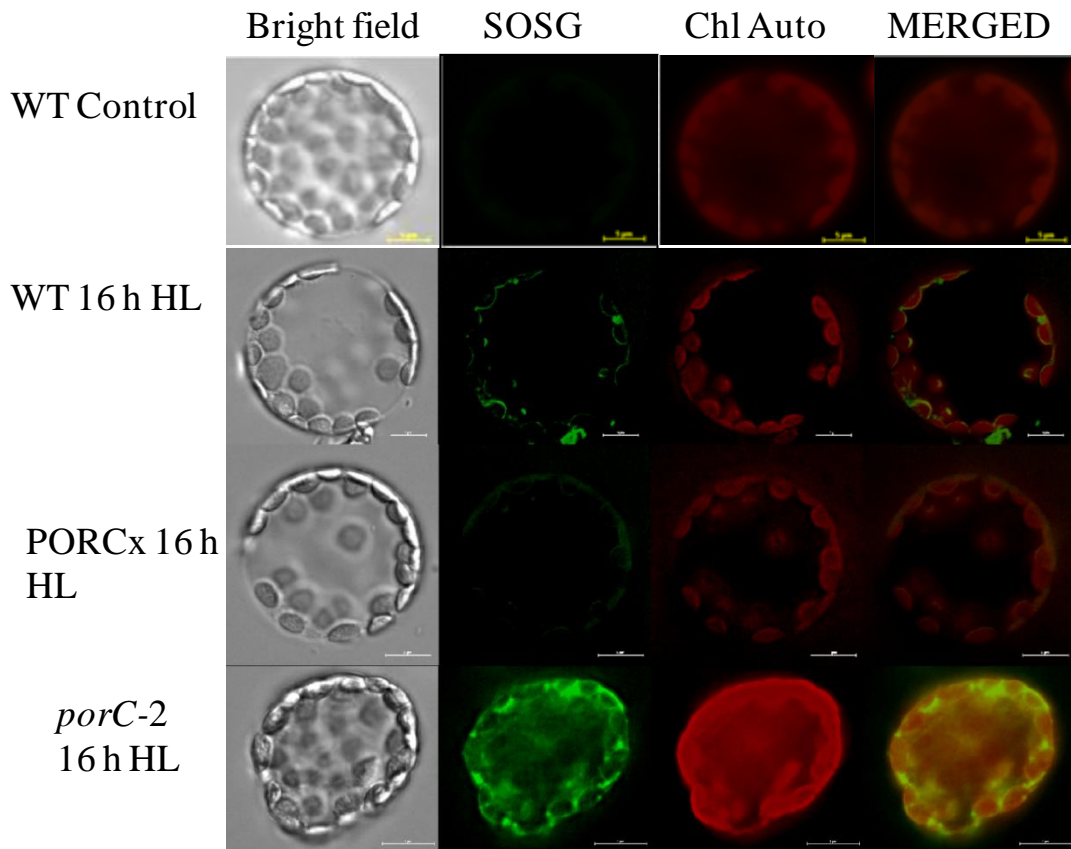


Figure 33. Measurement of singlet oxygen production in high light in WT, PORCx and *porC-2* plants. Arabidopsis protoplasts were isolated after exposing WT, PORCx and *porC-2* plants to 16 h high light ($800 \mu\text{mol photons m}^{-2}\text{s}^{-1}$) in a plant growth chamber maintained at 21°C . To the isolated protoplasts, SOSG dye was added to detect singlet oxygen. (b) Analysis of SOSG fluorescence by ImageJ software.

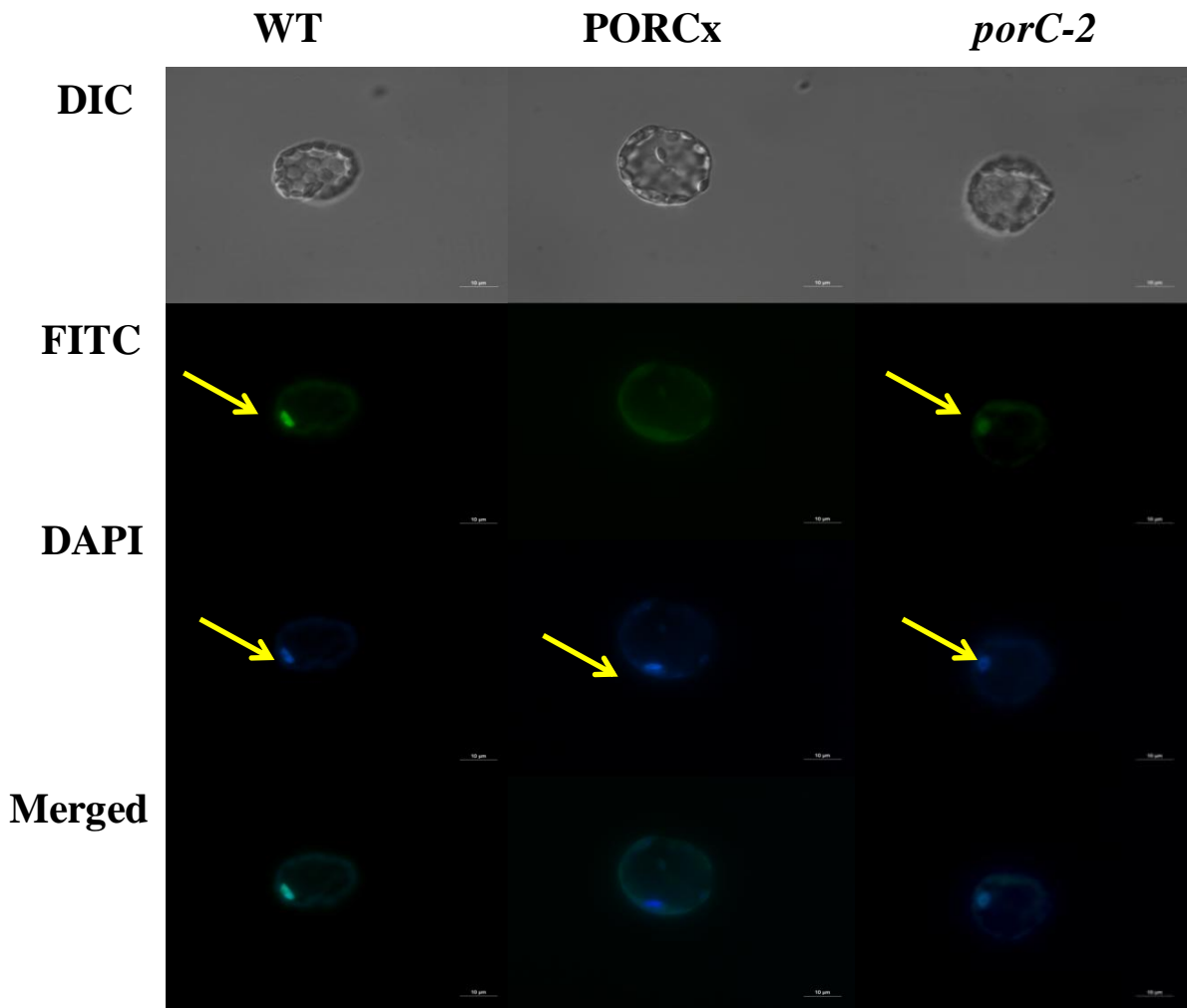


Figure. 34 Identification of DNA nick in the protoplasts isolated from WT, PORCx and *porC-2* plants under singlet oxygen (1O_2) generating condition. Arabidopsis protoplasts were isolated after exposing WT, PORCx and *porC-2* plants to 16 h high light ($800 \mu\text{mol photons m}^{-2}\text{s}^{-1}$) in a plant growth chamber maintained at 21°C . The harvested protoplasts were labeled according to the manufacturer's protocol for TUNEL assay. Yellow arrows indicate localization of nucleus.

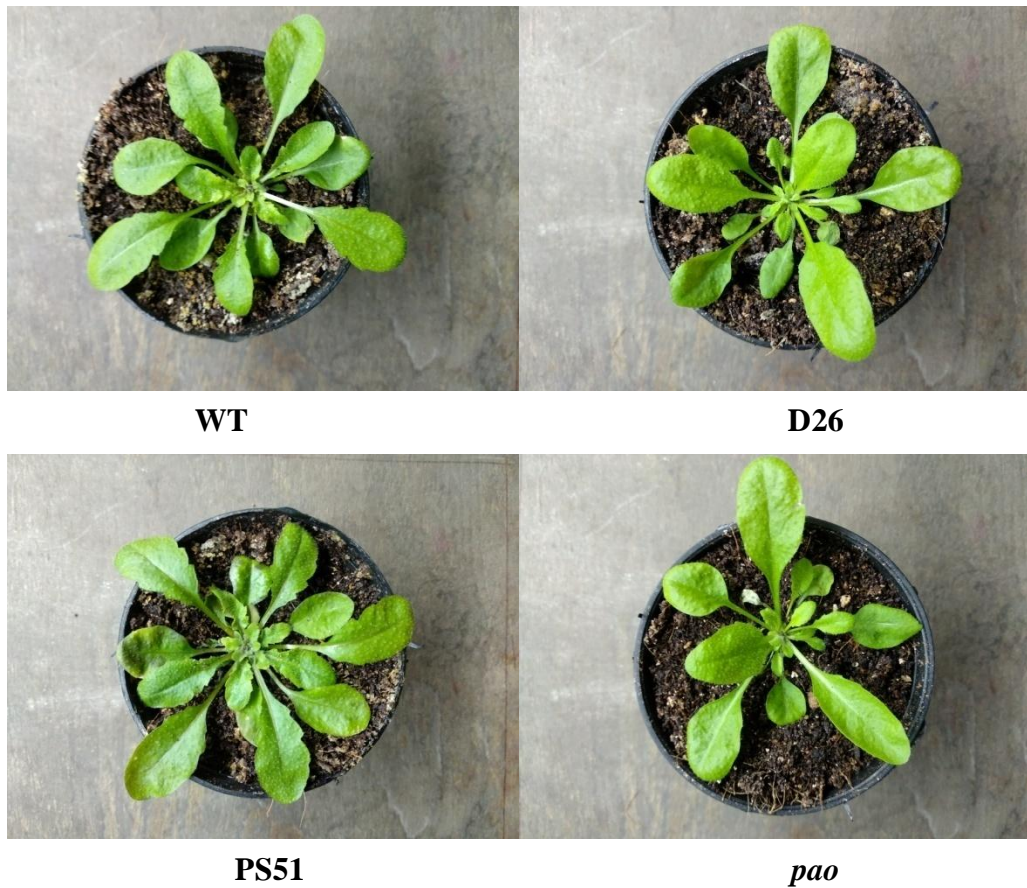


Figure 35. Phenotype of WT, *AtPaO/RCCR* Double overexpressor (D26), *AtPaO* overexpressor (PS51) and *pao* mutant. Plants were grown at 21°C under 10h L and 14h D photoperiod in cool-white-fluorescent light (100 $\mu\text{mol photons m}^{-2} \text{s}^{-1}$).

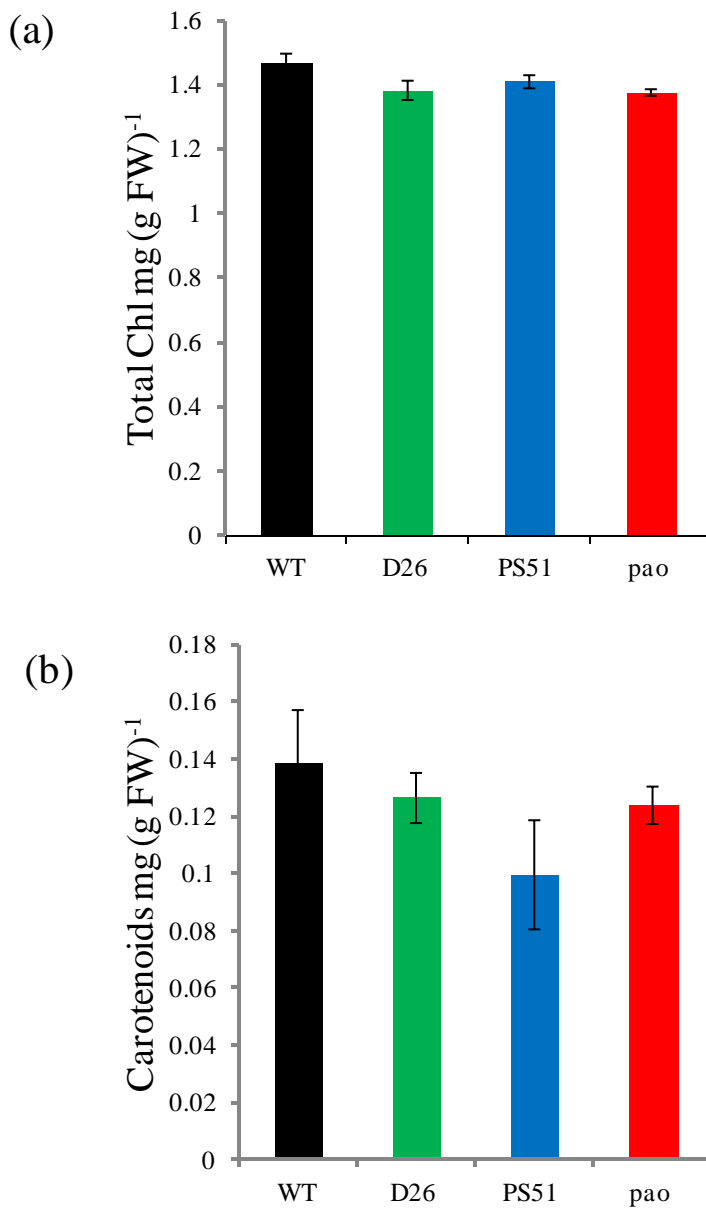


Figure 36. Pigment content in WT, *AtPaO/AtRCCR* Double overexpressor (D26), *AtPaO* overexpressor (PS51) and its mutant *pao*. Plants were grown at 21⁰C under 10h L and 14h D photoperiod in cool-white-fluorescent light (100 μmol photons m⁻² s⁻¹). (a) Total Chl, and their (b) Carotenoid content were measured as in materials and methods. Each data point is an average of six replicates. The error bar represents standard error (±SE).

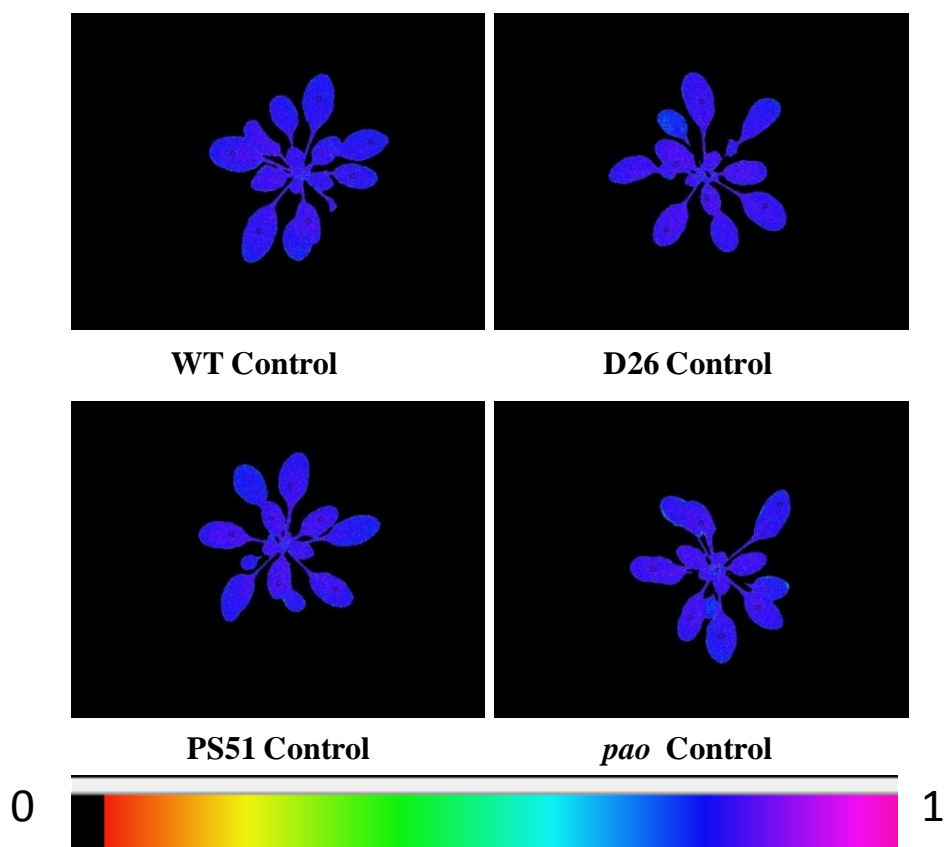


Figure 37. Analysis of PSII quantum yield in dark-adapted control plants. WT, D26, PS51 and *pao* mutant plants were grown at 21⁰C under 10h L and 14h D photoperiod in cool-white-fluorescent light (100 $\mu\text{mol photons m}^{-2} \text{s}^{-1}$). Chlorophyll fluorescence parameters were determined by Imaging PAM fluorometer. False color images of Fv/Fm in non-stressed plants. The color code beneath the image depict values from 0 to 1

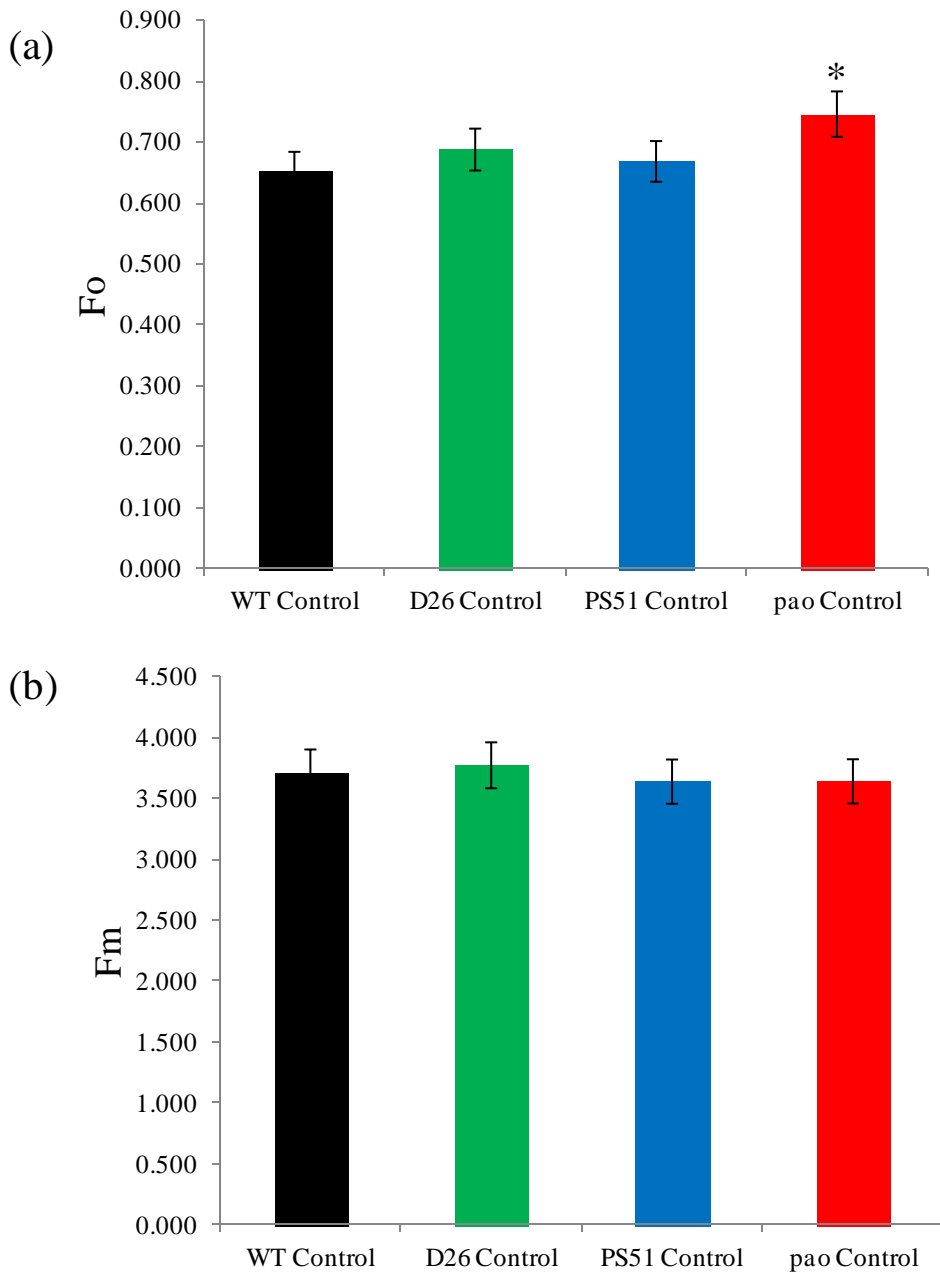


Figure 38. Chlorophyll a fluorescence yield in WT and *AtPaO/RCCR* Double (D26) and *AtPaO* single (PS51) transgenic and its mutant *pao* plants under control conditions. Plants were grown at 21⁰C under 10h L and 14h D photoperiod in cool-white-fluorescent light (100 μ mol photons m^{-2} s^{-1}). The chlorophyll a fluorescence parameters (a) Minimum fluorescence (F_o) and (b) Maximum fluorescence (F_m) were calculated from Dual-PAM 100 fluorometer (Walz, Germany). Each data point is the average of six replicates and error bar represents \pm SE.

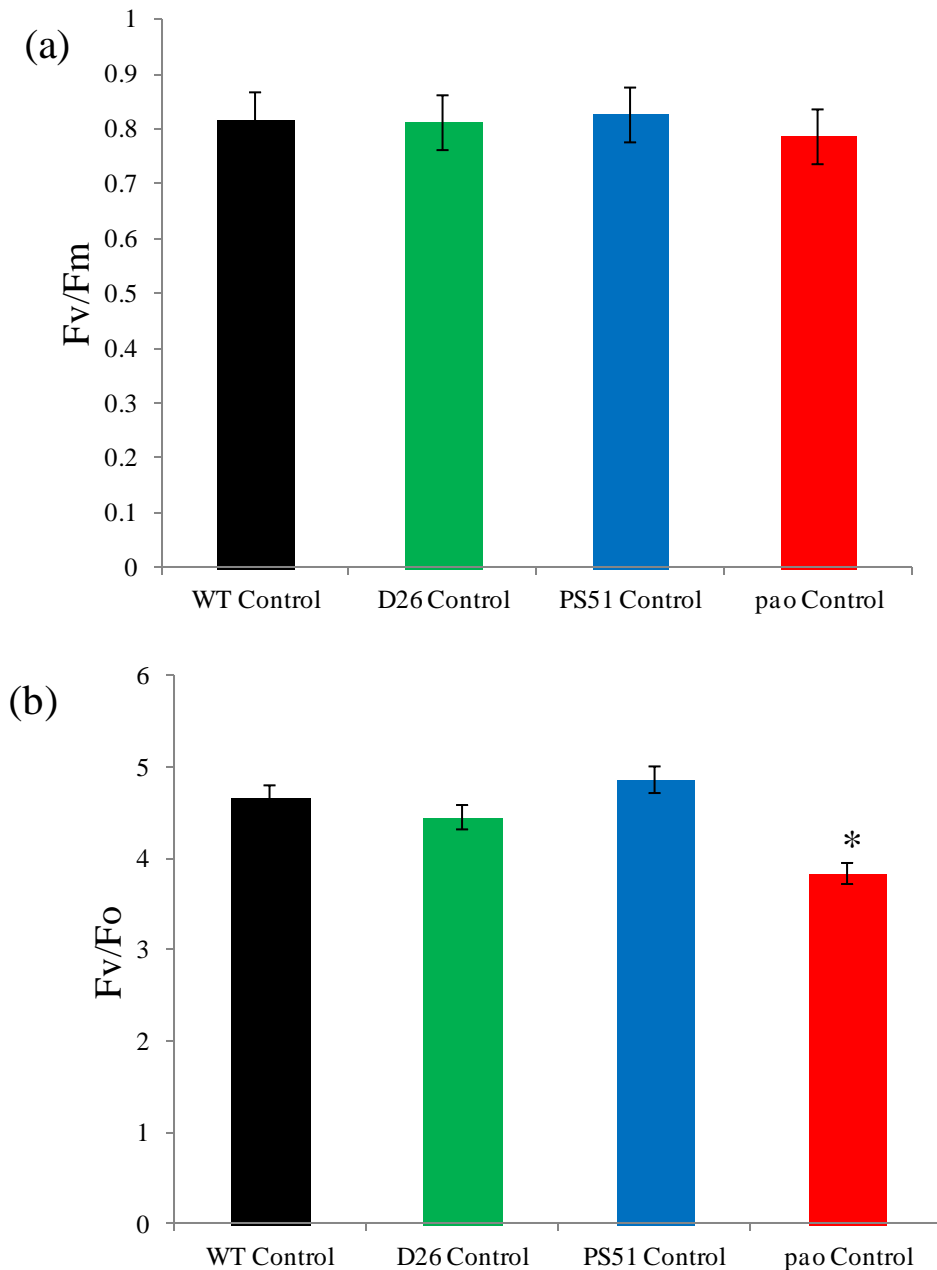


Figure 39. Chlorophyll a fluorescence parameters of WT, D26, PS51 and *pao* mutant plants. Plants were grown at 21⁰C under 10h L and 14h D photoperiod in cool-white-fluorescent light (100 $\mu\text{mol photons m}^{-2} \text{s}^{-1}$). The chlorophyll a fluorescence parameters (a) Maximal PS II quantum yield (b) Variable to minimum chlorophyll fluorescence (F_v/F_o) were calculated from Dual-PAM 100 fluorometer (Walz, Germany). Each data point is the average of six replicates and error bar represents \pm SE.

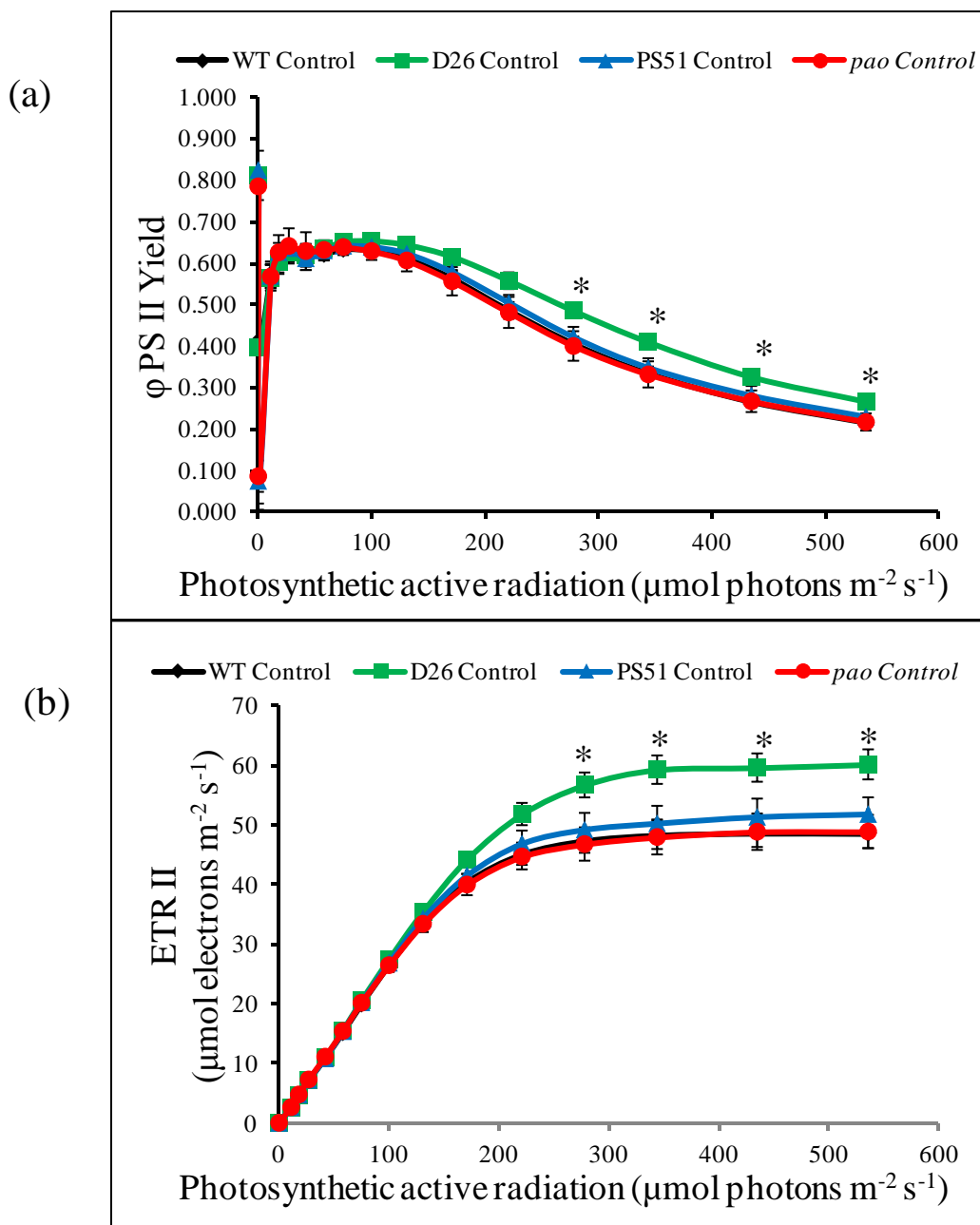


Figure 40. Quantum yield of PSII (ϕ PSII) and PSII-dependent electron transport rate (ETR) in WT, D26, PS51 and *pao* mutants. Plants were grown at 21⁰C under 10h L and 14h D photoperiod in cool-white-fluorescent light (100 $\mu\text{mol photons m}^{-2} \text{s}^{-1}$). The chlorophyll a fluorescence parameters (a) Quantum yield of PSII (ϕ PSII), and (b) Calculated electron transport rate of PSII were determined by using Dual PAM 100 fluorometer. Each data point is the average of six replicates and error bar represents \pm SE. Asterisk indicate significant difference determined by *t* test (**P*<0.05)

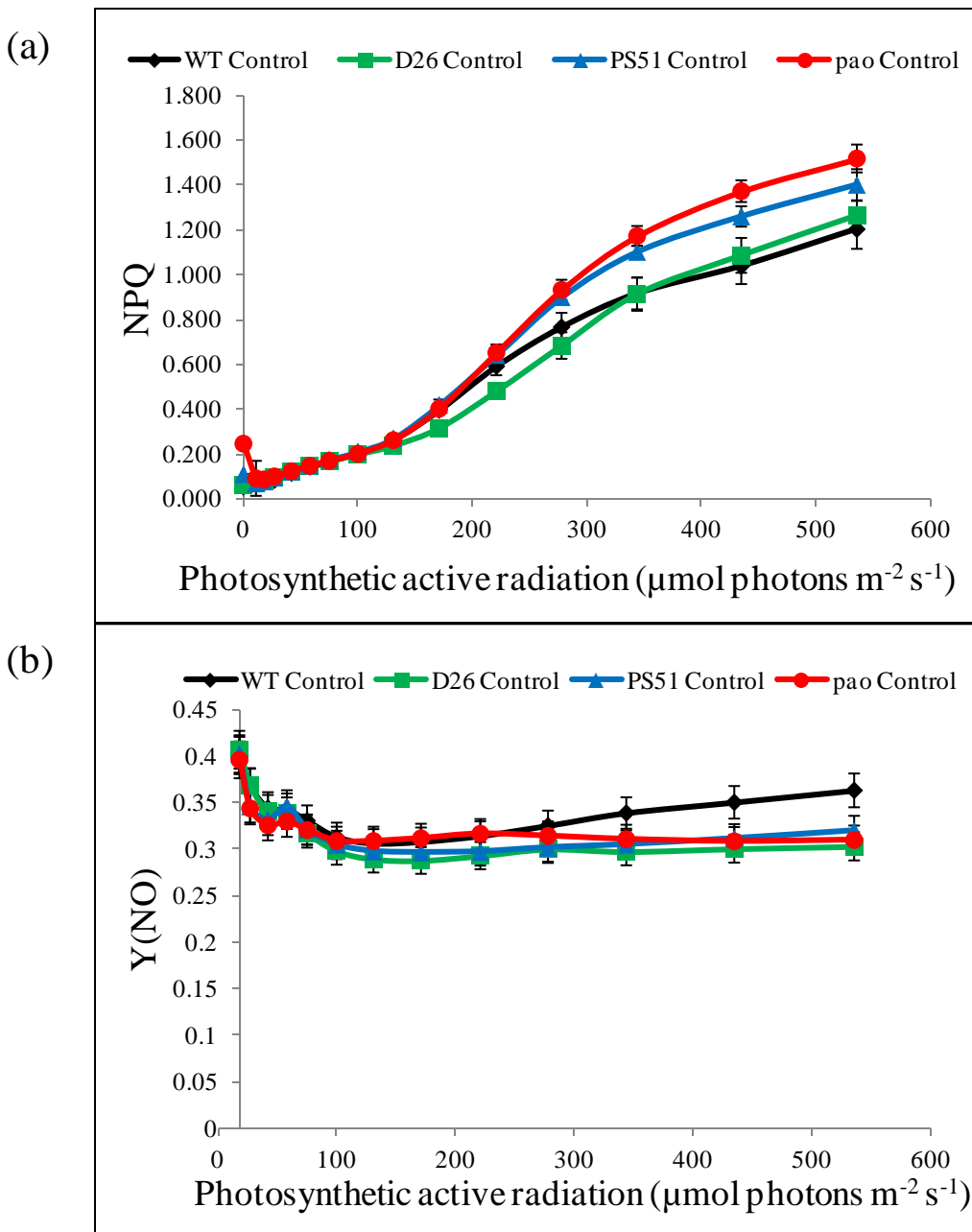
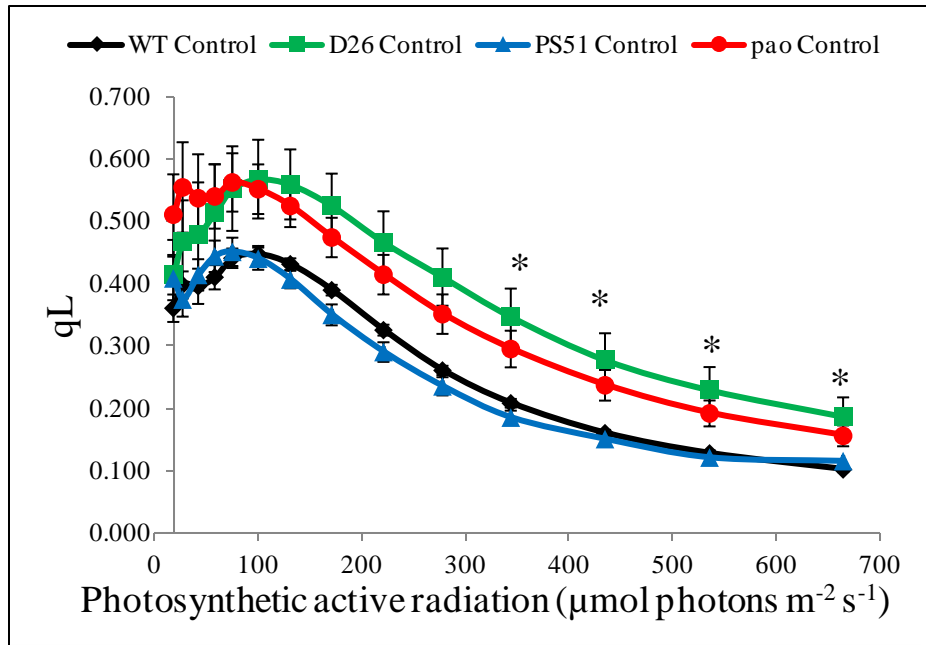


Figure 42. Analysis of (a) Non photochemical quenching, and (b) quantum yield of non-regulated energy dissipation Y(NO) in *Arabidopsis* WT D26, PS51 and its mutant *pao*. Plants were grown at 21°C under 10h L and 14h D photoperiod in cool-white-fluorescent light (100 $\mu\text{mol photons m}^{-2} \text{s}^{-1}$). Parameters were measured by using Dual PAM 100 fluorometer. Each data point is the average of six replicates and error bar represents $\pm\text{SE}$.

(a)



(b)

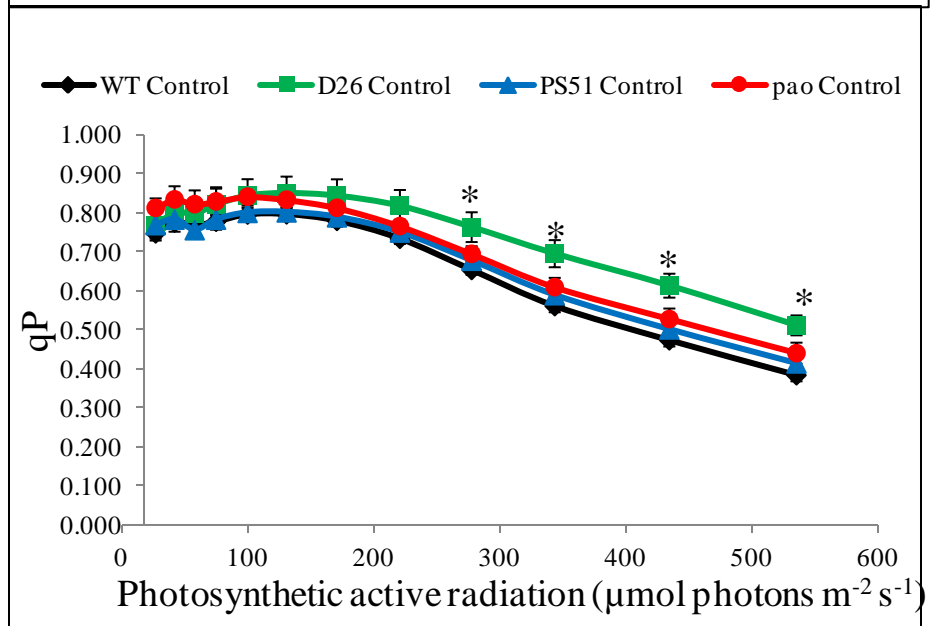


Figure 43. Coefficient of photochemical quenching (qL) in WT, D26,PS51 and pao mutant plants. Plants were grown at 21°C under 10h L and 14h D photoperiod in cool-white-fluorescent light (100 $\mu\text{mol photons m}^{-2} \text{s}^{-1}$). Parameters were measured by using Dual PAM 100 fluorometer Each data point is the average of six replicates and error bar represents $\pm\text{SE}$. Asterisk indicate significant difference determined by *t* test (* $P < 0.05$)

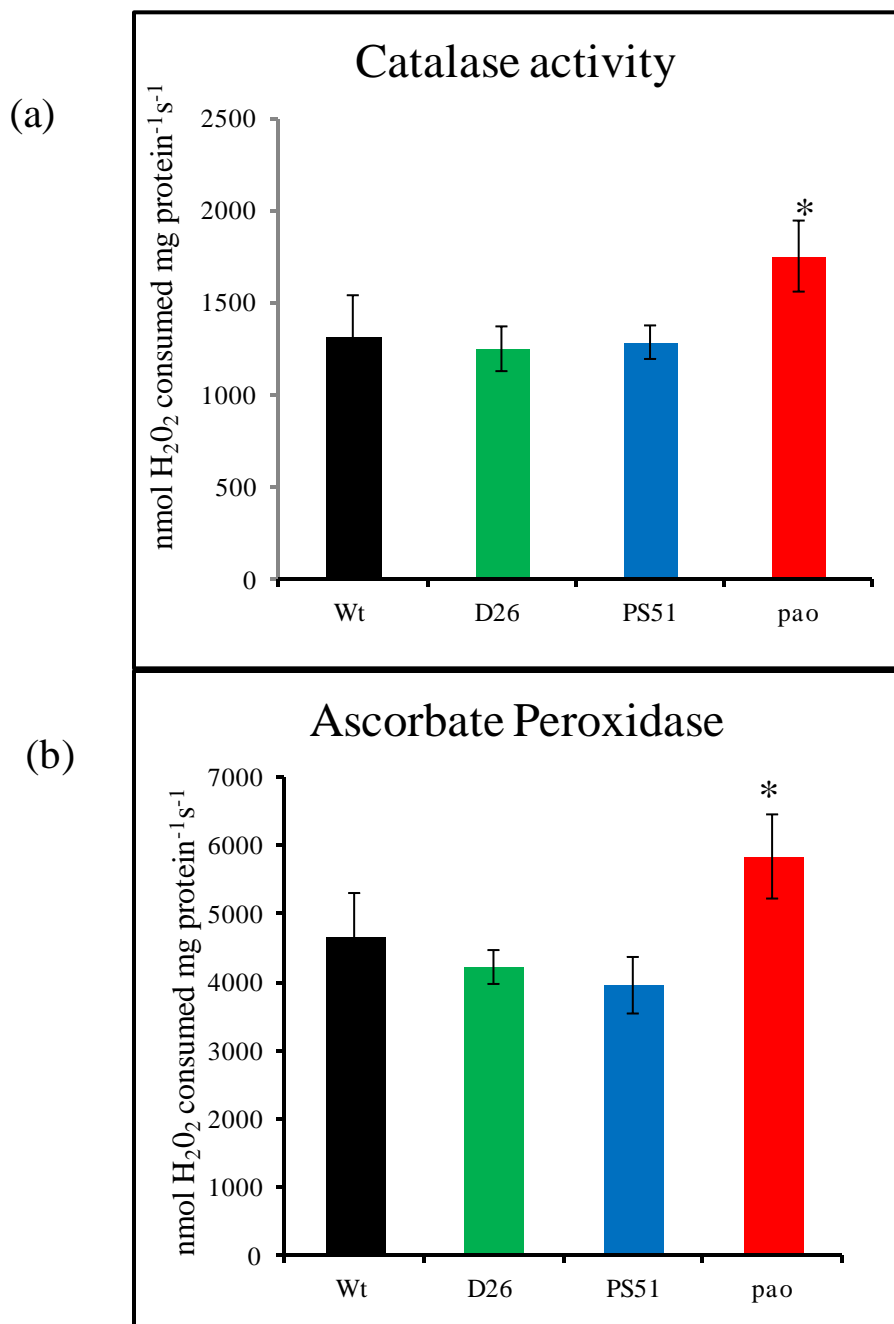


Figure 44. Measurement of (a) Catalase and (b) Ascorbate Peroxidase rate in WT D26, PS51 and its mutant *pao*. Plants were grown at 21°C under 10h L and 14h D photoperiod in cool-white-fluorescent light (100 $\mu\text{mol photons m}^{-2} \text{s}^{-1}$) for 5 weeks. Their antioxidative enzyme activities were measured as described in materials and methods. Asterisk indicate significant difference determined by *t* test (* $P < 0.05$)

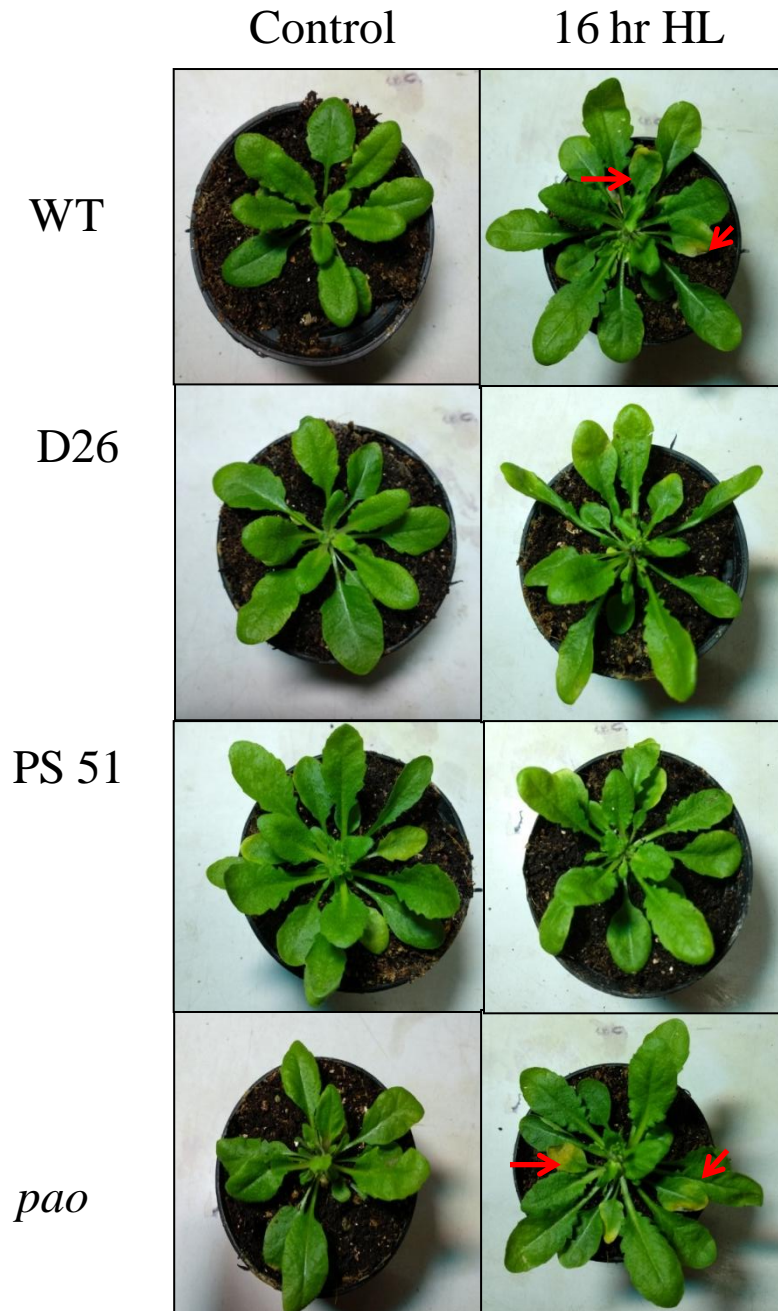


Figure 45. Morphological changes in WT, D26, PS51 and *pao* mutant plants after exposing them to high light intensity ($800 \mu\text{mol photons m}^{-2}\text{s}^{-1}$). Plants were grown at 21°C under 10h L and 14h D photoperiod in cool-white-fluorescent light ($100 \mu\text{mol photons m}^{-2} \text{s}^{-1}$) for 5 weeks. Well hydrated plants were exposed to either $100 \mu\text{mol photons m}^{-2} \text{s}^{-1}$ (control) or high light ($800 \mu\text{mol photons m}^{-2} \text{s}^{-1}$) for 16 h in the plant growth chamber maintained at 21°C . Minimum 6 plants from each type was used in the study. Red arrows indicate photo-bleached leaves due to high light stress.

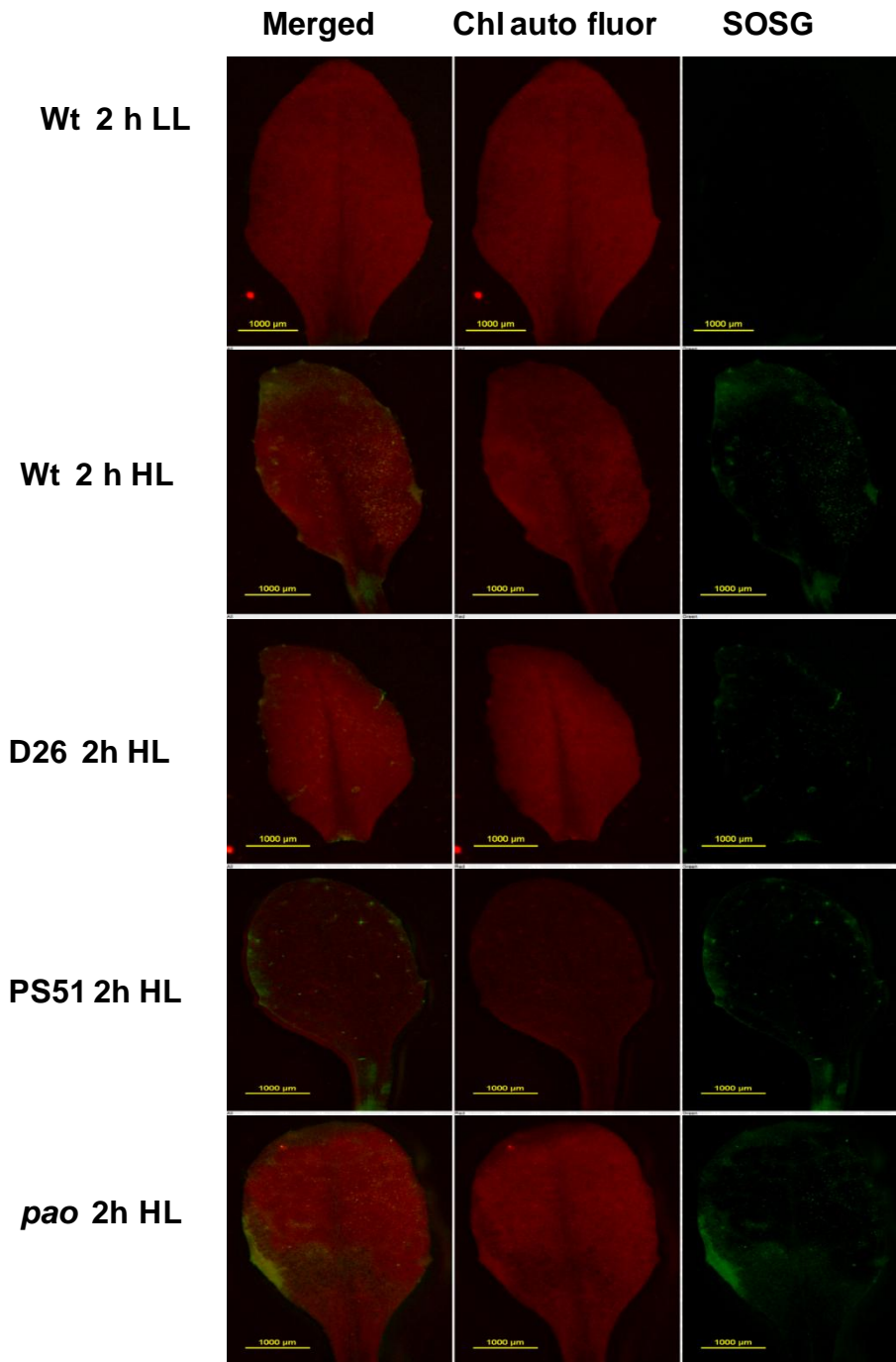


Figure 46. Monitoring of singlet oxygen level in D26, PS51 and *pao* mutant plants by Singlet oxygen sensor green (SOSG). Three-week-old arabidopsis plants were kept under growth light ($100 \mu\text{mol photons m}^{-2}\text{s}^{-1}$) or high light ($100 \mu\text{mol photons m}^{-2}\text{s}^{-1}$) for 2 h in the plant growth chamber maintained at 21°C . Singlet oxygen was detected by staining the detached leaves with SOSG dye. SOSG stained leaves were observed under 1.5X magnification using different fluorescent channels.

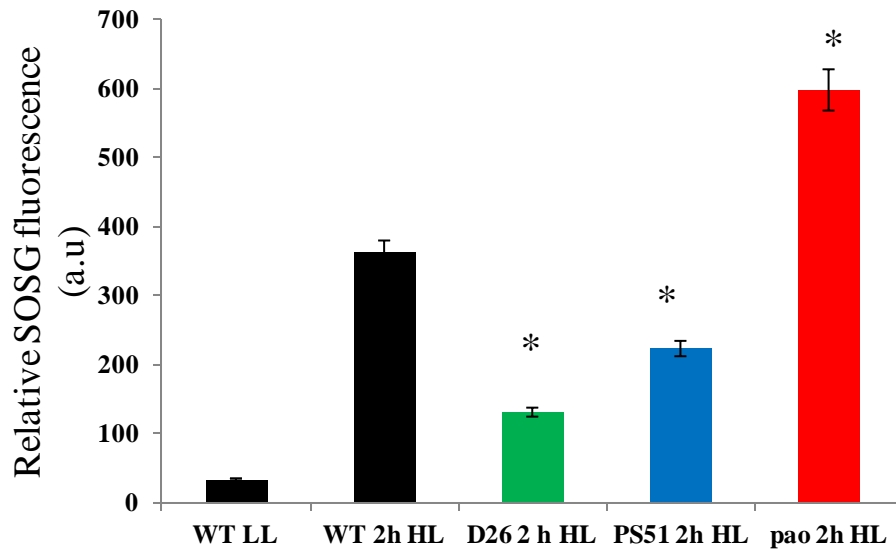
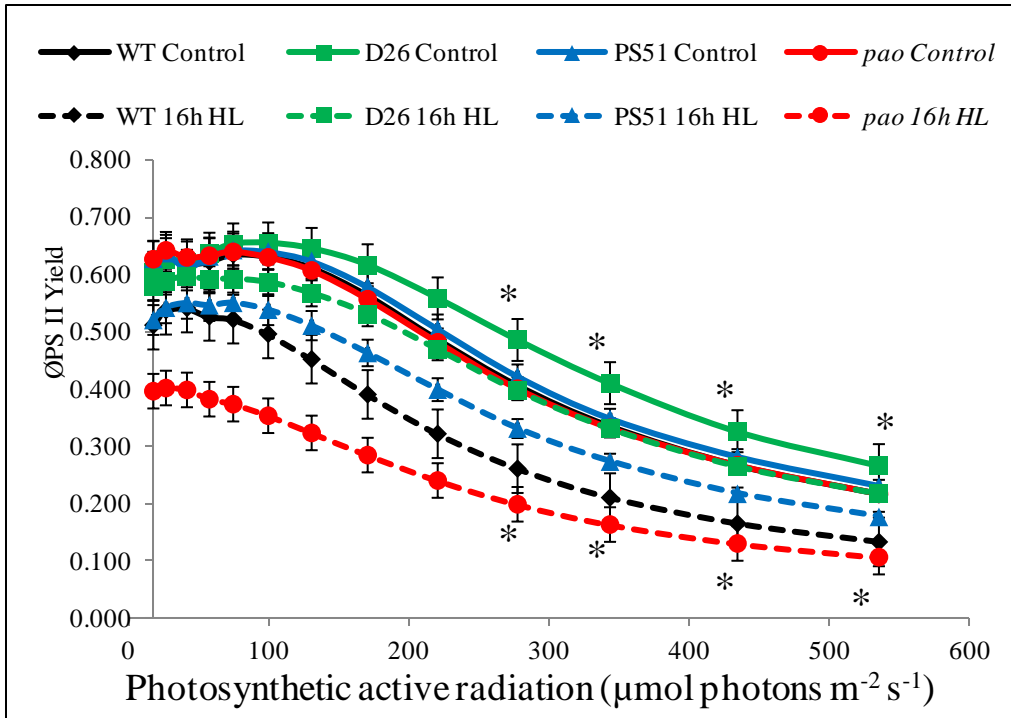


Figure 47. Estimation SOSG fluorescence emanating from light treated leaves. The captured images were analyzed using ImageJ software. Each data point is the average of six replicates and error bar represents \pm SE. Asterisk indicate significant difference determined by *t* test (* $P < 0.05$)

(a)



(b)

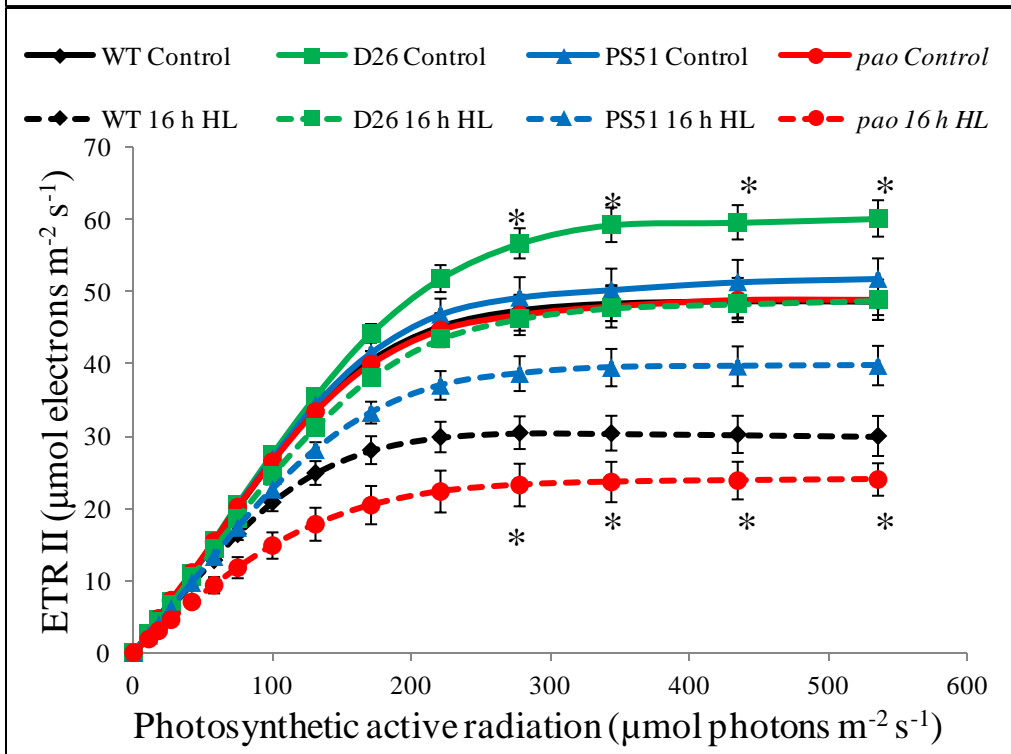


Figure 48. Quantum yield of PSII (ϕ PSII) and Electron transport rate (ETR) in WT, D26, PS51 and *pao* mutant. Plants were grown at 21°C under 10h L and 14h D photoperiod in cool-white-fluorescent light ($100 \mu\text{mol photons m}^{-2} \text{s}^{-1}$) for 5 weeks. Well hydrated plants were kept under high light ($800 \mu\text{mol photons m}^{-2} \text{s}^{-1}$) for 16 h in the plant growth chamber maintained at 21°C. The chlorophyll a fluorescence parameters (a) Quantum Yield Of PsII (ϕ PSII), and (b) Electron transport rate of PSII were determined by using Dual PAM 100 fluorometer. Each data point is the average of six replicates and error bar represents \pm SE. Asterisk indicate significant difference determined by *t* test (* $P < 0.05$)

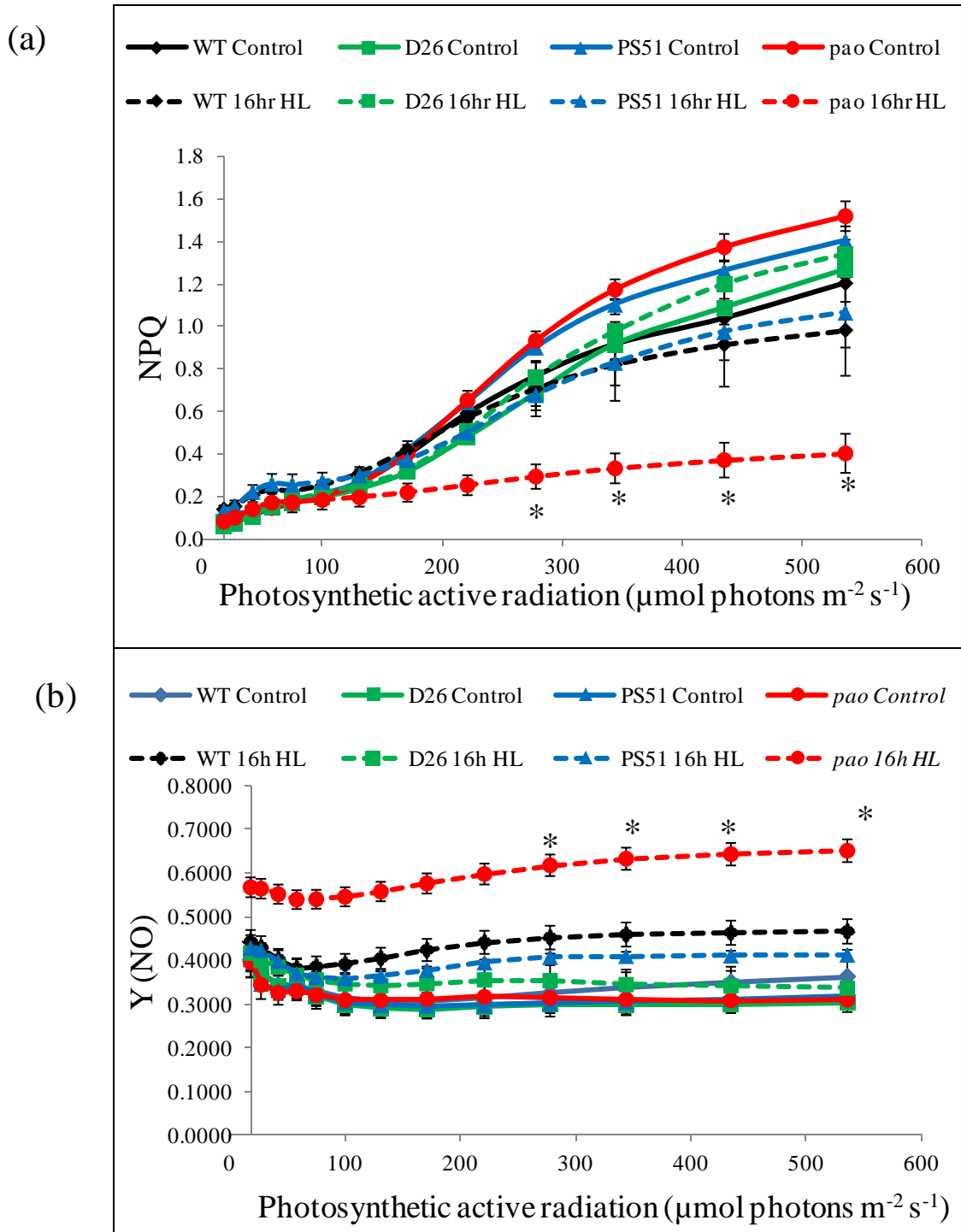


Figure 49. Analysis of (a) Non photochemical quenching and (b) Quantum yield of non-regulated energy dissipation Y(NO) in WT, D26, PS51 and its mutant *pao*. Plants were grown at 21^oC under 10h L and 14h D photoperiod in cool-white-fluorescent light (100 $\mu\text{mol photons m}^{-2} \text{s}^{-1}$) for 5 weeks. Well hydrated plants were kept under high light (800 $\mu\text{mol photons m}^{-2} \text{s}^{-1}$) for 16 h in the plant growth chamber maintained at 21^oC. The chlorophyll a fluorescence parameters were determined by using Dual PAM 100 fluorometer Each data point is the average of six replicates and error bar represents \pm SE. Asterisk indicate significant difference determined by *t* test (* $P < 0.05$)

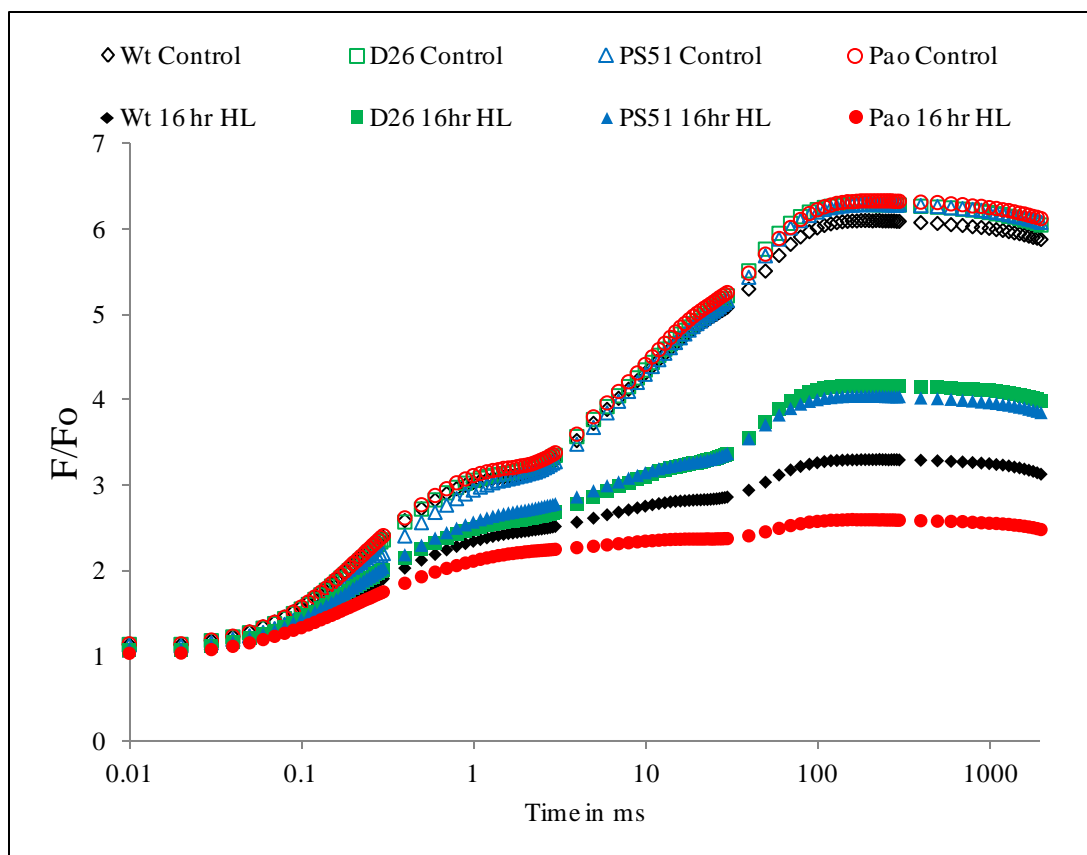


Figure 49. Analysis of chlorophyll a fluorescence induction curve WT, D26, PS51 and *pao* mutant plants. Well hydrated plants were kept under high light ($800 \mu\text{mol photons m}^{-2} \text{s}^{-1}$) for 16 h in the plant growth chamber maintained at 21°C . Control plants were kept under growth light ($100 \mu\text{mol photons m}^{-2} \text{s}^{-1}$). After light treatment, plants were incubated in dark for 20 min.. Data was normalized at F_0 where F denotes fluorescence at time t (F_t). Measurement was performed by photosynthetic efficiency analyzer, Handy-PEA.

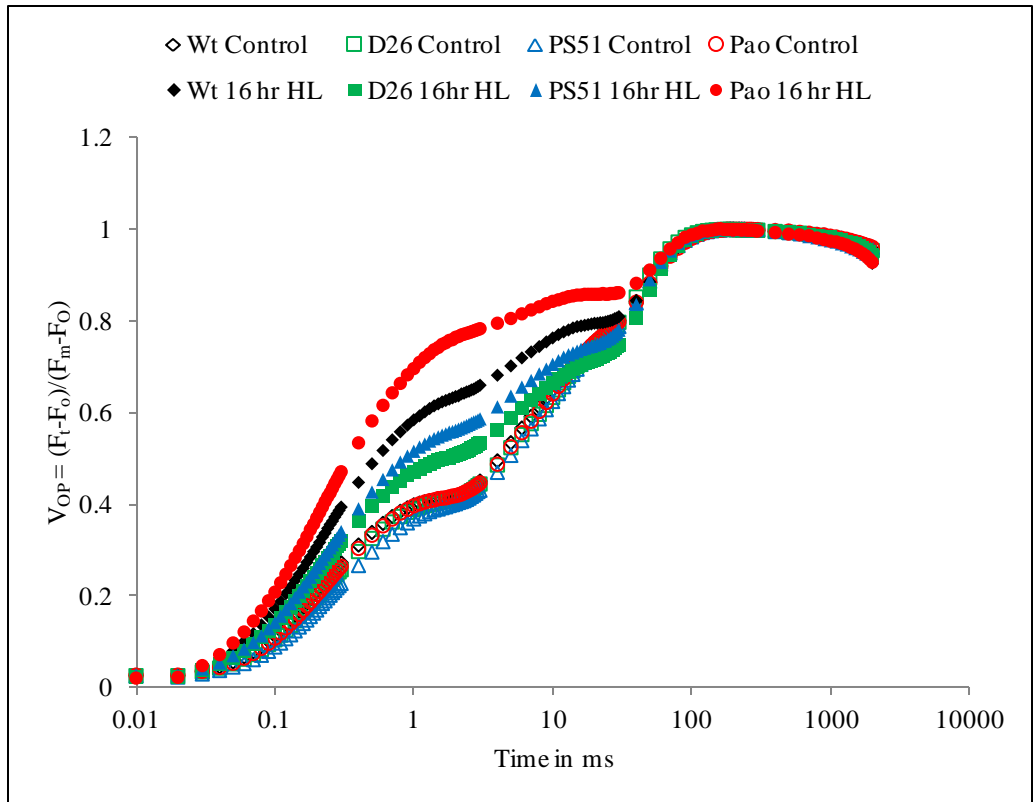


Figure 50. Analysis of chlorophyll a fluorescence induction curve double normalized at O and P level. Well hydrated WT, D26, PS51 and *pao* mutant plants were kept under high light ($800 \mu\text{mol photons m}^{-2} \text{s}^{-1}$) for 16 h in the plant growth chamber maintained at 21°C and later incubated in dark for 20 min after completion of HL stress. Control plants were kept under normal light ($100 \mu\text{mol photons m}^{-2} \text{s}^{-1}$). Measurement was performed by photosynthetic efficiency analyzer, Handy- PEA. Chlorophyll fluorescent transient were plotted against logarithmic time scale.

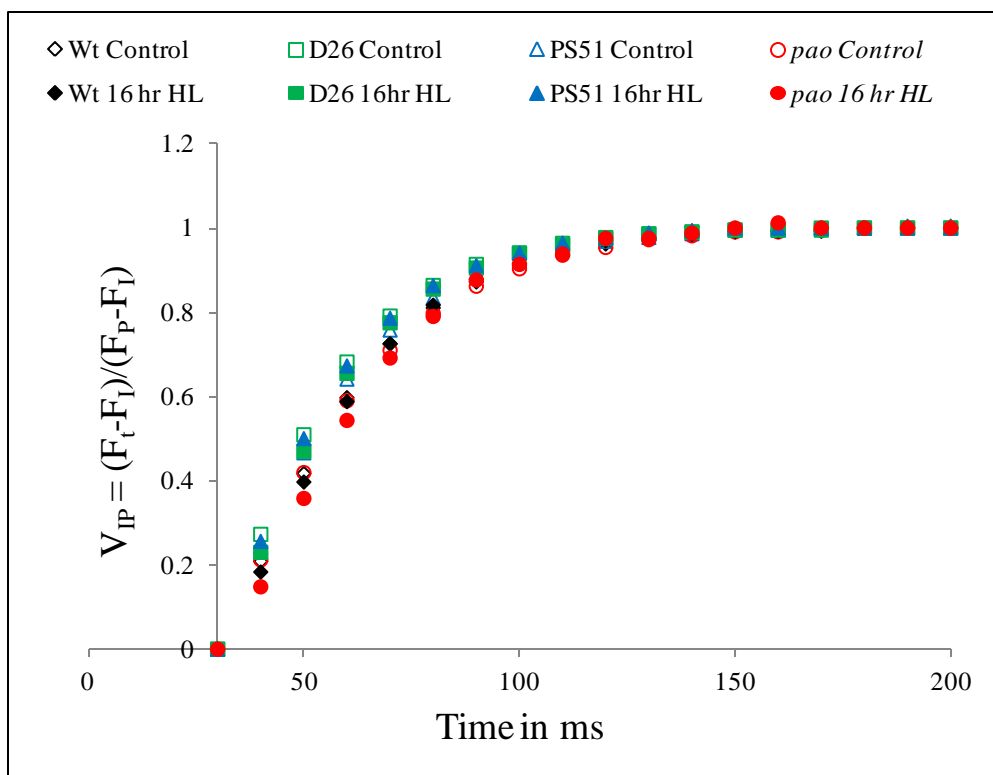


Figure 51. I to P rise transient normalized at both at I and P, deduced from the OJIP curves of figure-49. Variable fluorescence transients from the I to the P double normalized between I (F_I) and P (F_P) phases. Measurement was performed by photosynthetic efficiency analyzer, Handy-PEA.

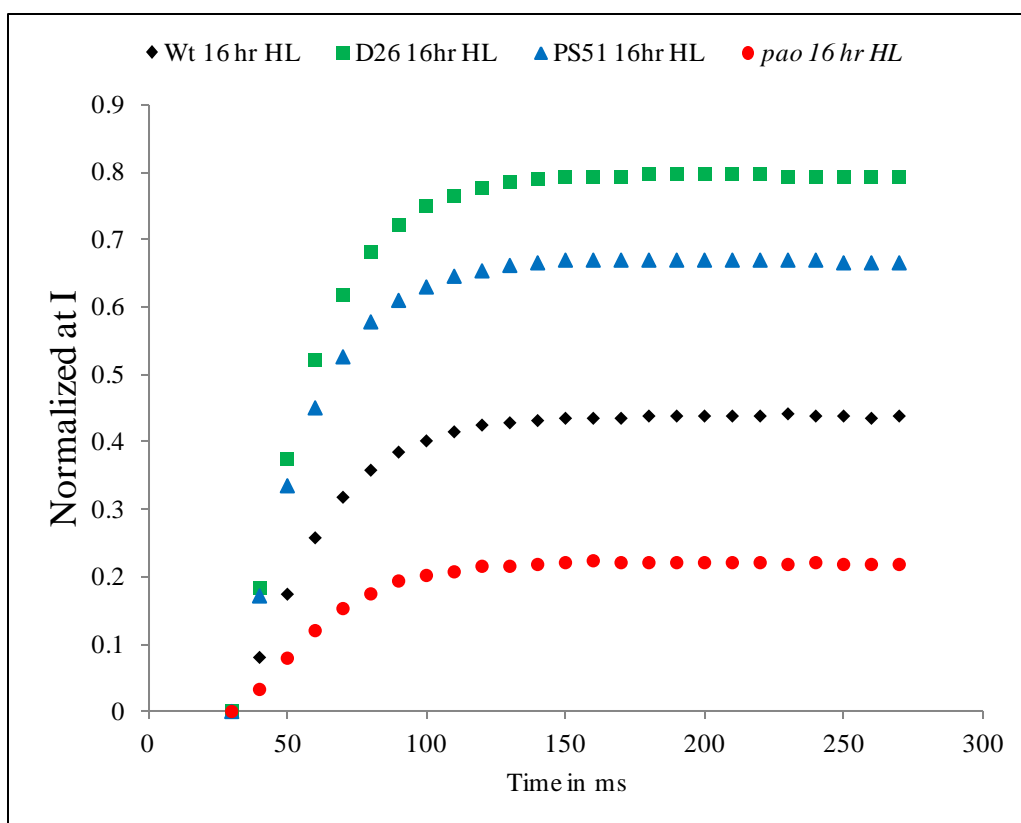


Figure 52. I to P rise normalized at I deduced from the analysis of chlorophyll a fluorescence transient. Variable fluorescence transients from the I to the P single normalized at I phase (30ms). Measurement was performed by photosynthetic efficiency analyzer, Handy-PEA

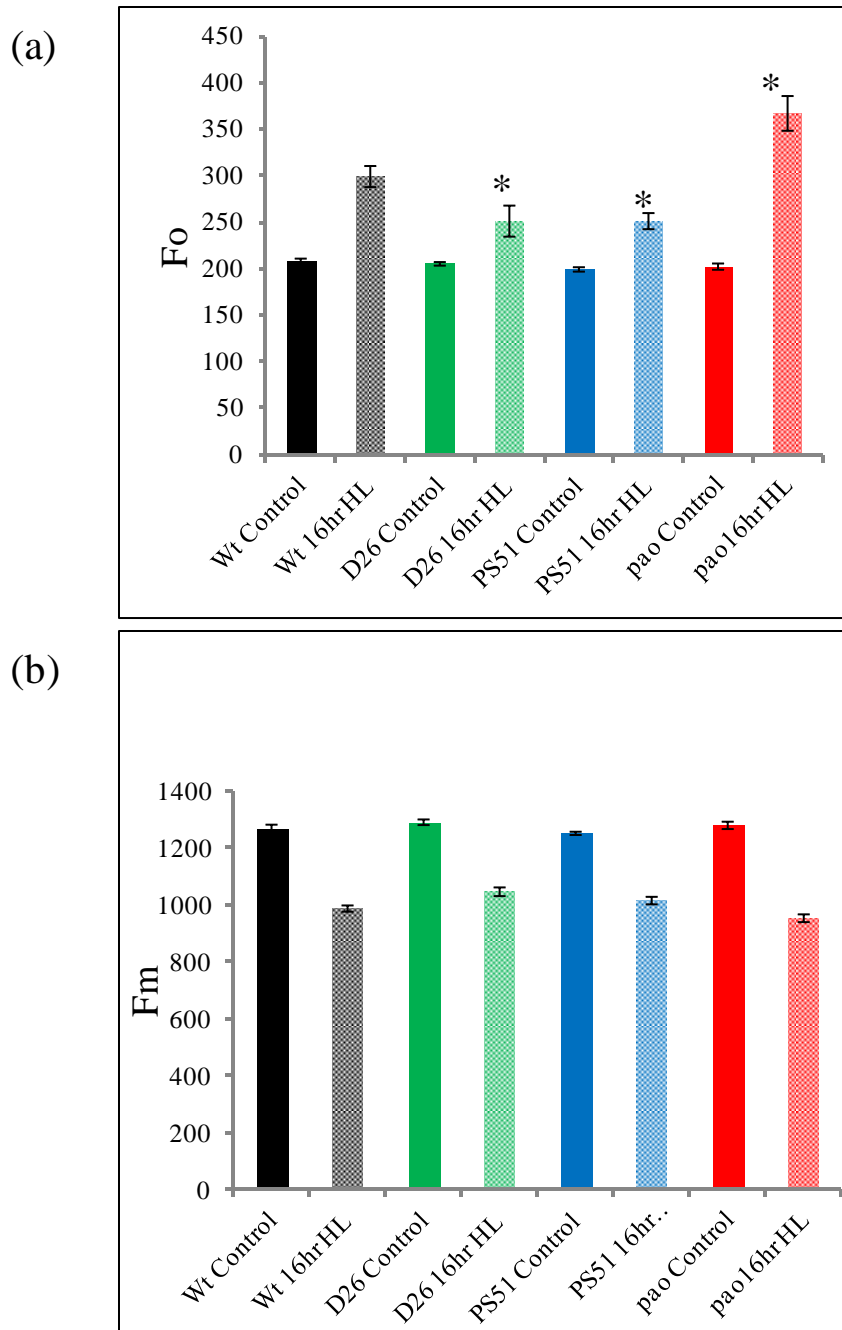


Figure 53. Chlorophyll a fluorescence yield in WT, D26, PS51 and *pao* mutant. Plants were kept in growth light ($100 \mu\text{mol photons m}^{-2} \text{s}^{-1}$) or high light ($800 \mu\text{mol photons m}^{-2} \text{s}^{-1}$ for 16 hours in the plant growth chamber maintained at 21°C). (a) Dark fluorescence yield (F_o) (b) Maximum fluorescence yield (F_m) were measured from Handy-PEA. The data points are average of 15 replicates and error bars represent $\pm\text{SE}$. Asterisk indicate significant difference determined by t test (* $P < 0.05$)

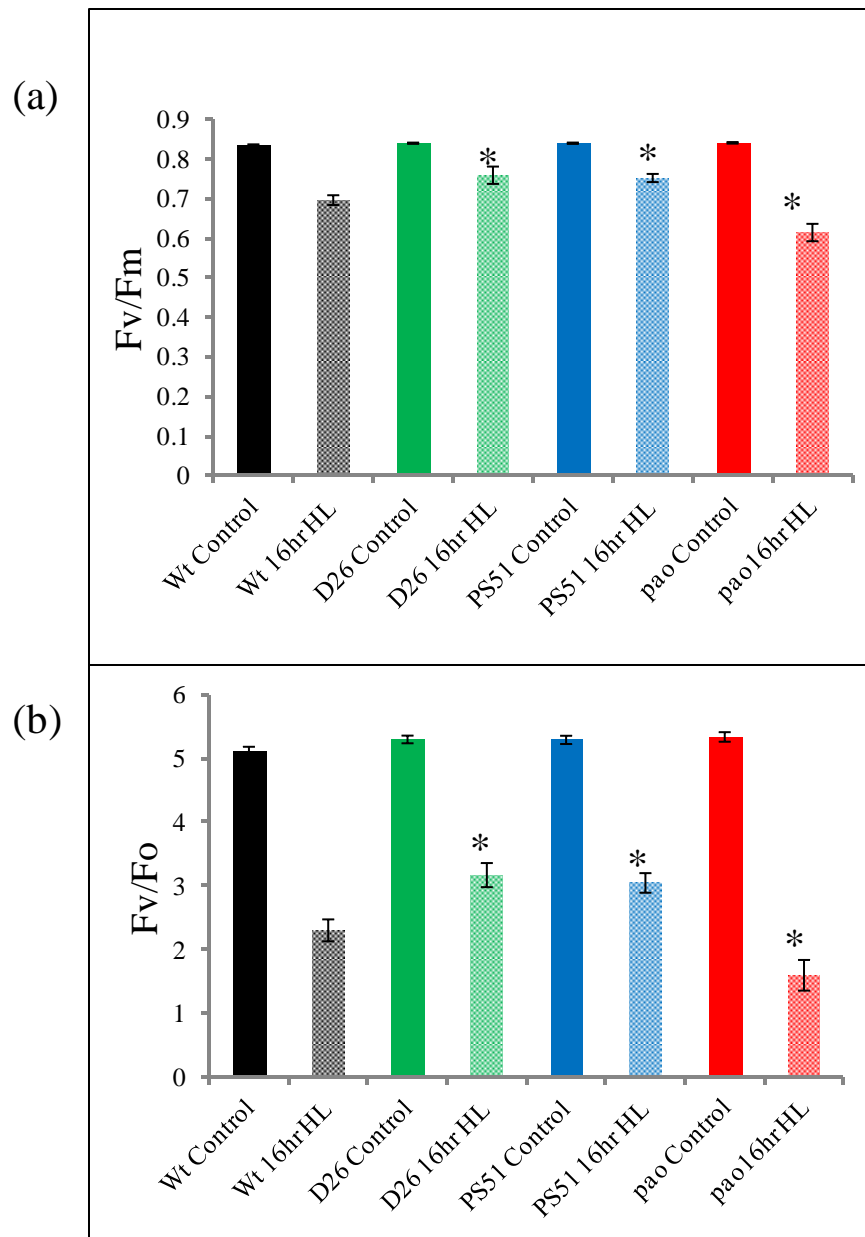


Figure 54. Chlorophyll a fluorescence parameters of WT, D26, PS51 and *pao* mutant. Plants were kept in controlled ($100 \mu\text{mol photons m}^{-2} \text{s}^{-1}$) and high light ($800 \mu\text{mol photons m}^{-2} \text{s}^{-1}$ for 16 hours in the plant growth chamber maintained at 21°C). (a) Ratio of variable to maximum fluorescence (F_v/F_m). (b) Ratio of variable to initial fluorescence were measure from photosynthetic efficiency analyzer. The data points are average of 15 replicates and error bars represent $\pm\text{SE}$. Asterisk indicate significant difference determined by *t* test (* $P<0.05$)

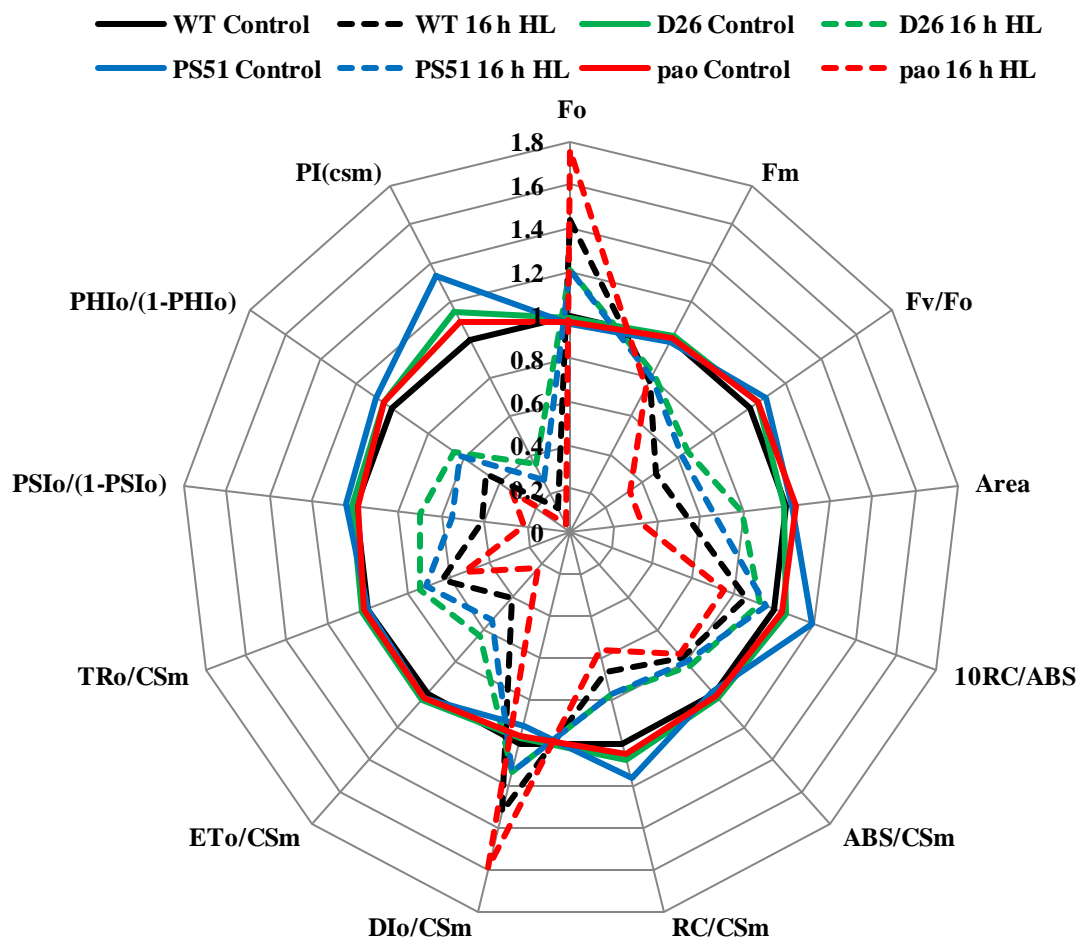


Figure 55. Radar plot depicting parameters derived from OJIP transient curve. After analysis of OJIP curve, different parameters were interpreted from Biolyzer software. WT Control was taken as reference.

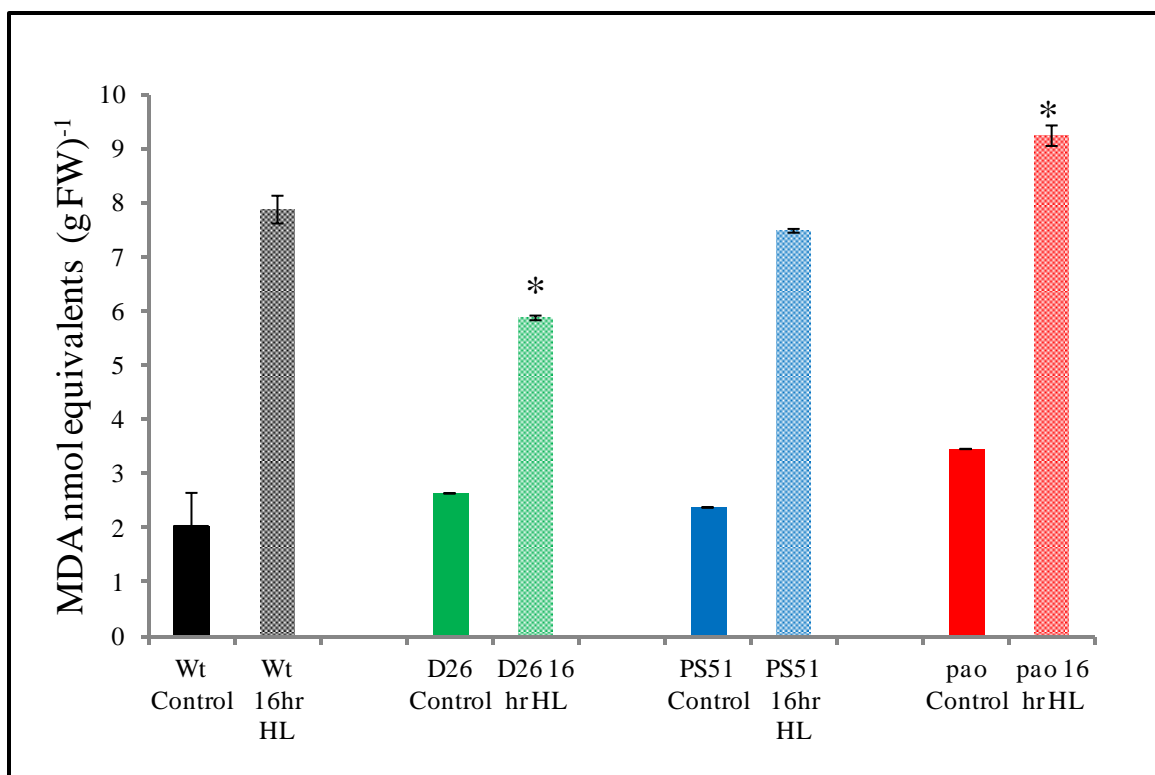


Figure 56. MDA assay to detect lipid peroxidation in WT, D26, PS51 and *pao* mutant. Plants were grown at 21°C under 10h L and 14h D photoperiod in cool-white-fluorescent light ($100 \mu\text{mol photons m}^{-2} \text{s}^{-1}$) for 5 weeks. Well hydrated plants were kept under high light ($800 \mu\text{mol photons m}^{-2} \text{s}^{-1}$) for 16 h in the plant growth chamber maintained at 21°C. The MDA (Thiobarbituric acid reactive substance-TBARS) content was measured from the leaves as in materials and methods. Each data point is an average of six replicates. The error bar represent standard error ($\pm\text{SE}$). Asterisk indicate significant difference determined by *t* test (* $P < 0.05$)

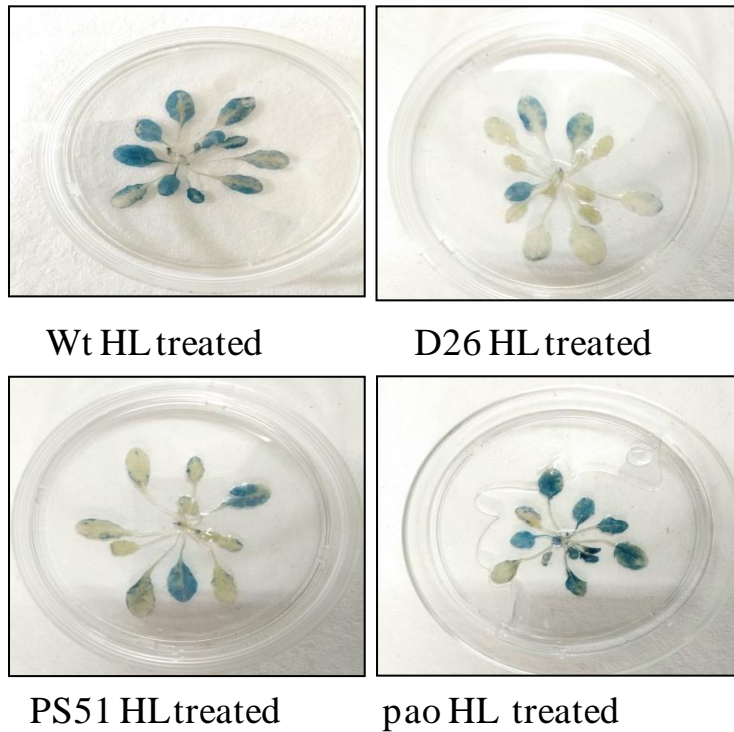


Figure 57. Detection of singlet oxygen induced cell death by Evans blue staining. 3 weeks old WT, D26, PS51 and *pao* plants kept under high light ($800 \mu\text{mol photons m}^{-2} \text{s}^{-1}$) in the plant growth chamber maintained at 21°C . After high light treatment, plants were stained with Evan's blue dye to monitor cell death.